

UNCLASSIFIED

SECURITY CLASSIFICATION OF THIS PAGE (When Data Entered)

REPORT DOCUMENTATION PAGE		READ INSTRUCTIONS BEFORE COMPLETING FORM
1. REPORT NUMBER	2. GOVT ACCESSION NO.	3. RECIPIENT'S CATALOG NUMBER
4. TITLE (and Subtitle) Ocean Surveillance Detection Studies: Part I. Detection in Gaussian Mixture Noise, Part II. An Investigation of Canonical Correlation As An Automatic Detection and Beamforming Technique		5. TYPE OF REPORT & PERIOD COVERED Final Report Jan. 1, 1985 - Sept. 30, 1985
7. AUTHOR(s) Jhong S. Lee, Leonard E. Miller, Robert H. French, and Young K. Kim		6. PERFORMING ORG. REPORT NUMBER JC-2034-N
9. PERFORMING ORGANIZATION NAME AND ADDRESS J. S. Lee Associates, Inc. 2001 Jefferson Davis Highway, Suite 601 Arlington, Virginia 22202		8. CONTRACT OR GRANT NUMBER(s) N00014-85-C-0091
11. CONTROLLING OFFICE NAME AND ADDRESS Office of Naval Research Statistics and Probability Program Arlington, Virginia 22217		10. PROGRAM ELEMENT, PROJECT, TASK AREA & WORK UNIT NUMBERS NR 661-007
14. MONITORING AGENCY NAME & ADDRESS (if different from Controlling Office)		12. REPORT DATE October, 1985
		13. NUMBER OF PAGES 261 + xv
		15. SECURITY CLASS. (of this report) UNCLASSIFIED
		15a. DECLASSIFICATION/DOWNGRADING SCHEDULE
16. DISTRIBUTION STATEMENT (of this Report) Approved for public release, distribution unlimited		
17. DISTRIBUTION STATEMENT (of the abstract entered in Block 20, if different from Report)		
18. SUPPLEMENTARY NOTES		
19. KEY WORDS (Continue on reverse side if necessary and identify by block number) Non-Gaussian Noise, Detection, Probability, Correlation, Beamforming		
20. ABSTRACT (Continue on reverse side if necessary and identify by block number) See Page iii		

DD FORM 1473
1 JAN 73EDITION OF 1 NOV 65 IS OBSOLETE
S/N 0102-014-6601

UNCLASSIFIED

ii SECURITY CLASSIFICATION OF THIS PAGE (When Data Entered)

In Part I, non-coherent detection of narrowband signals in Gaussian-Gaussian mixture noise is considered. The forms of the optimum detectors are found and evaluated for single and multiple observations. These detectors are sensitive to information on the signal and noise parameters. Also evaluated are several suboptimum detectors which perform well under certain conditions without requiring knowledge of signal and noise parameters.

In Part II, a new technique for detecting signals using arrays of sensors is investigated, based on the principles of canonical correlation. The theoretical results indicate that for a sufficient number of sensors, multiple, spatially separate signals, at the same frequency can be individually detected without knowledge of sensor position or using conventional beamforming. If sensor positions are known the algorithm supplies the direction of the signal arrivals. The limited numerical results show that a few sensors can automatically steer on and detect a single signal, but are incapable of resolving multiple signals successfully.

**OCEAN SURVEILLANCE
DETECTION STUDIES
PART I : DETECTION IN
GAUSSIAN MIXTURE NOISE
PART II : AN INVESTIGATION OF
CANONICAL CORRELATION AS AN
AUTOMATIC DETECTION
AND BEAMFORMING TECHNIQUE**

OCTOBER 1985

JC-2034-N

FINAL REPORT

UNDER CONTRACT N00014-85-C-0091

(NR 661-007)

Prepared For:

THE OFFICE OF NAVAL RESEARCH

Statistics and Probability Program

Arlington, Virginia 22217

Prepared By:

J.S.LEE ASSOCIATES, INC.

2001 Jefferson Davis Highway, Suite 601

Arlington, Virginia 22202

Approved for public release ; distribution unlimited

**OCEAN SURVEILLANCE
DETECTION STUDIES
PART I : DETECTION IN
GAUSSIAN MIXTURE NOISE
PART II : AN INVESTIGATION OF
CANONICAL CORRELATION AS AN
AUTOMATIC DETECTION
AND BEAMFORMING TECHNIQUE**

OCTOBER 1985

JC-2034-N

FINAL REPORT

UNDER CONTRACT N00014-85-C-0091

(NR 661-007)

Prepared For:

THE OFFICE OF NAVAL RESEARCH

Statistics and Probability Program

Arlington, Virginia 22217

Prepared By:

J.S.LEE ASSOCIATES, INC.

2001 Jefferson Davis Highway, Suite 601

Arlington, Virginia 22202

Approved for public release ; distribution unlimited

TABLE OF CONTENTS

LIST OF TABLES	ix
LIST OF FIGURES	x
<u>PART I: DETECTION IN GAUSSIAN MIXTURE NOISE</u>	
1.0 INTRODUCTION	1
1.1 BACKGROUND SUMMARY	1
1.1.1 Non-Gaussian Noise Models	2
1.1.2 Non-Gaussian Detector Designs (known signal)	4
1.1.3 Detector Design for Unknown Parameters	12
1.1.4 Intermittent Gaussian Interference as Non-Gaussian Noise	13
1.2 DETECTION THEORY FOR MIXTURE NOISE	16
1.2.1 PDF Formulations and Examples	16
1.2.2 Interpretation of the Mixture pdf	17
1.2.3 Form of Likelihood Ratio	17
1.2.4 Superposition of Detection Measures	19
1.3 TREATMENT OF BANDPASS NON-GAUSSIAN NOISE	21
1.3.1 Independent Quadrature Component Assumption	22
1.3.2 Circularly Symmetric Quadrature Assumption	24
2.0 NONCOHERENT DETECTION IN BANDPASS GAUSSIAN-GAUSSIAN MIXTURE NOISE USING CONVENTIONAL DETECTORS	27
2.1 DETECTION FORMULATIONS	27
2.2 PERFORMANCE OF SINGLE CHANNEL GAUSSIAN DETECTORS IN GAUSSIAN-GAUSSIAN MIXTURE NOISE	30
2.2.1 Forms of the Detectors	30
2.2.2 Single-Sample Detector Performance in Gaussian Mixture Noise	31
2.2.3 Multiple-Sample Detector Performance In Gaussian Mixture Noise	44

	2.2.3.1	Sum and Square Detector	45
	2.2.3.2	Square and Sum Detector	51
2.3		PERFORMANCE OF CORRELATION DETECTOR IN BANDPASS GAUSSIAN- GAUSSIAN MIXTURE NOISE	60
	2.3.1	Analysis for Gaussian mixture noise	63
	2.3.2	Probability integral	64
	2.3.2.1	False Alarm probability	66
	2.3.2.2	Detection performance	66
3.0		OPTIMUM NONCOHERENT DETECTION IN BANDPASS GAUSSIAN-GAUSSIAN MIXTURE NOISE	73
	3.1	NON-GAUSSIAN DETECTOR FORMULATION	73
	3.1.1	Conditional Gaussian Approach	75
	3.1.2	GLR For Constant Signal Phase	77
	3.1.3	GLR For Independent Phase Samples	78
	3.1.4	Example	79
	3.2	EFFECT OF VARIANCE DISTRIBUTION ASSUMPTIONS	81
	3.2.1	Slowly-varying Noise Power	81
	3.2.2	Independent Noise Samples	84
	3.3	PERFORMANCE OF SINGLE-SAMPLE DETECTORS	87
	3.3.1	Form of GLR Detector	87
	3.3.2	False Alarm Probability	96
	3.3.3	Detection Performance	103
	3.3.3.1	Results for known SNR	106
	3.3.3.2	Results for fixed <u>a priori</u> SNR	111
	3.4	PERFORMANCE FOR MULTIPLE SAMPLES	113
	3.4.1	Forms of the GLR for Multiple Samples	114
	3.4.2	Numerical Results for Independent Samples	117

J. S. LEE ASSOCIATES, INC.

4.0	SUBOPTIMUM DETECTORS	120
4.1	APPROXIMATIONS TO THE OPTIMUM DETECTOR	120
4.1.1	Large SNR Approximations	120
4.1.2	Small SNR Approximation and Locally Optimum Detector	121
4.1.3	Performance of the Locally Optimum Detector	122
4.1.3.1	False Alarm Probability	126
4.1.3.2	Detection probability for a single sample	126
4.1.4	Performance of the Weak Signal Locally Optimum Detector for Multiple Samples	136
4.2	SERIAL NORMALIZATION DETECTORS	139
4.2.1	Conceptual formulation	139
4.2.2	Analysis of the detector performance	140
4.2.2.1	False Alarm Probability	141
4.2.2.2	Detection Probability	142
4.2.3	Numerical results	143
4.3	PARALLEL NORMALIZATION DETECTORS	154
4.3.1	Parallel Normalization Concept	157
4.3.2	Distribution of Test Statistic	158
4.3.2.1	False Alarm Probability	159
4.3.2.2	Detection Probability	160
4.3.3	Numerical Results	162
4.4	COMPARISON OF DETECTOR PERFORMANCES	169
<u>APPENDICES TO PART I</u>		
3-A	FORTTRAN program to calculate false alarm and detection probabilities for optimum detector in bandpass Gaussian-Gaussian mixture noise	172
3-B	Numerical Technique for Evaluating Multiple Sample Detector Performance	195
4-A	Development of alternate expression for noncentral F probability integral	198
REFERENCES (PART I).		199

TABLE OF CONTENTS

PART II: AN INVESTIGATION OF CANONICAL CORRELATION AS AN AUTOMATIC DETECTION AND BEAMFORMING TECHNIQUE

1.0	<u>INTRODUCTION</u>	202
1.1	BACKGROUND	202
1.2	MOTIVATION FOR STUDY	205
1.3	REVIEW OF CANONICAL CORRELATION METHOD FOR REAL DATA	207
2.0	<u>EXTENSION OF CANONICAL CORRELATION TO COMPLEX DATA</u>	212
2.1	FORMULATION OF THE PROBLEM	212
2.1.1	Complex representation of the data	214
2.1.2	Correlation measure	215
2.1.3	Maximum correlation	216
2.1.4	Sample solution: single signal	218
2.2	SOLUTION FOR TWO SIGNALS	224
2.2.1	General formulation	224
2.2.2	Formulation for linear array	226
2.2.3	Special case of four sensors	227
3.0	<u>NUMERICAL STUDIES</u>	231
3.1	RESULTS FOR SINGLE SIGNAL	231
3.1.1	Cases without noise correlation	234
3.1.2	Cases with noise correlation	235
3.2	RESULTS FOR TWO SIGNALS	237
3.2.1	Effect of array configuration and size	237
3.2.2	Effect of relative signal strengths and angular spacings	246
3.2.3	Effect of noise correlation	253
3.3	INTERPRETATIONS OF THE NUMERICAL RESULTS.	257
4.0	RECOMMENDATIONS FOR FURTHER STUDY	260
	REFERENCES (PART II)	261

J. S. LEE ASSOCIATES, INC.

LIST OF TABLES - PART I

<u>TABLE</u>		<u>PAGE</u>
2.2-1	FALSE ALARM THRESHOLDS FOR SQUARE-LAW ENVELOPE DETECTOR (SINGLE SAMPLE)	34
2.3-1	FALSE ALARM THRESHOLDS FOR CORRELATION DETECTOR (SINGLE SAMPLE)	67
4.1-1	FALSE ALARM THRESHOLDS FOR LOCALLY OPTIMUM DETECTOR IN BANDPASS GAUSSIAN-GAUSSIAN MIXTURE NOISE	130

LIST OF TABLES - PART II

<u>TABLE</u>		
3-1	PARAMETERS USED IN NUMERICAL STUDIES	233
3-2	CANONICAL CORRELATION RESULTS FOR ONE SIGNAL WHEN INTER-SENSOR NOISE CORRELATION EXISTS	236
3-3	CANONICAL CORRELATION FOR $\rho = 10$, $r = 1$, AND DIFFERENT SENSOR NOISE CORRELATIONS	255
3-4	CANONICAL CORRELATIONS FOR WEAK SIGNALS AND DIFFERENT SENSOR NOISE CORRELATIONS	256

LIST OF FIGURES - PART I

<u>FIGURE</u>		<u>PAGE</u>
1.1-1	LOCALLY OPTIMUM NON-GAUSSIAN DETECTOR STRUCTURE	7
1.1-2	SAMPLE VARIANCE VS RECORD NUMBER, ARTIC UNDER-ICE AMBIENT ACOUSTIC NOISE (FROM [10])	9
1.1-3	SIMPLIFIED NONLINEARITIES FOR LOCALLY OPTIMUM DETECTORS	10
2.2-1	DETECTORS FOR A BANDPASS SIGNAL IN GAUSSIAN NOISE	32
2.2-2	FALSE ALARM PROBABILITY FOR GAUSSIAN DETECTOR IN GAUSSIAN-GAUSSIAN MIXTURE NOISE, MIXTURE PARAMETER $\epsilon = 0.01$	36
2.2-3	FALSE ALARM PROBABILITY FOR GAUSSIAN DETECTOR IN GAUSSIAN-GAUSSIAN MIXTURE NOISE, MIXTURE PARAMETER $\epsilon = 0.1$	37
2.2-4	FALSE ALARM PROBABILITY FOR GAUSSIAN DETECTOR IN GAUSSIAN-GAUSSIAN MIXTURE NOISE, MIXTURE PARAMETER $\epsilon = 0.2$	38
2.2-5	FALSE ALARM PROBABILITY FOR GAUSSIAN DETECTOR IN GAUSSIAN-GAUSSIAN MIXTURE NOISE, MIXTURE PARAMETER $\epsilon = 0.5$	39
2.2-6	RECEIVER OPERATING CHARACTERISTICS FOR GAUSSIAN DETECTOR IN GAUSSIAN-GAUSSIAN MIXTURE NOISE, MIXTURE PARAMETER $\epsilon = 0.01$	40
2.2-7	RECEIVER OPERATING CHARACTERISTICS FOR GAUSSIAN DETECTOR IN GAUSSIAN-GAUSSIAN MIXTURE NOISE, MIXTURE PARAMETER $\epsilon = 0.1$	41
2.2-8	RECEIVER OPERATING CHARACTERISTICS FOR GAUSSIAN DETECTOR IN GAUSSIAN-GAUSSIAN MIXTURE NOISE, MIXTURE PARAMETER $\epsilon = 0.2$	42
2.2-9	RECEIVER OPERATING CHARACTERISTICS FOR GAUSSIAN DETECTOR IN GAUSSIAN-GAUSSIAN MIXTURE NOISE, MIXTURE PARAMETER $\epsilon = 0.5$	43
2.2-10	RECEIVER OPERATING CHARACTERISTICS FOR THE SUM-AND-SQUARE GAUSSIAN DETECTOR IN GAUSSIAN-GAUSSIAN MIXTURE NOISE ($\epsilon = 0.1, V^2 = 100$) WHEN MULTIPLE SAMPLES ARE USED AND THE NOISE POWER IS SLOWLY VARYING	48
2.2-11	RECEIVER OPERATING CHARACTERISTICS FOR THE SUM-AND-SQUARE GAUSSIAN DETECTOR IN GAUSSIAN-GAUSSIAN MIXTURE NOISE ($\epsilon = 0.1, V^2 = 100$) WHEN INDEPENDENT MULTIPLE SAMPLES ARE USED	50
2.2-12	RECEIVER OPERATING CHARACTERISTICS FOR THE SQUARE-AND-SUM GAUSSIAN DETECTOR IN GAUSSIAN-GAUSSIAN MIXTURE NOISE ($\epsilon = 0.1, V^2 = 100$) WHEN MULTIPLE SAMPLES ARE USED AND THE NOISE POWER IS SLOWLY VARYING	54

J. S. LEE ASSOCIATES, INC.

<u>FIGURE</u>	<u>PAGE</u>
2.2-13(a) RECEIVER OPERATING CHARACTERISTICS FOR THE SQUARE AND SUM GAUSSIAN DETECTOR IN GAUSSIAN-GAUSSIAN MIXTURE NOISE ($\epsilon = 0.1$, $V^2 = 100$) WHEN INDEPENDENT MULTIPLE SAMPLES ARE USED, AND $P_{FA} = 10^{-1}$	57
2.2.13(b) RECEIVER OPERATING CHARACTERISTICS FOR THE SQUARE AND SUMS GAUSSIAN DETECTOR IN GAUSSIAN-GAUSSIAN MIXTURE NOISE ($\epsilon = 0.1$, $V^2 = 100$) WHEN INDEPENDENT MULTIPLE SAMPLES ARE USED, AND $P_{FA} = 10^{-2}$	58
2.3-1 BANDPASS CORRELATOR	61
2.3-2 PERFORMANCE OF BANDPASS CORRELATION DETECTOR IN UNCORRELATED GAUSSIAN NOISE	69
2.3.3 PERFORMANCE OF BANDPASS CORRELATION DETECTOR IN GAUSSIAN-GAUSSIAN MIXTURE NOISE ($\epsilon = 0.1$, $V^2 = 10$) FOR DIFFERENT DEGREES OF CORRELATION IN "IMPULSIVE" COMPONENT	70
2.3-4 PERFORMANCE OF BANDPASS CORRELATION DETECTOR IN GAUSSIAN-GAUSSIAN MIXTURE NOISE ($\epsilon = 0.1$, $V^2 = 100$) FOR DIFFERENT DEGREES OF CORRELATION IN "IMPULSIVE" COMPONENT	71
3.2-1 OPTIMUM DETECTOR FOR SINUSOIDAL SIGNAL IN SLOWLY-VARYING GAUSSIAN-GAUSSIAN MIXTURE NOISE	83
3.2-2 OPTIMUM DETECTOR FOR NONCOHERENT SIGNAL AND INDEPENDENT GAUSSIAN-GAUSSIAN MIXTURE NOISE SAMPLES	86
3.3-1 LIKELIHOOD RATIO FOR GAUSSIAN-GAUSSIAN MIXTURE NOISE ($\epsilon = 0.01$, $V^2 = 10$), PARAMETERIZED BY SNR	89
3.3-2 LIKELIHOOD RATIO FOR GAUSSIAN-GAUSSIAN MIXTURE NOISE ($\epsilon = 0.01$, $V^2 = 100$), PARAMETERIZED BY SNR	90
3.3-3 LIKELIHOOD RATIO FOR GAUSSIAN-GAUSSIAN MIXTURE NOISE ($\epsilon = 0.01$, $V^2 = 1000$), PARAMETERIZED BY SNR	91
3.3-4 LIKELIHOOD RATIO FOR GAUSSIAN-GAUSSIAN MIXTURE NOISE ($\epsilon = 0.1$, $V^2 = 10$), PARAMETERIZED BY SNR	92
3.3-5 LIKELIHOOD RATIO FOR GAUSSIAN-GAUSSIAN MIXTURE NOISE ($\epsilon = 0.01$, $V^2 = 10$), PARAMETERIZED BY SNR (DETAIL OF FIGURE 3.3-4)	93
3.3-6 LIKELIHOOD RATIO FOR GAUSSIAN-GAUSSIAN MIXTURE NOISE ($\epsilon = 0.1$, $V^2 = 100$), PARAMETERIZED BY SNR	94
3.3-7 DEPENDENCE OF DETECTOR FALSE ALARM THRESHOLDS ON SHAPE OF LIKELIHOOD RATIO	97

<u>FIGURE</u>	<u>PAGE</u>
3.3-8	CONCEPTUAL IMPLEMENTATION OF GLR DETECTOR 98
3.3-9	FALSE ALARM PROBABILITY FOR OPTIMUM DETECTOR IN GAUSSIAN-GAUSSIAN MIXTURE NOISE ($\epsilon = 0.01$), WITH ASSUMED SNR OF 0.0 dB AND PARAMETRIC IN VARIANCE RATIO 101
3.3-10	FALSE ALARM PROBABILITY FOR OPTIMUM DETECTOR IN GAUSSIAN-GAUSSIAN MIXTURE NOISE ($\epsilon = 0.01$), WITH ASSUMED SNR OF 15 dB AND PARAMETRIC IN VARIANCE RATIO 102
3.3-11	FALSE ALARM PROBABILITY FOR OPTIMUM DETECTOR IN GAUSSIAN-GAUSSIAN MIXTURE NOISE ($\epsilon = 0.1$), WITH ASSUMED SNR OF 0.0 dB AND PARAMETRIC IN VARIANCE RATIO 104
3.3-12	FALSE ALARM PROBABILITY FOR OPTIMUM DETECTOR IN GAUSSIAN-GAUSSIAN MIXTURE NOISE ($\epsilon = 0.1$), WITH ASSUMED SNR OF 15 dB AND PARAMETRIC IN VARIANCE RATIO 105
3.3-13	RECEIVER OPERATING CHARACTERISTICS FOR OPTIMUM DETECTOR IN BANDPASS GAUSSIAN-GAUSSIAN MIXTURE NOISE ($\epsilon = 0.01$), FOR DIFFERENT FALSE ALARM PROBABILITIES AND VARIANCE RATIOS 107
3.3-14	RECEIVER OPERATING CHARACTERISTICS FOR OPTIMUM DETECTOR IN BANDPASS GAUSSIAN-GAUSSIAN MIXTURE NOISE ($\epsilon = 0.1$) FOR DIFFERENT FALSE ALARM PROBABILITIES AND VARIANCE RATIOS 109
3.3-15	RECEIVER OPERATING CHARACTERISTICS FOR OPTIMUM DETECTOR IN BANDPASS GAUSSIAN-GAUSSIAN MIXTURE NOISE ($\epsilon = 0.5$) FOR DIFFERENT FALSE ALARM PROBABILITIES AND VARIANCE RATIOS 110
3.3-16	RECEIVER OPERATING CHARACTERISTICS FOR OPTIMUM DETECTOR IN BANDPASS GAUSSIAN-GAUSSIAN MIXTURE NOISE: EFFECT OF USING FIXED VALUE OF \underline{A} PRIORI SNR 112
3.4-1	PERFORMANCE OF OPTIMUM DETECTOR FOR SIGNALS IN BANDPASS GAUSSIAN-GAUSSIAN MIXTURE NOISE ($\epsilon = 0.1$, $V^2 = 10$) FOR $P_{FA} = 10^{-1}$ AND MULTIPLE, INDEPENDENT SAMPLES 118
3.4-2	PERFORMANCE OF OPTIMUM DETECTOR FOR SIGNALS IN BANDPASS GAUSSIAN-GAUSSIAN MIXTURE NOISE ($\epsilon = 0.1$, $V^2 = 100$) FOR $P_{FA} = 10^{-1}$ AND MULTIPLE, INDEPENDENT SAMPLES 119
4.1-1	LOCALLY OPTIMUM DETECTOR CHARACTERISTIC FOR BANDPASS GAUSSIAN-GAUSSIAN MIXTURE NOISE ($\epsilon = 0.01$) FOR SEVERAL VALUES OF VARIANCE RATIO 123
4.1-2	LOCALLY OPTIMUM DETECTOR CHARACTERISTIC FOR BANDPASS GAUSSIAN-GAUSSIAN MIXTURE NOISE ($\epsilon = 0.1$) FOR SEVERAL VALUES OF VARIANCE RATIO 124
4.1-3	LOCALLY OPTIMUM DETECTOR CHARACTERISTIC FOR BANDPASS GAUSSIAN-GAUSSIAN MIXTURE NOISE ($\epsilon = 0.5$) FOR SEVERAL VALUES OF VARIANCE RATIO 125

<u>FIGURE</u>	<u>PAGE</u>
4.1-4 FALSE ALARM PROBABILITY VS. FIRST THRESHOLD FOR LOCALLY OPTIMUM DETECTOR IN BANDPASS GAUSSIAN-GAUSSIAN MIXTURE NOISE ($\epsilon = 0.01$) .	127
4.1-5 FALSE ALARM PROBABILITY VS. FIRST THRESHOLD FOR LOCALLY OPTIMUM DETECTOR IN BANDPASS GAUSSIAN-GAUSSIAN MIXTURE NOISE ($\epsilon = 0.01$) .	128
4.1-6 FALSE ALARM PROBABILITY VS. FIRST THRESHOLD FOR LOCALLY OPTIMUM DETECTOR IN BANDPASS GAUSSIAN-GAUSSIAN MIXTURE NOISE ($\epsilon = 0.5$) .	129
4.1-7 RECEIVER OPERATING CHARACTERISTICS FOR LOCALLY OPTIMUM DETECTOR IN BANDPASS GAUSSIAN-GAUSSIAN MIXTURE NOISE ($\epsilon = 0.01$)	132
4.1-8 RECEIVER OPERATING CHARACTERISTICS FOR LOCALLY OPTIMUM DETECTOR IN BANDPASS GAUSSIAN-GAUSSIAN MIXTURE NOISE ($\epsilon = 0.1$)	133
4.1-9 RECEIVER OPERATING CHARACTERISTICS FOR LOCALLY OPTIMUM DETECTOR IN BANDPASS GAUSSIAN-GAUSSIAN MIXTURE NOISE- ($\epsilon = 0.5$)	134
4.1-10 RECEIVER OPERATING CHARACTERISTICS FOR LOCALLY OPTIMUM DETECTOR IN BANDPASS GAUSSIAN-GAUSSIAN MIXTURE NOISE FOR $\epsilon = 0.1$, $V^2 = 10$, AND $P_{FA} = 10^{-1}$	135
4.1-11 MULTIPLE-SAMPLE PERFORMANCE OF LOCALLY OPTIMUM DETECTOR FOR BANDPASS SIGNALS IN GAUSSIAN-GAUSSIAN MIXTURE NOISE, FOR $\epsilon = 0.1$, $V^2 = 100$ AND $P_{FA} = 10^{-1}$	137
4.1-12 MULTIPLE-SAMPLE PERFORMANCE OF LOCALLY OPTIMUM DETECTOR FOR BANDPASS SIGNALS IN GAUSSIAN-GAUSSIAN MIXTURE NOISE, FOR $\epsilon = 0.1$, $V^2 = 100$, AND $P_{FA} = 10^{-2}$	138
4.2-1 PERFORMANCE OF SERIAL NORMALIZATION DETECTOR IN BANDPASS GAUSSIAN-GAUSSIAN MIXTURE NOISE ($\epsilon = 0.01$) FOR TWO TIME SAMPLES .	145
4.2-2 PERFORMANCE OF SERIAL NORMALIZATION DETECTOR IN BANDPASS GAUSSIAN-GAUSSIAN MIXTURE NOISE ($\epsilon = 0.1$) FOR TWO TIME SAMPLES .	146
4.2-3 PERFORMANCE OF SERIAL NORMALIZATION DETECTOR IN BANDPASS GAUSSIAN-GAUSSIAN MIXTURE NOISE ($\epsilon = 0.5$) FOR TWO TIME SAMPLES .	147
4.2-4 PERFORMANCE OF SERIAL NORMALIZATION DETECTOR IN BANDPASS GAUSSIAN-GAUSSIAN MIXTURE NOISE ($\epsilon = 0.01$) FOR THREE TIME SAMPLES	148
4.2-5 PERFORMANCE OF SERIAL NORMALIZATION DETECTOR IN BANDPASS GAUSSIAN-GAUSSIAN MIXTURE NOISE ($\epsilon = 0.1$) FOR THREE TIME SAMPLES	149

J. S. LEE ASSOCIATES, INC.

<u>FIGURE</u>		<u>PAGE</u>
4.2-6	PERFORMANCE OF SERIAL NORMALIZATION DETECTOR IN BANDPASS GAUSSIAN-GAUSSIAN MIXTURE NOISE ($\epsilon = 0.5$) FOR THREE TIME SAMPLES .	150
4.2-7	PERFORMANCE OF SERIAL NORMALIZATION DETECTOR IN BANDPASS GAUSSIAN-GAUSSIAN MIXTURE NOISE ($\epsilon = 0.01$) FOR FOUR TIME SAMPLES .	151
4.2-8	PERFORMANCE OF SERIAL NORMALIZATION DETECTOR IN BANDPASS GAUSSIAN-GAUSSIAN MIXTURE NOISE ($\epsilon = 0.1$) FOR FOUR TIME SAMPLES .	152
4.2-9	PERFORMANCE OF SERIAL NORMALIZATION DETECTOR IN BANDPASS GAUSSIAN-GAUSSIAN MIXTURE NOISE ($\epsilon = 0.5$) FOR FOUR TIME SAMPLES .	153
4.3-1	DETECTOR FOR WEAK SIGNAL IN LOWPASS, SWITCHED BURST NOISE	155
4.3-2	SWITCHED GAIN DETECTOR FOR BANDPASS GAUSSIAN-GAUSSIAN MIXTURE NOISE	156
4.3-3	PERFORMANCE OF TWO-CHANNEL PARALLEL NORMALIZATION DETECTOR IN BANDPASS GAUSSIAN-GAUSSIAN MIXTURE NOISE ($\epsilon = 0.01$) FOR A SINGLE TIME SAMPLE	163
4.3-4	PERFORMANCE OF TWO-CHANNEL PERALLEL NORMALIZATION DETECTOR IN BANDPASS GAUSSIAN-GAUSSIAN MIXTURE NOISE ($\epsilon = 0.1$) FOR A SINGLE TIME SAMPLE	164
4.3-5	PERFORMANCE OF TWO-CHANNEL PARALLEL NORMALIZATION DETECTOR IN BANDPASS GAUSSIAN-GAUSSIAN MIXTURE NOISE ($\epsilon = 0.5$) FOR A SINGLE TIME SAMPLE	165
4.3-6	PERFORMANCE OF TWO-CHANNEL PARALLEL NORMALIZATION DETECTOR IN BANDPASS GAUSSIAN-GAUSSIAN MIXTURE NOISE ($\epsilon = 0.01$) FOR TWO TIME SAMPLES	166
4.3-7	PERFORMANCE OF TWO-CHANNEL PARALLEL NORMALIZATION DETECTOR IN BANDPASS GAUSSIAN-GAUSSIAN MIXTURE NOISE ($\epsilon = 0.1$) FOR TWO TIME SAMPLES	167
4.3-8	PERFORMANCE OF TWO-CHANNEL PARALLEL NORMALIZATION DETECTOR IN BANDPASS GAUSSIAN-GAUSSIAN MIXTURE NOISE ($\epsilon = 0.5$) FOR TWO TIME SAMPLES	168
4.4-1	COMPARISON OF SUBOPTIMUM DETECTOR PERFORMANCES IN BANDPASS GAUSSIAN-GAUSSIAN MIXTURE NOISE ($\epsilon = 0.1, V^2 = 100$) FOR $P_{FA} = 0.1$ AND $K = 2$ SAMPLES	170
4.4-2	COMPARISON OF SUBOPTIMUM DETECTOR PERFORMANCES IN BANDPASS GAUSSIAN-GAUSSIAN MIXTURE NOISE ($\epsilon = 0.1, V^2 = 100$) FOR $P_{FA} = 0.01$ AND $K = 2$ SAMPLES	171

LIST OF FIGURES - PART II

<u>FIGURE</u>		<u>PAGE</u>
1-1	ARRAY SUM CONCEPT	203
1-2	CORRELATION PROCESSING OF SENSORS AND OF ARRAYS	204
2-1	ILLUSTRATED SENSOR PLACEMENT AND RECEIVED SIGNAL ARRIVALS	213
2-2	LINEAR ARRAY CONFIGURATION	228
3-1	ARRAY CONFIGURATIONS USED IN NUMERICAL STUDIES	232
3-2	EFFECT OF ARRAY CONFIGURATION ON CANONICAL CORRELATIONS VS. 10 dB SIGNAL BEARING WHEN A SECOND, 0 dB SIGNAL IS PRESENT AT A BEARING OF $3\pi/4$ ($d = \lambda/4$)	238
3-3	EFFECT OF ARRAY CONFIGURATION ON AGREEMENT OF STEERING VECTOR SOLUTION WITH 10 dB SIGNAL DELAY VECTOR WHEN A SECOND, 0 dB SIGNAL IS PRESENT AT A BEARING OF $3\pi/4$ ($d = \lambda/4$)	239
3-4	EFFECT OF CROSSED PAIR ARRAY SIZE (d/λ) ON CANONICAL CORRELATIONS VS. 10 dB SIGNAL BEARING WHEN A SECOND 0 dB SIGNAL IS PRESENT AT A BEARING OF $3\pi/4$	241
3-5	EFFECT OF CROSSED PAIR ARRAY SIZE (d/λ) ON AGREEMENT OF STEERING VECTOR SOLUTION WITH 10 dB SIGNAL DELAY VECTOR WHEN A SECOND, 0 dB SIGNAL IS PRESENT AT A BEARING OF $3\pi/4$	242
3-6	EFFECT OF LINEAR ARRAY SIZE (d/λ) ON CANONICAL CORRELATIONS VS. 10 dB SIGNAL BEARING WHEN A SECOND, 0 dB SIGNAL IS PRESENT AT $-\pi/2$ BEARING RELATIVE TO FIRST SIGNAL	244
3-7	EFFECT OF LINEAR ARRAY SIZE (d/λ) ON AGREEMENT OF STEERING VECTOR SOLUTION WITH 10 dB SIGNAL DELAY VECTOR WHEN A SECOND, 0 dB SIGNAL IS PRESENT AT $-\pi/2$ BEARING RELATIVE TO FIRST SIGNAL	245
3-8	EFFECT OF ARRAY CONFIGURATION ON CANONICAL CORRELATION VS. 10 dB SIGNAL BEARING WHEN A SECOND, 0 dB SIGNAL IS PRESENT AT A BEARING OF $3\pi/4$ ($d = 0.3\lambda/4$)	247

<u>FIGURE</u>	<u>PAGE</u>
3-9	EFFECT OF ARRAY CONFIGURATION ON AGREEMENT OF STEERING VECTOR SOLUTION WITH 10 dB SIGNAL DELAY VECTOR WHEN A SECOND, 0 dB SIGNAL IS PRESENT AT A BEARING OF $3\pi/4$ ($d = 0.3\lambda/4$) 248
3-10	EFFECT OF SECOND SIGNAL STRENGTH ON CANONICAL CORRELATION SOLUTIONS VS. 10 dB SIGNAL BEARING WHEN THE SECOND SIGNAL IS PRESENT AT $-\pi/2$ BEARING RELATIVE TO FIRST SIGNAL 249
3-11	EFFECT OF SECOND SIGNAL STRENGTH ON AGREEMENT OF STEERING VECTOR SOLUTION WITH 10 dB SIGNAL DELAY VECTOR WHEN THE SECOND SIGNAL IS PRESENT AT $-\pi/2$ BEARING RELATIVE TO FIRST SIGNAL 250
3-12	EFFECT OF SECOND SIGNAL STRENGTH ON AGREEMENT OF STEERING VECTOR SOLUTION WITH 10 dB SIGNAL DELAY VECTOR WHEN THE SECOND SIGNAL IS PRESENT AT $-\pi/4$ BEARING RELATIVE TO FIRST SIGNAL 251
3-13	EFFECT OF SECOND SIGNAL STRENGTH ON AGREEMENT OF STEERING VECTOR SOLUTION WITH 10 dB SIGNAL DELAY VECTOR WHEN THE SECOND SIGNAL IS PRESENT AT $-\pi/4$ BEARING RELATIVE TO FIRST SIGNAL (EXPANDED SCALE) 252
3-14	EFFECT OF SENSOR NOISE CORRELATION ON AGREEMENT OF VECTOR SOLUTION WITH DELAY VECTOR FOR ONE SIGNAL WHEN A SECOND SIGNAL IS PRESENT AT A BEARING OF $3\pi/4$ (LINEAR ARRAY) 254

PART I: DETECTION IN GAUSSIAN MIXTURE NOISE

1.0 INTRODUCTION

1.1 BACKGROUND SUMMARY

In many applications, the passive detection of signals in noise is not adequately performed if the detector design is based on Gaussian noise assumptions. Particularly in the LF and VLF portions of the electromagnetic spectrum and in the acoustic environment, the ambient noise observed by the receiver contains impulsive components which cause the noise probability distribution to depart from the Gaussian model. As a result, the sensitivity of a Gaussian-based detector is degraded for given false alarm probability. Therefore, much effort has been focused on realizing improved detector and receiver designs that are matched to realistic noise distributions, using measured values of noise parameters.

The detector design problem is complicated by the fact that the parameters describing the noise distribution are difficult to measure and vary with time. Since it is not practical in these situations to employ theoretically "optimum" detectors which rely on a priori knowledge of noise parameters, current research is aimed at discovering effective detection procedures which are "robust", or relatively insensitive to uncertainties in the values of distributional parameters, if not "nonparametric", or "distribution-free". Also of interest are realistic noise models whose parameters are easily measured physical quantities.

Noise due to man-made sources can degrade detection and communication performance in every portion of the spectrum. Impulsive interference

due to multiple-access communications emissions, for example, results in a non-Gaussian received noise distribution. The threat of intentional interference or jamming has forced system designers to take this possibility into account by modifying their detection procedures. Without formulating the problem as a non-Gaussian noise problem per se, many heuristic receivers have been developed to make the detection and communication systems operate satisfactorily whether jammed or not jammed.

The success of certain heuristic detectors in adapting to non-Gaussian noise implies that their designers have made correct assumptions concerning the noise process. For the most part, these practical detectors are based on recognizing the "short term" or time varying nature of the noise, rather than its "long term" or marginal (unconditional) distribution. Therefore, it seems likely that modelling non-Gaussian noise as nonstationary noise would yield better results than the present theoretical emphasis on marginal non-Gaussian noise models.

In order to show the motivation for our efforts, in the following paragraphs we give further background on non-Gaussian modelling, on receiver design, and on jamming interference.

1.1.1 Non-Gaussian Noise Models

The modelling effort evidenced in the current detection literature has been approached from two directions: empirical and theoretical.

A good example of the empirical noise modelling approach is the work reported by Fennick [1], who gathered statistics of telecommunication channels and postulated on the basis of measured pdf's that the underlying distribution could be characterized by the sum of a Gaussian pdf and an exponential term:

$$\begin{aligned} \text{pdf} &= \text{Gaussian} + \text{exponential} \\ &= a \exp(-x^2/2\sigma^2) + b \exp(-c|x|). \end{aligned} \quad (1.1-1)$$

In this manner, the "larger than Gaussian" tails of the observed statistics were accounted for.

The theoretical approach, one working from the physics of the situation, can be exemplified by the work of Hall [2], who supposed that the received noise is a narrowband Gaussian process multiplied by a time-varying weighting factor. Hall's pdf was found to take the form

$$\text{pdf} = \text{const.} (x^2 + a^2)^{-(m+1)/2}. \quad (1.1-2)$$

Good fits to data were reported, using certain values of the parameters. However, the parameters themselves were not identified with the physical processes because of simplifications chosen to make the mathematics tractable.

Middleton [3, 4, 5] asserts that he has found tractable pdf's that fit known data well by approaching the problem from the physical/theoretical point of view, and that the parameters of the distribution retain physical interpretations (therefore being suitable for measurement). Moreover, the "Class A, B, and C" noise models Middleton has developed are claimed to be "canonical", or capable of generating the wide variety of observable statistics while keeping the same functional form. For example, the pdf for Middleton's Class A noise, for which the noise bandwidth is said to be less than that of the desired signal, takes the form of an infinite sum of weighted Gaussian pdf's with increasing variances:

$$\text{pdf} = \frac{1}{\sqrt{2\pi}} e^{-A} \sum_{m=0}^{\infty} \frac{A^m}{m! \sigma_m} \exp(-x^2/2\sigma_m^2), \quad \sigma_m^2 = \frac{m + A\Gamma}{A(1 + \Gamma)}, \quad (1.1-3)$$

where Γ is the ratio of the power in the Gaussian portion of the interference to that in the impulsive (Poisson) component, and A is called the "impulsive index," a kind of counting function for the impulsive interference and related to the amount of overlap in individual interference waveforms (large A corresponds to a trend toward Gaussian). An excellent approximation for small values of A is given by Middleton [5] and by Vastola [16] as

$$\text{pdf} = a \exp(-x^2/2\sigma_1^2) + b \exp(-x^2/2\sigma_2^2), \quad (1.1-4)$$

or the weighted sum of two Gaussian density functions. Although we have simplified the notation somewhat in this presentation, each of the parameters is given a physical, measurable interpretation by Middleton.

1.1.2 Non-Gaussian Detector Designs (known signal)

If N independent samples $\{x_i\}$ of a received waveform $x(t)$ are to be tested as to whether $x(t)$ contains noise only or known signal $s(t)$ plus noise, the log-likelihood ratio takes the form

$$\log \Lambda(x_1, x_2, \dots, x_N) = \sum_{i=1}^N \log \left[\text{pdf}(x_i | s_i) / \text{pdf}(x_i | s_i=0) \right] \underset{n}{\overset{s+n}{>}} \text{threshold} \quad (1.1-5)$$

where $x_i \equiv x(t_i)$ and $s_i \equiv s(t_i)$. For stationary Gaussian noise the resulting statistical test is the linear detector

$$\sum_{i=1}^N x_i s_i \underset{n}{\overset{s+n}{>}} \text{threshold}; \quad (1.1-6)$$

the receiver needs only to perform a weighted sum (filtering) of the input data and to compare the value of that sum to a threshold value.

If the noise is not Gaussian, the likelihood function may be difficult to interpret in terms of a discrete component or analog implementation, depending on the form of the noise pdf. For Hall's pdf, (1.1.2), the closed form permits solving directly for the optimum receiver structure as

$$\sum_{i=1}^N \left\{ \log \left[(x_i - s_i)^2 + a^2 \right] - \log \left[x_i^2 + a^2 \right] \right\} \underset{s+n}{\gtrsim} \text{threshold} \quad (1.1.7)$$

where a is the parameter shown in (1.1-2). For pdf's which are not closed forms, implementation may be performed using digital processing; however, analysis may require making some approximations. For example, even for the two-term approximation to Middleton's pdf given by (1.1-4), the likelihood ratio is

$$\log \Lambda = \sum_{i=1}^N \log \left\{ \frac{a \exp \left[- (x_i - s_i)^2 / 2\sigma_1^2 \right] + b \exp \left[- (x_i - s_i)^2 / 2\sigma_2^2 \right]}{a \exp(-x_i^2 / 2\sigma_1^2) + b \exp(-x_i^2 / 2\sigma_2^2)} \right\}. \quad (1.1-8)$$

A way out of the analytical difficulty which has been used extensively is to treat the special case of weak, or "threshold" signals and therefore to obtain what are termed locally optimal or threshold receivers. How this approach works may be explained as follows: since the signal is "small", to a good degree of approximation the pdf may be written as the pdf for no signal plus a first order term in a Taylor series expansion [5, 6], giving

$$\Lambda_i = \frac{p(x_i - s_i)}{p(x_i - 0)} \approx 1 - \frac{s_i p'(x_i)}{p(x_i)} = 1 - s_i \frac{a}{\partial x_i} \left[\log p(x_i) \right]. \quad (1.1-9)$$

This results in the statistical test

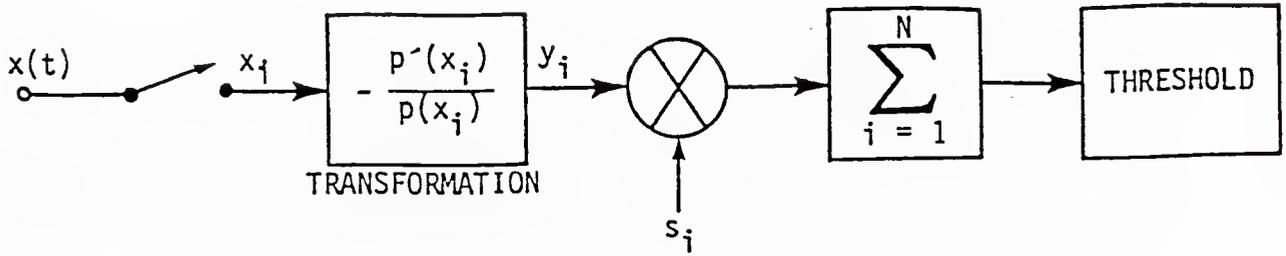
$$\sum_{i=1}^N s_i y_i = \sum_{i=1}^N s_i g(x_i) \geq \text{threshold} \equiv n, \quad (1.1-10)$$

which resembles the "linear" test (1.1-6) after the data has been transformed by the nonlinearity

$$g(x_i) = - \frac{p'(x_i)}{p(x_i)} = y_i. \quad (1.1-11)$$

The form of this nonlinearity is highly sensitive to the parameters and functional form of the assumed pdf, as illustrated in Figure 1.1-1. In that figure, we observe that for Gaussian noise, $g(x)$ is simply a linear dependence, whereas for the other assumed distributions shown the transformation can be almost any form, depending on the shape and parameters of the noise pdf.

The form of the nonlinearity requires either knowledge of adaptation to the noise conditions which exist. Therefore, Middleton [5, 8] stresses the correspondence between the parameters of his pdf model and measurable quantities. The ability of the receiver to perform satisfactory adaptation to time-varying noise parameters can make the difference between success of failure for practical non-Gaussian detectors [9]. Martinez and



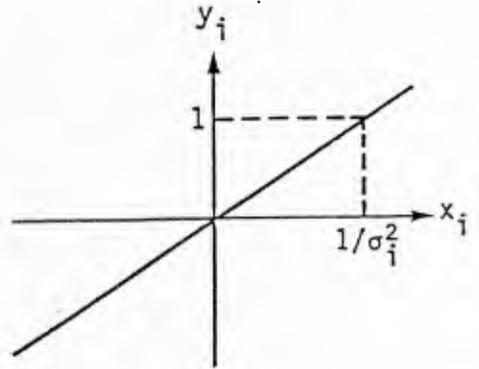
NOISE DENSITY

Gaussian

$$p(x_i) = K \exp\left\{-x_i^2/2\sigma_i^2\right\}$$

TRANSFORMATION

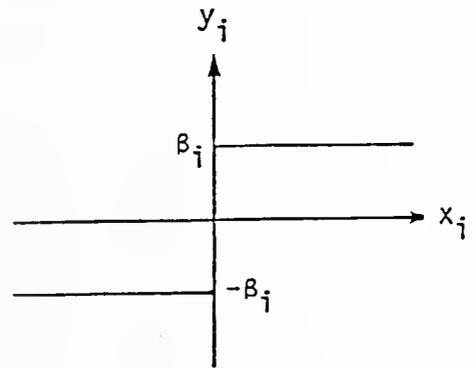
$$x_i/\sigma_i^2$$



DOUBLE EXPONENTIAL

$$p(x_i) = k \exp\left\{-\beta_i |x_i|\right\}$$

$$\beta_i \text{sgn}(x_i)$$



BISTATIC WAVEFORM IN GAUSSIAN

$$p(x_i) = K\{e_1(x_i) + e_2(x_i)\}$$

$$e_1 = \exp\left\{-(x_i-A)^2/2\sigma_i^2\right\}$$

$$e_2 = \exp\left\{-(x_i+A)^2/2\sigma_i^2\right\}$$

$$\frac{1}{\sigma_i^2} \frac{(x_i-A)e_1 + (x_i+A)e_2}{e_1 + e_2}$$

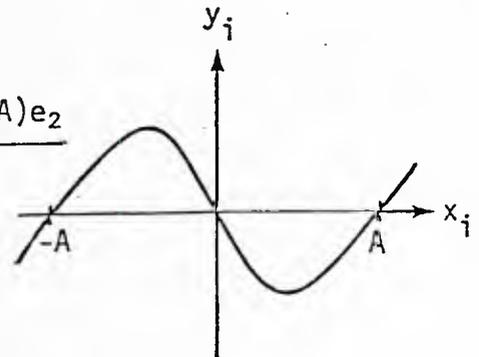


FIGURE 1.1-1. LOCALLY OPTIMUM NON-GAUSSIAN DETECTOR STRUCTURE

Thomas [10], for example, report that sampled Arctic under-ice ambient acoustic noise data reveal a nonstationary process with impulsive components; this behavior is well illustrated by the time history of sample variance shown in Figure 1.1-2. Because the impulsive components occur relatively infrequently, large sample sizes are required to determine accurate estimates of impulsive parameters. This requirement conflicts with the need to take time-varying noise properties into account over a smaller sample size.

Since the form of the nonlinearity for locally optimum detection is often complicated as well as sensitive to the accuracy of measured noise distribution parameters, investigations have been made to determine whether simplified or approximate versions of the transformations, which use fewer parameters, can be used with success. For example, Miller and Thomas [11] report that relatively simple piecewise linear approximations can give nearly as good asymptotic performance (relative to a Gaussian detector) as the locally optimal nonlinearity. Among the simplified nonlinearities they studied were the "amplifier-limiter" (also known as a "clipper" or "soft limiter"), the "hard limiter", and the "noise blanker" approximations to the optimum nonlinearity for detection in a Gaussian-Laplace mixture noise distribution. These transformations are shown in Figure 1.1-3.

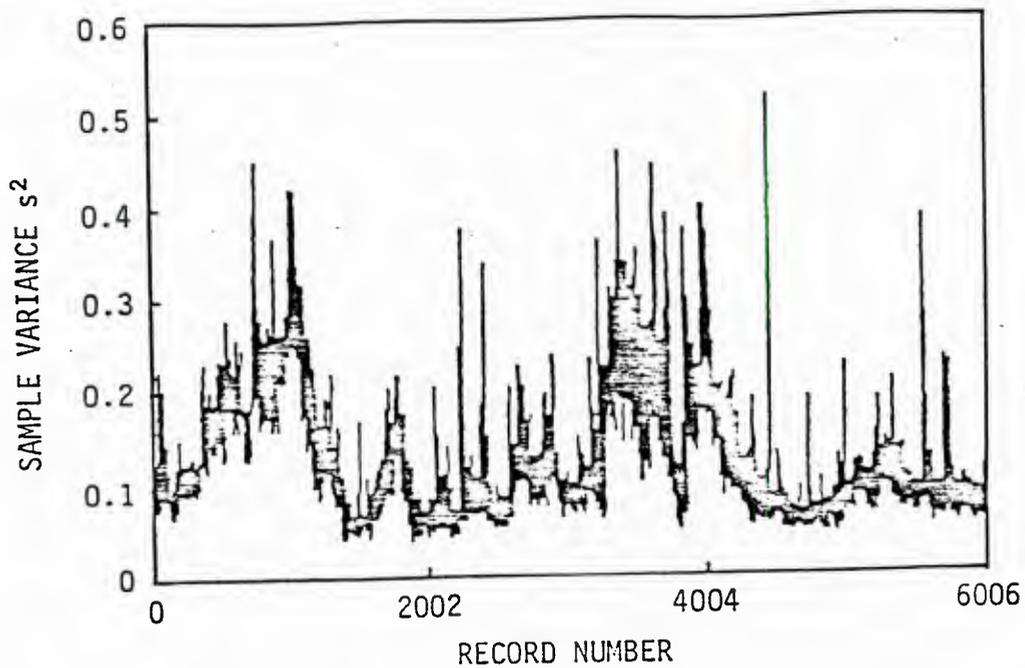
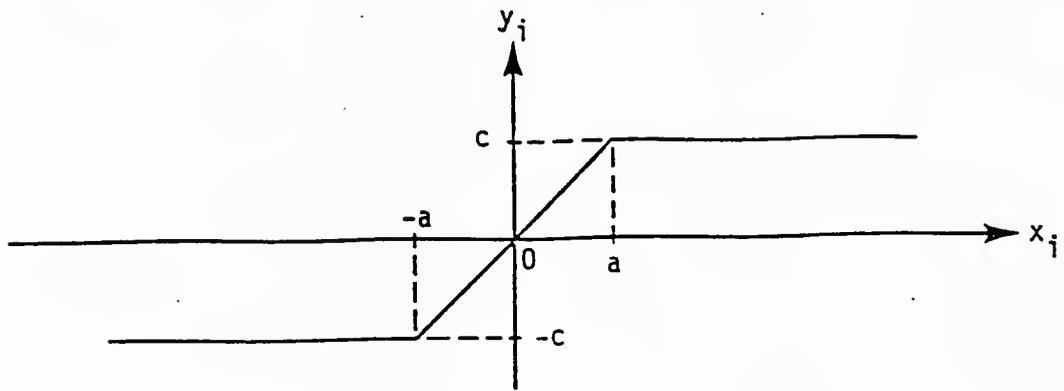
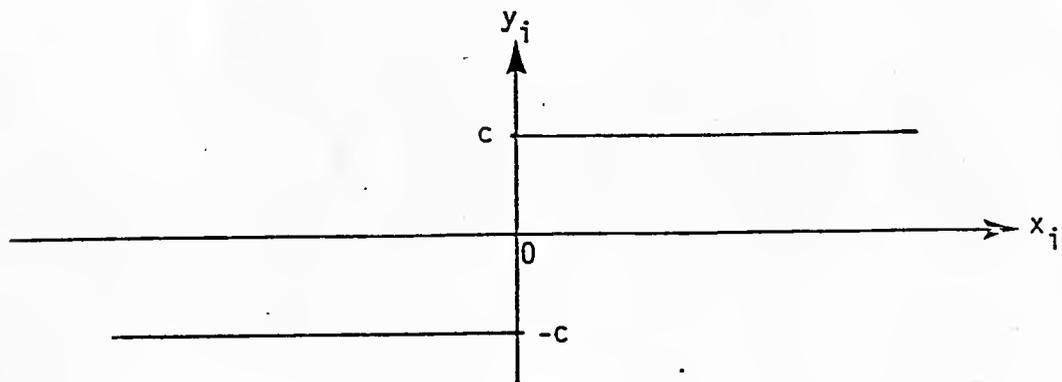


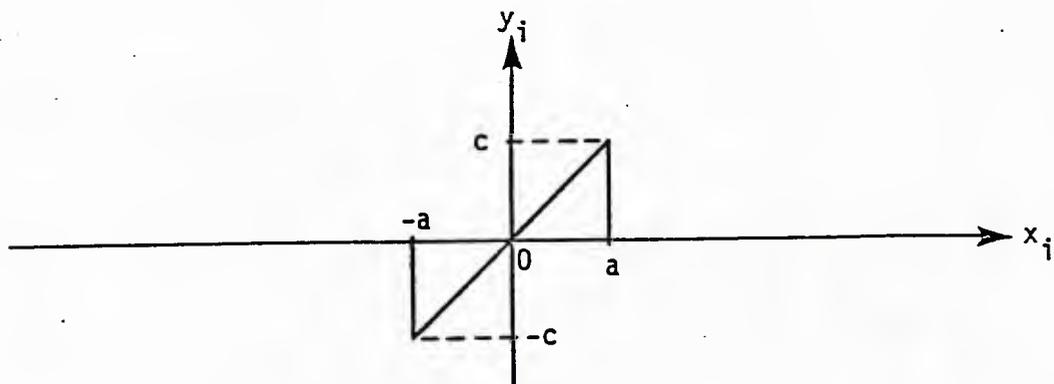
FIGURE 1.1-2. SAMPLE VARIANCE VS RECORD NUMBER,
ARTIC UNDER-ICE AMBIENT ACOUSTIC NOISE
(FROM [10])



(a) Amplifier-limiter



(b) Hard Limiter



(c) Noise Blanker

FIGURE 1.1-3. SIMPLIFIED NONLINEARITIES FOR LOCALLY OPTIMUM DETECTORS

We note that in equation (1.1-9) above, if the true signal values are the same ($s_i = s, \forall i$), the receiver design becomes

$$s \sum_{i=1}^N g(x_i) \geq n \quad \text{or} \quad \sum_{i=1}^N g(x_i) \geq \frac{n}{s} = n' \quad (1.1-12)$$

The receiver does not use any information on the value of the (constant) signal, since the threshold n' is to be determined by false alarm probability requirements. Therefore, an advantage of threshold or weak signal locally optimum detector designs is that they do not require prior knowledge of the signal parameters if they are "slowly varying" over the N samples of the input..

In general, the log-likelihood ratio for known signal values $\{s_i\}$ depends strongly on these values. Therefore, a penalty in loss of performance can be expected if the actual received signal values differ (for example, due to loss of synchronization). This statement is true even for a constant signal ($s_i=s$) except for the special case of Gaussian noise, as seen from equation (1.1-6), so we expect to see, for example, close agreement of detection performance between locally optimum and optimum detectors when the signal is actually weak, and a loss in the locally optimum detector's performance relative to the optimum when the signal is actually strong.

For a single sample ($N=1$), all distributions of transformed variables giving likelihood ratios which are monotonic yield the same detection performance, since then

$$\Pr \{ \Lambda(x_1) \geq n \} = \Pr \{ x_1 \geq n' \} \quad (1.1-13)$$

1.1.3 Detector Design for Unknown Parameters.

When either signal or noise parameters (or both) are unknown, we can choose to use estimated values of these parameters, risking a loss in detection performance if the actual values differ significantly from those assumed. However, if the distributions of the unknown parameters are known, decision theory for composite hypothesis testing [19] requires that we use the unconditional likelihood ratio (LR) test

$$\Lambda(X) = \frac{\int d\theta_1 p(X|\theta_1, H_1) p(\theta_1|H_1)}{\int d\theta_0 p(X|\theta_0, H_0) p(\theta_0|H_0)} \quad (1.1-14)$$

where the data X and the parameters θ_0 and θ_1 can be vectors or sets.

If the distributions for the unknown parameters are not available, or if they are considered "unknown nonrandom", the best test procedure is not clearly specified by decision theory. However, since the optimum performance would be achieved if somehow a perfect measurement were made of the unknown parameters, it is reasonable to use the generalized likelihood ratio (GLR)

$$\Lambda_g(X) = \frac{\max_{\theta_1} p(X|\theta_1, H_1)}{\max_{\theta_0} p(X|\theta_0, H_0)} \quad (1.1-15)$$

For example, testing the hypothesis $H_0: x_i = G(0, \sigma^2)$ against $H_1: x_i = G(m, \sigma^2)$, where neither the mean m nor the variance σ^2 is known, results in the test [20]

$$\frac{n \left(\frac{1}{n} \sum_{i=1}^N x_i \right)^2}{\sum_{i=1}^N \left[x_i - \frac{1}{n} \sum_{k=1}^N x_k \right]^2} = \frac{n(\bar{x})^2}{\sum_{i=1}^N (x_i - \bar{x})^2} \geq n, \quad (1.1-16)$$

which is equivalent to comparing the ratio of estimates $(\hat{m})^2/\hat{\sigma}^2$ to a threshold. (If m is the value of a constant "signal", then the ratio is a form of estimated signal-to-noise ratio.)

1.1.4 Intermittent Gaussian Interference as Non-Gaussian Noise

An understanding of non-Gaussian noise as arising from intermittent or time-varying noise is evident in the present communications literature, which reflects much concern over the disruption of communications and/or detections due to intentional interference or jamming. In frequency hopping communications systems, for example, it has been shown that for limited jammer power an effective jamming strategy is one for which the jamming is present in the dehopped bandwidth some fraction of the time (γ), rather than continuously. Thus the marginal pdf of the received noise at a given time, assuming Gaussian noise jamming, is given by

$$\sqrt{2\pi} p(x) = (1-\gamma) \frac{1}{\sigma_N} \exp(-x^2/2\sigma_N^2) + \gamma \frac{1}{\sqrt{\sigma_N^2 + \sigma_J^2}} \exp\left[-x^2/2(\sigma_N^2 + \sigma_J^2)\right],$$

$$(\sigma_N^2 = \text{background noise power, } \sigma_J^2 = \text{jamming noise power}) \quad (1.1-17)$$

which has the same form as (1.1-4). However, this Gaussian-Gaussian mixture type of non-Gaussian noise in these jamming situations is the result of the nonstationary or time-varying properties of the total noise, which is Gaussian at a given time. That is,

$$p(x_t) = \frac{1}{\sqrt{2\pi} \sigma_t} \exp\left\{-x_t^2/2\sigma_t^2\right\} \quad (1.1-18a)$$

where

$$\sigma_t^2 = \begin{cases} \sigma_N^2 & \text{with probability } 1-\gamma \\ \sigma_N^2 + \sigma_J^2 & \text{with probability } \gamma. \end{cases} \quad (1-1.18b)$$

Thus we observe that in this case a correspondence or analogy exists between "non-Gaussian" noise and "nonstationary Gaussian" noise. For example, the joint pdf of L independent samples of noise from the distribution given by (1.1-4) is, using $a=(1-\gamma)/\sigma_1\sqrt{2\pi}$ and $b=\gamma/\sigma_2\sqrt{2\pi}$,

$$\begin{aligned} p_L(\underline{x}) &= \prod_{k=1}^L \left[(1-\gamma) p_G(x_k; \sigma_1) + \gamma p_G(x_k; \sigma_2) \right] \\ &= \sum_{\ell=0}^L \binom{L}{\ell} \gamma^\ell (1-\gamma)^{L-\ell} \frac{1}{(2\pi\sigma_1^2)^{(L-\ell)/2}} \\ &\quad \cdot \exp\left\{-\frac{1}{2\sigma_1^2} \sum_{k_1=1}^{L-\ell} x_{k_1}^2\right\} \cdot \frac{1}{(2\pi\sigma_2^2)^{\ell/2}} \\ &\quad \cdot \exp\left\{-\frac{1}{2\sigma_2^2} \sum_{k_2=1}^{\ell} x_{k_2}^2\right\} \cdot \end{aligned} \quad (1.1-19)$$

This may be written

$$p_L(\underline{x}) = \sum_{\ell=0}^L p_\ell p_L(\underline{x}|\ell), \quad (1.1-20)$$

where p_ℓ may be interpreted as the probability that " ℓ of the noise samples have variance σ_2^2 and $L-\ell$ have variance σ_1^2 ", and $p_L(\underline{x}|\ell)$ is the joint density of the samples conditioned on this event.

With this viewpoint we can interpret Middleton's Class A pdf (1.1-3) as

$$p(x_t) = p_G(x_t; \sigma_t^2) \quad \text{where } \sigma_t^2 = \sigma_m^2 \text{ with probability}$$

$$p_m = e^{-A} A^m/m!, \quad m = 1, 2, \dots; \quad (1.1-21)$$

that is, conditionally the noise is Gaussian, with the variance selected randomly from a discrete set of values.

1.2 DETECTION THEORY FOR MIXTURE NOISE

1.2.1 PDF Formulations and Examples

We consider the situation in which the noise is modelled as having the mixture probability density function (pdf)

$$p_n(x) = \sum_m \kappa_m f_m(x), \quad \sum_m \kappa_m = 1 \quad (1.2-1)$$

where each function $f_m(x)$ is a pdf weighted by a positive constant κ_m , $0 < \kappa_m < 1$. The argument x may be considered a scalar for lowpass noise or complex (two-dimensional) for bandpass noise. For example, the model proposed by Middleton [3] has the form in which each pdf $f_m(x)$ is Gaussian:

$$p_n(x) = \sum_{m=0}^{\infty} \frac{e^{-\lambda} \lambda^m}{m!} f_G(x; \sigma_m), \quad f_G(x; \sigma) = \frac{e^{-x^2/2\sigma^2}}{\sigma\sqrt{2\pi}} \quad (1.2-2)$$

Often two terms are used in the mixture model, for example, the Gaussian-Gaussian mixture

$$p_n(x) = (1-\epsilon) f_G(x; \sigma_1) + \epsilon f_G(x; \sigma_2), \quad \sigma_2 > \sigma_1, \quad (1.2-3)$$

or the Gaussian-Laplace mixture

$$p_n(x) = (1-\epsilon) f_G(x; \sigma_1) + \epsilon \cdot \frac{\alpha}{2} e^{-\alpha|x|}. \quad (1.2-4)$$

In that the two-term models express the condition that the noise is nearly Gaussian (the first term) but with distributional tails higher than the Gaussian (contributed by the second term), they are sometimes called "contamination" models.

1.2.2 Interpretation of the Mixture pdf

Consider the class of mixture densities in which the component pdf's $f_m(x)$ take the same functional form, but with different parameter values, that is,

$$f_m(x) = f_A(x; \xi_m),$$

where $f_A(;)$ is the common functional form for the family "A" of the pdf's, and ξ_m is a particular value of a parameter (or set of parameters) determining the scaling, location, etc., of the pdf. Then the mixture pdf has the interpretation

$$\begin{aligned} p_n(x) &= \sum_m \kappa_m f_A(x; \xi_m) \\ &= \int d\xi f_A(x; \xi) p_\xi(\xi). \end{aligned} \tag{1.2-5}$$

Under this view, $p_n(x)$ is the result of averaging the parametric pdf $f_A(x; \xi)$ over a discrete pdf for the values of ξ :

$$p_\xi(\xi) = \sum_m \kappa_m \delta(\xi - \xi_m), \quad \sum_m \kappa_m = 1. \tag{1.2-6}$$

For example, in Middleton's non-Gaussian noise model, the parameter ξ is the variance of a zero-mean Gaussian pdf, and the κ_m describe a Poisson (discrete) pdf for occurrence of the variance values.

1.2.3 Form of Likelihood Ratio

For additive and independent signals and noise, the pdf under the alternative hypothesis under the mixture model of noise becomes

$$p_{s+n}(x) = p_n(x-s) = \sum_m \kappa_m f_m(x-s). \tag{1.2-7}$$

The likelihood ratio (LR) then takes the form

$$\begin{aligned} \Lambda(x) &\triangleq \frac{p_{s+n}(x)}{p_n(x)} = \frac{\sum_m \kappa_m f_m(x-s)}{\sum_m \kappa_m f_m(x)} \\ &= \frac{\sum_m \kappa_m f_m(x) [f_m(x-s)/f_m(x)]}{\sum_m \kappa_m f_m(x)} \\ &= \sum_m W_m(x) \Lambda_m(x), \quad \sum_m W_m(x) = 1, \end{aligned} \quad (1.2-8)$$

a mixture of individual LR's $\Lambda_m(x)$ weighted by the (nonconstant) functions

$$W_m(x) = \frac{\kappa_m f_m(x)}{\sum_m \kappa_m f_m(x)}. \quad (1.2-9)$$

For example, for the Gaussian-Gaussian mixture (1.2-3),

$$W_1(x) = \frac{(1-\epsilon)\sigma_1^{-1}e^{-x^2/2\sigma_1^2}}{(1-\epsilon)\sigma_1^{-1}e^{-x^2/2\sigma_1^2} + \epsilon\sigma_2^{-1}e^{-x^2/2\sigma_2^2}} = 1 - W_2(x). \quad (1.2-10)$$

In the case that the signal has unknown parameters $\{\theta\}$, the LR formulation (1.2-8) becomes the generalized likelihood ratio

$$\begin{aligned} \Lambda(x) &= \frac{E_\theta \{p_{s+n}(x; \theta)\}}{p_n(x)} = E_\theta \{ \Lambda(x; \theta) \} \\ &= \sum_m W_m(x) E_\theta \{ \Lambda_m(x; \theta) \}. \end{aligned} \quad (1.2-11)$$

1.2.4 Superposition of Detection Measures

It has been shown that the pdf for mixture noise is an additive combination of individual pdf's:

$$p_n(x) = \sum_m \kappa_m f_m(x), \quad \sum_m \kappa_m = 1. \quad (1.2-12)$$

For this reason the probability of false alarm (P_{FA}) or Type I detection error is, given the threshold n ,

$$\begin{aligned} P_{FA}(n) &= \Pr\{\Lambda(x) > n | H_0\} \\ &= \Pr\{x \in R_n | H_0\} \\ &= \int_{R_n} dx p_n(x) \\ &= \sum_m \kappa_m \int_{R_n} dx f_m(x) \\ &= \sum_m \kappa_m P_{FA,m}(n). \end{aligned} \quad (1.2-13)$$

We see that $P_{FA}(n)$ is the superposition of PFA's arising from the individual terms in the pdf. Similarly, the detection probability (P_D) is a superposition of individual probabilities:

$$\begin{aligned}
 P_D(n;s) &\equiv \Pr\{\Lambda(x) > n | H_1\} \\
 &= \Pr\{X \in R_n | H_1\} \\
 &= \int_{R_n} dx p_n(x-s) \\
 &= \sum_m \kappa_m \int_{R_n} dx f_m(x-s) \\
 &= \sum_m \kappa_m P_{D,m}(n;s) \tag{1.2-14}
 \end{aligned}$$

Thus in a significant manner the use of mixture densities to characterize non-Gaussian noise facilitates calculation of detection measures.

1.3 TREATMENT OF BANDPASS NON-GAUSSIAN NOISE

For zero-mean, stationary bandpass Gaussian noise, it has long been understood that the sample function of the noise random process can be represented in quadrature form by the decomposition

$$n(t) = n_c(t) \cos \omega_0 t - n_s(t) \sin \omega_0 t, \quad (1.3-1)$$

where $f_0 = \omega_0/2\pi$ is the center frequency of the band, $n_c(t)$ is an "in-phase" random process, and $n_s(t)$ is a "quadrature" random process. Both $n_c(t)$ and $n_s(t)$ are lowpass Gaussian random processes, with

$$\begin{aligned} E\{n_c(t)\} &= E\{n_s(t)\} = 0, \text{ for } E\{n(t)\} = 0 \\ E\{n_c^2(t)\} &= E\{n_s^2(t)\} = E\{n^2(t)\} = \sigma^2. \end{aligned} \quad (1.3-2)$$

The correlation functions pertaining to the quadrature components $n_c(t)$ and $n_s(t)$ are

$$\begin{aligned} R_c(\tau) &= E\{n_c(t)n_c(t+\tau)\} = E\{n_s(t)n_s(t+\tau)\} \\ &= \int_{-B}^B df S_n(f-f_0) \cos 2\pi f \tau \end{aligned} \quad (1.3-3)$$

and

$$\begin{aligned} R_{cs}(\tau) &= E\{n_c(t)n_s(t+\tau)\} \\ &= \int_{-B}^B df S_n(f-f_0) \sin 2\pi f \tau. \end{aligned} \quad (1.3-4)$$

From these correlation functions we observe that at the same time instant ($\tau=0$), $R_{CS}=0$ and therefore n_C and n_S are uncorrelated. Further, if the noise power spectral density $S_n(f)$ is even about the center frequency, f_0 , then $R_{CS}(\tau)=0$ for all τ , implying that n_C and n_S are uncorrelated for all pairs of time instants.

For $n_C(t)$ and $n_S(t)$ Gaussian, zero correlation is equivalent to statistical independence, and we can write their joint pdf as

$$p_{n_C, n_S}(\alpha, \beta) = p_{n_C}(\alpha)p_{n_S}(\beta) = \frac{1}{2\pi\sigma^2} \exp\left\{-\frac{n_C^2 + n_S^2}{2\sigma^2}\right\}. \quad (1.3-5)$$

Now the question we wish to address is how to model the joint pdf of the quadrature components of a bandpass non-Gaussian process. Under the assumption that the noise spectrum is even about the center frequency, we can state that n_C and n_S are uncorrelated. If they are not Gaussian, the lack of correlation no longer implies independence, although of course independence implies they are uncorrelated.

1.3.1 Independent Quadrature Component Assumption

One assumption which can be made concerning the quadrature components of bandpass non-Gaussian noise is that they are independent. Thus, for example, for Gaussian-Gaussian mixture noise we could write

$$\begin{aligned}
 p_{nc,ns}(\alpha, \beta) &= p_{nc}(\alpha) p_{ns}(\beta) \\
 &= \left[(1-\epsilon) \frac{1}{\sigma_1} p_G\left(\frac{\alpha}{\sigma_1}\right) + \epsilon \frac{1}{\sigma_2} p_G\left(\frac{\alpha}{\sigma_2}\right) \right] \\
 &\quad \times \left[(1-\epsilon) \frac{1}{\sigma_1} p_G\left(\frac{\beta}{\sigma_1}\right) + \epsilon \frac{1}{\sigma_2} p_G\left(\frac{\beta}{\sigma_2}\right) \right] \\
 &= \frac{(1-\epsilon)^2}{2\pi\sigma_1^2} \exp\left\{-\frac{\alpha^2 + \beta^2}{2\sigma_1^2}\right\} + \frac{\epsilon(1-\epsilon)}{2\pi\sigma_1\sigma_2} \exp\left\{-\frac{\alpha^2}{2\sigma_1^2} - \frac{\beta^2}{2\sigma_2^2}\right\} \\
 &\quad + \frac{\epsilon(1-\epsilon)}{2\pi\sigma_1\sigma_2} \exp\left\{-\frac{\alpha^2}{2\sigma_2^2} - \frac{\beta^2}{2\sigma_1^2}\right\} + \frac{\epsilon^2}{2\pi\sigma_2^2} \exp\left\{-\frac{\alpha^2 + \beta^2}{2\sigma_2^2}\right\} \quad (1.3-6)
 \end{aligned}$$

Such a model was used by Trunk [20] to study the performance of radar detectors in sea clutter.

For noncoherent detection, we are interested in the distribution of the envelope of the noise. Using the independent quadrature version of Gaussian-Gaussian noise, the pdf of the envelope is

$$\begin{aligned}
 p_{env}(u) &= u \int_0^{2\pi} d\phi p_{nc,ns}(u \cos\phi, u \sin\phi) \\
 &= (1-\epsilon)^2 \cdot \frac{1}{\sigma_1} p_R\left(\frac{u}{\sigma_1}\right) + \epsilon^2 \cdot \frac{1}{\sigma_2} p_R\left(\frac{u}{\sigma_2}\right) \\
 &\quad + \frac{2\epsilon(1-\epsilon)u}{\sigma_1\sigma_2} \exp\left\{-\frac{u^2}{4} \left(\frac{\sigma_1^2 + \sigma_2^2}{\sigma_1^2\sigma_2^2}\right)\right\} I_0\left\{\frac{u^2}{4} \left(\frac{\sigma_2^2 - \sigma_1^2}{\sigma_1^2\sigma_2^2}\right)\right\}, \quad (1.3-7a)
 \end{aligned}$$

where $p_R(\cdot)$ is the Rayleigh pdf:

$$p_R(x) = x e^{-x^2/2}, \quad x \geq 0. \quad (1.3-7b)$$

It can be observed from the above expression that the assumption of independent quadrature components yields an envelope pdf with some complexity. With a signal present, the envelope pdf is very difficult to analyze, not having a closed form [20].

Another aspect of this noise modelling assumption is revealed by the pdf of the phase of the noise, found to be

$$\begin{aligned}
 p_{\text{phase}}(\phi) &= \int_0^{\infty} du \, u \, p_{nc,ns}(u \cos \phi, u \sin \phi) \\
 &= \frac{(1-\epsilon)^2 + \epsilon^2}{2\pi} \\
 &\quad + \frac{\epsilon(1-\epsilon)}{2\pi} \frac{\sigma_1 \sigma_2 (\sigma_1^2 + \sigma_2^2)}{\sigma_1^2 \sigma_2^2 + (\sigma_1^2 - \sigma_2^2)^2 \sin^2 \phi \cos^2 \phi}. \quad (1.3-8)
 \end{aligned}$$

Obviously, the phase of the bandpass Gaussian-Gaussian mixture noise is not uniformly distributed when it is assumed that the noise quadrature components are independent, nor is the phase independent of the envelope.

1.3.2 Circularly Symmetric Quadrature Assumption

If it is understood that the quadrature components n_c and n_s of the bandpass noise are in general statistically dependent when the noise is nonGaussian, then finding the form of the joint density of n_c and n_s becomes the problem. Two methods [21] are available for constructing a joint pdf when it is assumed that the joint pdf has the form

$$p_{nc,ns}(\alpha, \beta) = g(\sqrt{\alpha^2 + \beta^2}), \quad (1.3-9)$$

some function of $\sqrt{\alpha^2 + \beta^2}$, that is, the pdf possesses "circular symmetry".

The first method is to select the function $g(R)$, recognizing that R is the envelope of the noise, and assuming that the phase of noise relative to the center frequency is independent of the envelope. Then the joint pdf of envelope and phase becomes

$$p_{R,\theta}(u,\theta) = K \frac{u g(u)}{2\pi} \quad (1.3-10)$$

where K is a normalization constant. This approach has been used to analyze the performance of communications in VLF atmospheric noise [22], with the envelope assumed to have a log normal distribution. The marginal distributions of the individual quadrature components, $p_{nc}(\alpha)$ and $p_{ns}(\beta)$ follow from the joint pdf and we do not have control over their form using this method.

The second method for constructing a joint pdf is based on generalizing the marginal pdf's of the quadrature components. Let the characteristic function of the individual quadrature components be

$$C(v) = E\left\{e^{jv n_c}\right\} = E\left\{e^{jv n_s}\right\}. \quad (1.3-11)$$

A circularly symmetric joint distribution can be assigned to the quadrature components by defining the joint characteristic function to be

$$C_{nc,ns}(v,\mu) = C\left(\sqrt{v^2 + \mu^2}\right). \quad (1.3-12)$$

For example, if the quadrature components are Gaussian-Gaussian mixtures, then

$$C(v) = (1-\epsilon)e^{-\frac{1}{2}\sigma_1^2 v^2} + \epsilon e^{-\frac{1}{2}\sigma_2^2 v^2}, \quad (1.3-13)$$

and the circularly symmetric joint characteristic function is

$$C_{nc,ns}(v,\mu) = (1-\epsilon) e^{-\frac{1}{2}\sigma_1^2 (v^2 + \mu^2)} + \epsilon e^{-\frac{1}{2}\sigma_2^2 (v^2 + \mu^2)}. \quad (1.3-14)$$

From this assumption it follows that

$$p_{nc,ns}(\alpha, \beta) = \frac{(1-\epsilon)}{2\pi\sigma_1^2} \exp\left\{-\frac{\alpha^2 + \beta^2}{2\sigma_1^2}\right\} + \frac{\epsilon}{2\pi\sigma_2^2} \exp\left\{-\frac{\alpha^2 + \beta^2}{2\sigma_2^2}\right\}. \quad (1.3-15)$$

Throughout our subsequent analysis, we shall use the circularly symmetric, rather than independent, quadrature assumption.

2.0 NONCOHERENT DETECTION IN BANDPASS GAUSSIAN-GAUSSIAN MIXTURE NOISE USING CONVENTIONAL DETECTORS

In this section we examine the effects on detection performance that occur as the noise departs from a Gaussian distribution. The detectors will be based on the assumption that the noise is Gaussian.

As we develop these results, several purposes are in mind. First, the performance of Gaussian detectors in the non-Gaussian noise environment will serve as a useful reference or yardstick for evaluation of the performance of improved detectors. Second, the results will reveal whether the use of multiple samples will overcome the loss in single-sample detector performance, so that acceptable performance is achieved in spite of the fact that the noise is not Gaussian. Third, by comparing the performance of single-channel Gaussian detectors in non-Gaussian noise with that of detectors utilizing two channels of data (specifically, a correlator-detector), we will learn whether one type of these common detectors is less vulnerable to the degradation from non-Gaussian noise than the other.

2.1 DETECTION FORMULATIONS

As a particular case of detection of signals in non-Gaussian noise, we turn to the problem defined as follows: on the basis of the received waveform $r(t)$, $0 < t \leq T$, we wish to accept or reject the null hypothesis

$$H_0: r(t) = n(t) \quad (\text{noise only}) \quad (2.1-1)$$

when the noise is bandpass Gaussian-Gaussian mixture noise,

$$n(t) = n_c(t)\cos\omega_0 t - n_s(t)\sin\omega_0 t \quad (2.1-2)$$

where $f_0 = \omega_0/2\pi$ is the center frequency of the band, and the joint pdf of the quadrature components $n_c(t)$, $n_s(t)$ at a given instant is the bivariate Gaussian-Gaussian mixture pdf

$$p_{n_c, n_s}(\alpha, \beta) = \frac{1-\epsilon}{2\pi\sigma_1^2} \exp\left\{-\frac{\alpha^2 + \beta^2}{2\sigma_1^2}\right\} + \frac{\epsilon}{2\pi\sigma_2^2} \exp\left\{-\frac{\alpha^2 + \beta^2}{2\sigma_2^2}\right\}. \quad (2.1-3)$$

Detection occurs when H_0 is rejected in favor of the alternative hypothesis

$$H_1: r(t) = n(t) + A\cos[\omega_0 t + \theta(t)], \quad (2.1-4)$$

in which the signal amplitude A is constant during the observation interval* and the signal phase $\theta(t)$ is random. Two different assumptions will be made about the phase: (a) the random phase is constant ("slowly varying") during the observation interval (type 1 signal); or (b) the random phases of samples taken during the observation interval are independent (type 2 signal).

We assume that K samples of r_c and r_s , the quadrature components of $r(t)$, are taken on the interval $(0, T)$. Under the two hypotheses, the joint pdf's of these samples are

$$H_0: p_{\underline{r}_c, \underline{r}_s}(\underline{\alpha}, \underline{\beta} | H_0) = p_{\underline{n}_c, \underline{n}_s}(\underline{\alpha}, \underline{\beta}) \quad (2.1-5a)$$

$$H_1: p_{\underline{r}_c, \underline{r}_s}(\underline{\alpha}, \underline{\beta} | H_1, \underline{s}) = p_{\underline{n}_c, \underline{n}_s}(\underline{\alpha} - \underline{s}_c, \underline{\beta} - \underline{s}_s) \quad (2.1-5b)$$

where the vector notation signifies

* In certain cases shown below, the extension of the analysis to amplitude variations is possible in a simple manner. The assumption of constant amplitude signals is commonly made as a means to simplifying the analysis, realizing that in practice variation is almost always observed.

$$\underline{r}_c = [r_c(t_1), r_c(t_2), \dots, r_c(t_k)]$$

$$\underline{r}_s = [r_s(t_1), r_s(t_2), \dots, r_s(t_k)]$$

$$\underline{s}_c = [s_c(t_1), s_c(t_2), \dots, s_c(t_k)]$$

$$= A \cos \theta [1, 1, \dots, 1] \quad (\text{Type 1})$$

$$= A [\cos \theta_1, \cos \theta_2, \dots, \cos \theta_k] \quad (\text{Type 2})$$

$$\underline{s}_s = [s_s(t_1), s_s(t_2), \dots, s_s(t_k)]$$

$$= A \sin \theta [1, 1, \dots, 1] \quad (\text{Type 1})$$

$$= A [\sin \theta_1, \sin \theta_2, \dots, \sin \theta_k] \quad (\text{Type 2}). \quad (2.1-5c)$$

The test for rejecting H_0 in favor of H_1 is to be based on the generalized likelihood ratio (GLR)

$$\Lambda_{\underline{r}}(\underline{\alpha}, \underline{\beta}) = \frac{E_{\theta} \{ p_{\underline{r}_c, \underline{r}_s}(\underline{\alpha}, \underline{\beta} | H_1, \underline{s}) \}}{p_{\underline{r}_c, \underline{r}_s}(\underline{\alpha}, \underline{\beta} | H_0)}. \quad (2.1-6)$$

We also shall consider the extension of this formula to the situation in which two channels of data (from perhaps two sensors) are to be tested for the presence of the same signal. In this case, the GLR becomes

$$\Lambda_{\underline{r}_1, \underline{r}_2}(\underline{\alpha}_1, \underline{\beta}_1, \underline{\alpha}_2, \underline{\beta}_2) = \Lambda_{\underline{r}_1}(\underline{\alpha}_1, \underline{\beta}_1) \Lambda_{\underline{r}_2}(\underline{\alpha}_2, \underline{\beta}_2), \quad (2.1-7)$$

assuming that the noises in the two channels are independent, and expanding the notation of (2.1-5) and (2.1-6) in an obvious way.

2.2 PERFORMANCE OF SINGLE CHANNEL GAUSSIAN DETECTORS IN GAUSSIAN-GAUSSIAN MIXTURE NOISE

When the mixture parameter ϵ in the noise pdf (2.1-3) is zero, the likelihood ratio (2.1-6) becomes

$$\begin{aligned} \Lambda_r(\underline{\alpha}, \underline{\beta}) &= E_{\underline{\theta}} \prod_{k=1}^K \exp \left\{ - \frac{(\alpha_k - A \cos \theta_k)^2 + (\beta_k - A \sin \theta_k)^2}{2\sigma_1^2} + \frac{\alpha_k^2 + \beta_k^2}{2\sigma_1^2} \right\} \\ &= \exp \left\{ - \frac{KA}{2\sigma_1^2} \right\} E_{\underline{\theta}} \left\{ \exp \left\{ \frac{A}{\sigma_1^2} \sum_{k=1}^K (\alpha_k \cos \theta_k + \beta_k \sin \theta_k) \right\} \right\}, \end{aligned} \quad (2.2-1)$$

assuming the samples (α_k, β_k) are independent.

2.2.1 Forms of the Detectors

For the Type I signal, the phases $\{\theta_k\}$ are all equal, and the result of the expectation taken in (2.2-1) is

$$\Lambda_r(\underline{\alpha}, \underline{\beta}) = \exp \left\{ - \frac{KA^2}{2\sigma_1^2} \right\} I_0 \left\{ \frac{A}{\sigma_1^2} \sqrt{f(\underline{\alpha}, \underline{\beta})} \right\} \quad (2.2-2)$$

where $I_0(\cdot)$ is the modified Bessel function of the first kind and order zero, and

$$f(\underline{\alpha}, \underline{\beta}) = \left(\sum_{k=1}^K \alpha_k \right)^2 + \left(\sum_{k=1}^K \beta_k \right)^2 \quad (2.2-3)$$

Since the likelihood ratio is monotonic or directly proportional to $f(\underline{\alpha}, \underline{\beta})$, testing the likelihood ratio is equivalent to testing $f(\underline{\alpha}, \underline{\beta})$, that is,

$$\Lambda_{\underline{r}}(\underline{\alpha}, \underline{\beta}) \underset{H_0}{\geq} n_1 \iff f(\underline{\alpha}, \underline{\beta}) \underset{H_0}{\geq} n_2. \quad (2.2-4)$$

The detector based on (2.2-4) is diagrammed in Figure 2.2-1(a).

For the Type II signal, the phases $\{\theta_k\}$ are all independent, and the result of the expectation taken in (2.2-1) is

$$\begin{aligned} \Lambda_{\underline{r}}(\underline{\alpha}, \underline{\beta}) &= \exp \left\{ -\frac{KA^2}{2\sigma_1^2} \right\} \prod_{k=1}^K I_0 \left(\frac{A}{\sigma_1^2} \sqrt{\alpha_k^2 + \beta_k^2} \right) \\ &= \exp \left\{ -\frac{KA^2}{2\sigma_1^2} + \sum_{k=1}^K \ln I_0 \left(\frac{A}{\sigma_1^2} \sqrt{\alpha_k^2 + \beta_k^2} \right) \right\}. \end{aligned} \quad (2.2-5)$$

When the signal is weak, we can simplify (2.2-5) greatly by using the approximation

$$\ln I_0 \left(\frac{A}{\sigma_1^2} \sqrt{\alpha_k^2 + \beta_k^2} \right) \approx \frac{A}{4\sigma_1^4} (\alpha_k^2 + \beta_k^2) \quad (2.2-6)$$

to arrive at the equivalent detection test

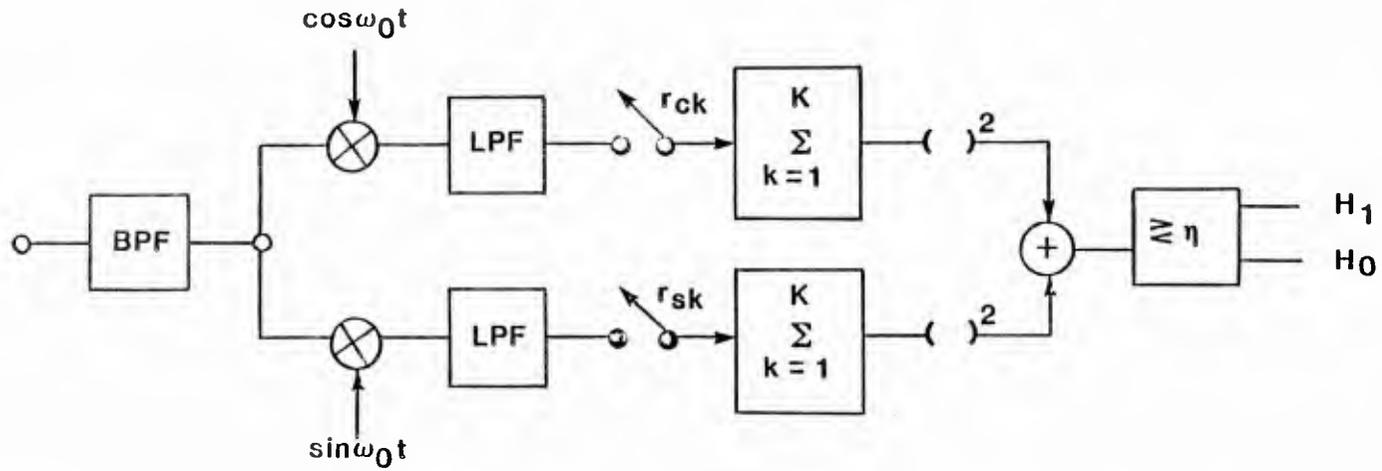
$$\sum_{k=1}^K (\alpha_k^2 + \beta_k^2) \underset{H_0}{\geq} n. \quad (2.2-7)$$

This practical implementation of the test of (2.2-7) is diagrammed in Figure 2.2-1(b).

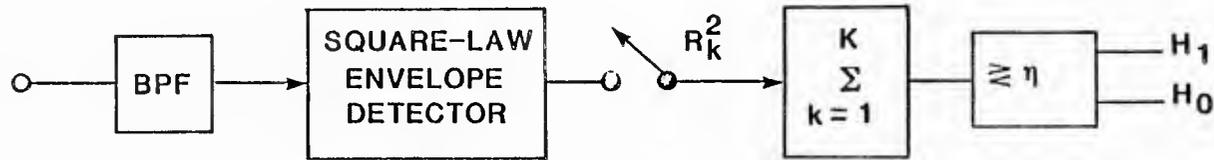
2.2.2 Single-Sample Detector Performance in Gaussian Mixture Noise

For one sample ($K=1$), the two detectors implement the test

$$r_C^2 + r_S^2 = R^2 \underset{H_0}{\geq} n, \quad (2.2-8)$$



(a) Type 1 signal (constant, random phase)



$$R_k^2 = r_{ck}^2 + r_{sk}^2$$

(b) Type 2 signal (independent, phase samples)

Figure 2.2-1 Detectors for a bandpass signal in Gaussian noise.

where R is the envelope of the received waveform at the sample time. Thus instead of quadrature sampling, we may employ an envelope or square-law envelope detector. It is well-known that in Gaussian noise, R^2 is a constant times a noncentral chi-squared random variable with two degrees of freedom and noncentrality parameter

$$\lambda = \begin{cases} 2\rho, & H_1 \text{ true, } \rho = A^2/2\sigma^2; \\ 0, & H_0 \text{ true.} \end{cases} \quad (2.2-9)$$

The performance of the quadrature detector for Gaussian-Gaussian noise in terms of false alarm and detection probabilities is found to be

$$\begin{aligned} P_{FA}(\eta) &= \Pr\{R^2 > \eta | H_0\} \\ &= (1-\epsilon) e^{-\eta/2\sigma_1^2} + \epsilon e^{-\eta/2\sigma_2^2} \end{aligned} \quad (2.2-10)$$

and

$$\begin{aligned} P_D(\eta) &= \Pr\{R^2 > \eta | H_1\} \\ &= (1-\epsilon) Q\left(A/\sigma_1, \sqrt{\eta/\sigma_1^2}\right) + \epsilon Q\left(A/\sigma_2, \sqrt{\eta/\sigma_2^2}\right), \end{aligned} \quad (2.2-11)$$

where η is the detection threshold and $Q(a,b)$ is Marcum's Q-function.

The effect of the mixture parameters ϵ and $V^2 \triangleq \sigma_2^2/\sigma_1^2$ on the false alarm threshold for the square-law envelope detector is shown in Table 2.2-1. It is evident from this table that for P_{FA} small (<0.1), the tendency is for the first term in (2.2-10) to be negligible, resulting in

$$\frac{\eta}{\sigma_1^2} = -2V^2 \ln(P_{FA}/\epsilon), \quad V^2 \neq 1, \quad (2.2-12)$$

TABLE 2.2-1
 FALSE ALARM THRESHOLDS
 FOR SQUARE-LAW ENVELOPE DETECTOR (SINGLE SAMPLE)

P_{FA}	Gaussian Noise n/σ_1^2	GAUSSIAN-GAUSSIAN NOISE			
		$\epsilon = 0.1$		$\epsilon = .01$	
		$V^2 = 10$ n/σ_1^2	$V^2 = 100$ n/σ_1^2	$V^2 = 10$ n/σ_1^2	$V^2 = 100$ n/σ_1^2
0.1	4.60517	6.8662	10.3657	4.7494	4.7905
0.01	9.21034	46.0517	460.5170	10.9215	14.5094
0.001	13.8151	92.1034	921.0340	46.0517	460.5170

and the threshold is raised to a value much higher than that for Gaussian noise. Therefore, for the same false alarm probability, a higher SNR will be required to achieve the same detection probability. Note that if either $\epsilon=0$ or $V^2 = 1$, then the probabilities of false alarm and detection become those for the Gaussian noise case.

In Figures 2.2-2 to 2.2-5, the false alarm probability, as a function of the normalized threshold η/σ_1^2 , is plotted for different values of the mixture parameter, ϵ , and the variance ratio, V^2 :

$$\begin{aligned} \epsilon &= (.01, .1, .2, .5) \\ V^2 &= (1, 2, 10, 100, 1000). \end{aligned} \tag{2.2-13}$$

It is evident from these figures that for P_{FA} less than or equal to the mixture parameter ϵ , the threshold is determined by the second term in (2.2-10), as noted already in (2.2-12).

In Figures 2.2-6 to 2.2-9, the detection probability is plotted as a function of SNR for the same parametric conditions as described by (2.2-13), and for fixed false alarm probabilities of 10^{-1} , 10^{-2} , and 10^{-3} . As anticipated; for each value of ϵ , the detection probability decreases as V^2 , the variance ratio, increases, except in some cases for high SNR. We observe also that the degradation in performance for $P_D > .5$ is proportional to ϵ , and that in general the amount of degradation is greater for smaller values of P_{FA} , the false alarm probability. This result is consistent with the fact that the tails of the distribution are extended by the contaminating Gaussian noise with variance σ_2^2 . Even with ϵ as small as 0.01 (Figure 2.2-6), a loss in detectability of over 4 db is experienced

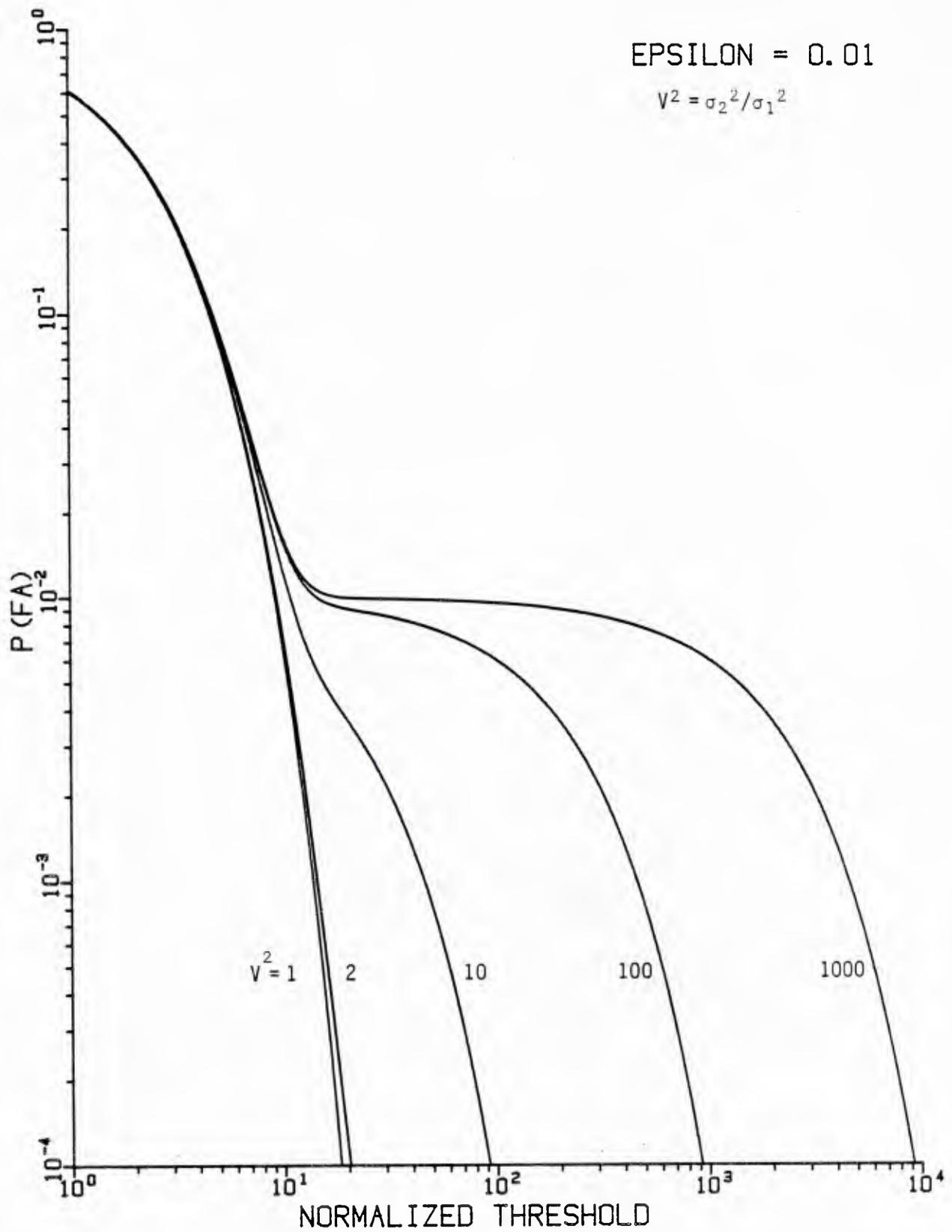


Figure 2.2-2. False alarm probability for Gaussian detector in Gaussian-Gaussian mixture noise, mixture parameter $\epsilon = 0.01$.

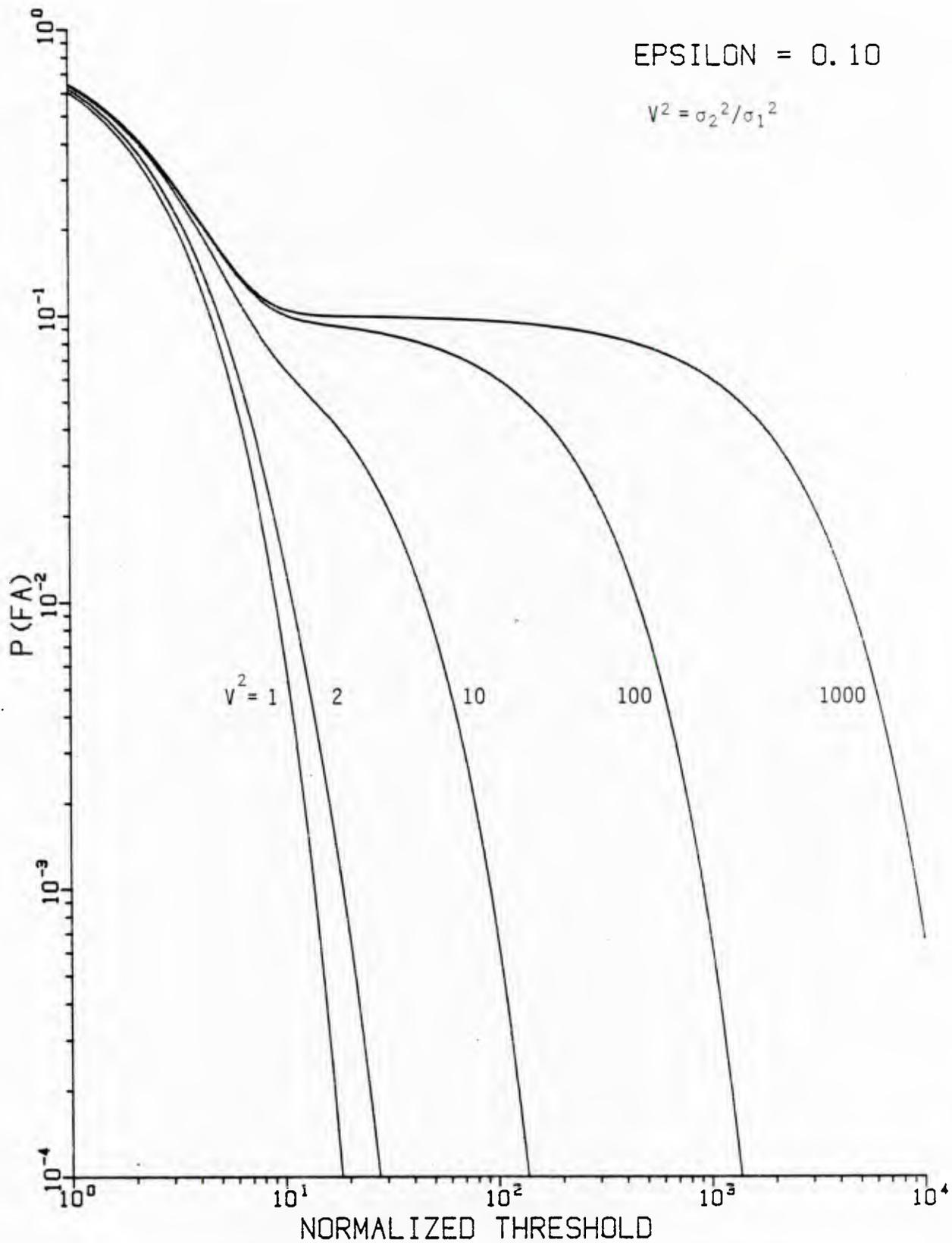


Figure 2.2-3. False alarm probability for Gaussian detector in Gaussian-Gaussian mixture noise, mixture parameter $\epsilon = 0.1$.

C100.0141SSDDGFA 10-APR-85 15:20:45 2

[100, 014]SSEDCGFA 10-APR-85 15, 20, 45 3

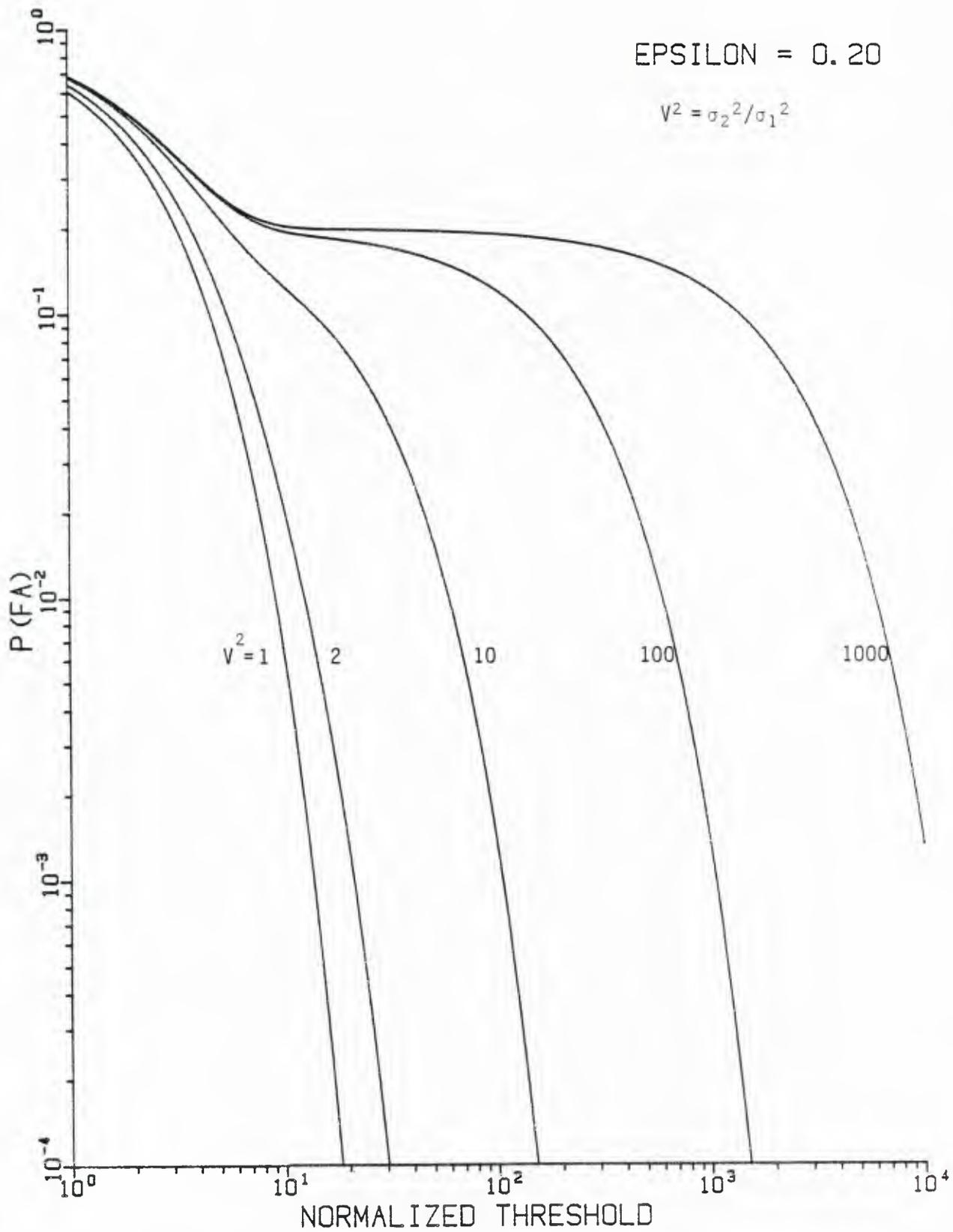


Figure 2.2-4. False alarm probability for Gaussian detector in Gaussian-Gaussian mixture noise, mixture parameter $\epsilon = 0.2$.

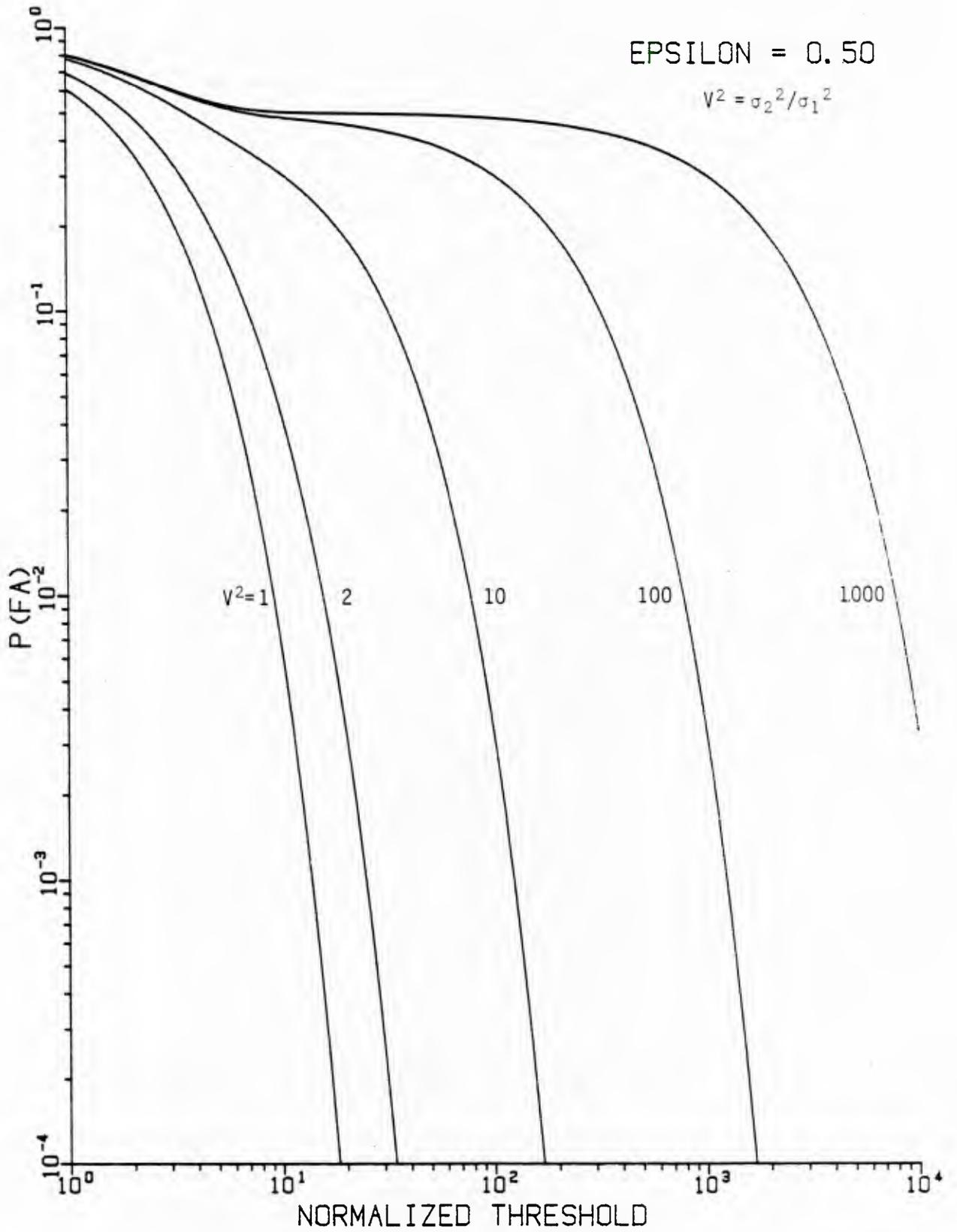


Figure 2.2-5. False alarm probability for Gaussian detector in Gaussian-Gaussian mixture noise, mixture parameter $\epsilon = 0.5$.

[100, 014]SSEDGFA 10-APR-85 15:20:45 4

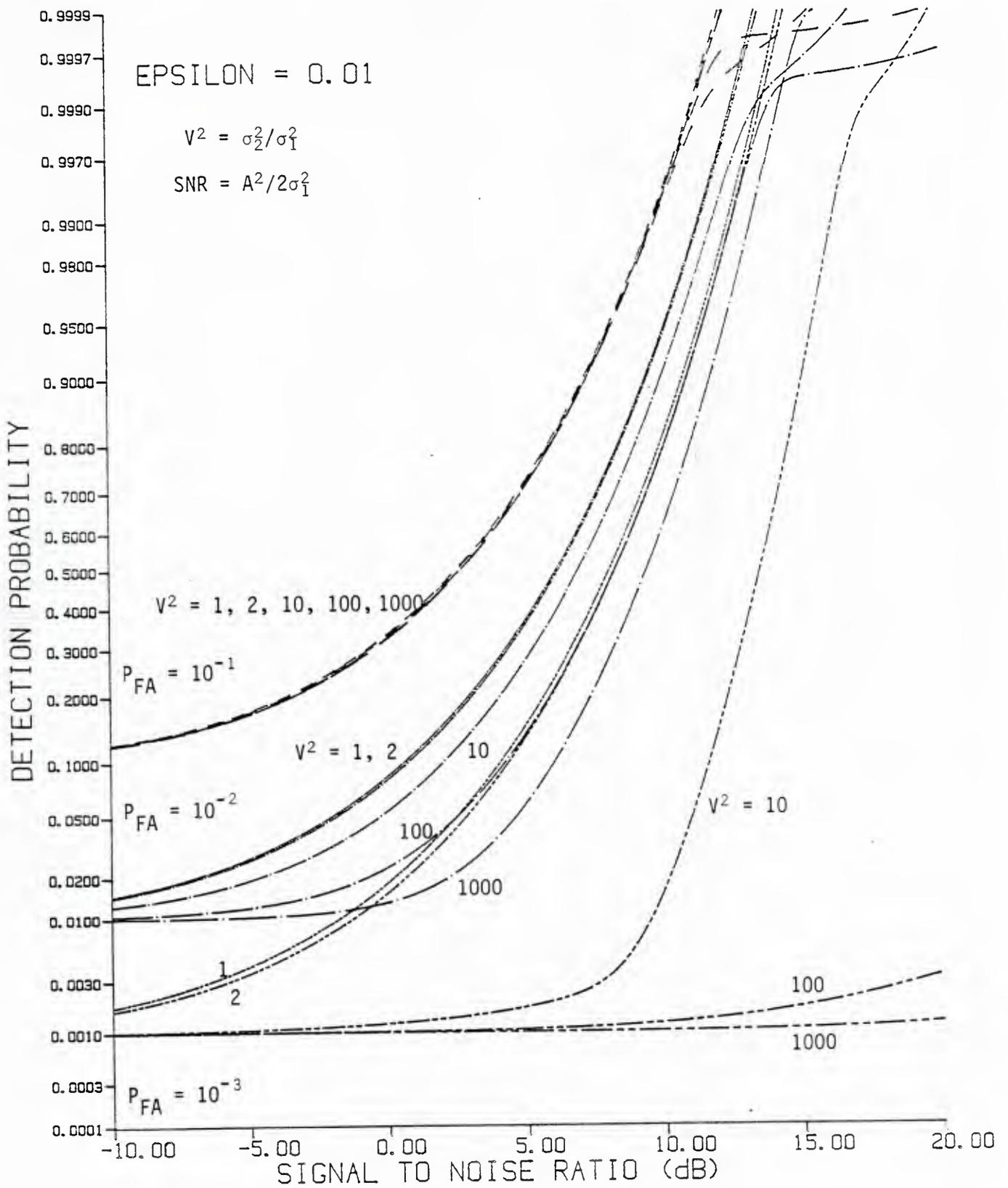


Figure 2.2-6 Receiver operating characteristics for Gaussian detector in Gaussian-Gaussian mixture noise, mixture parameter $\epsilon = 0.01$.

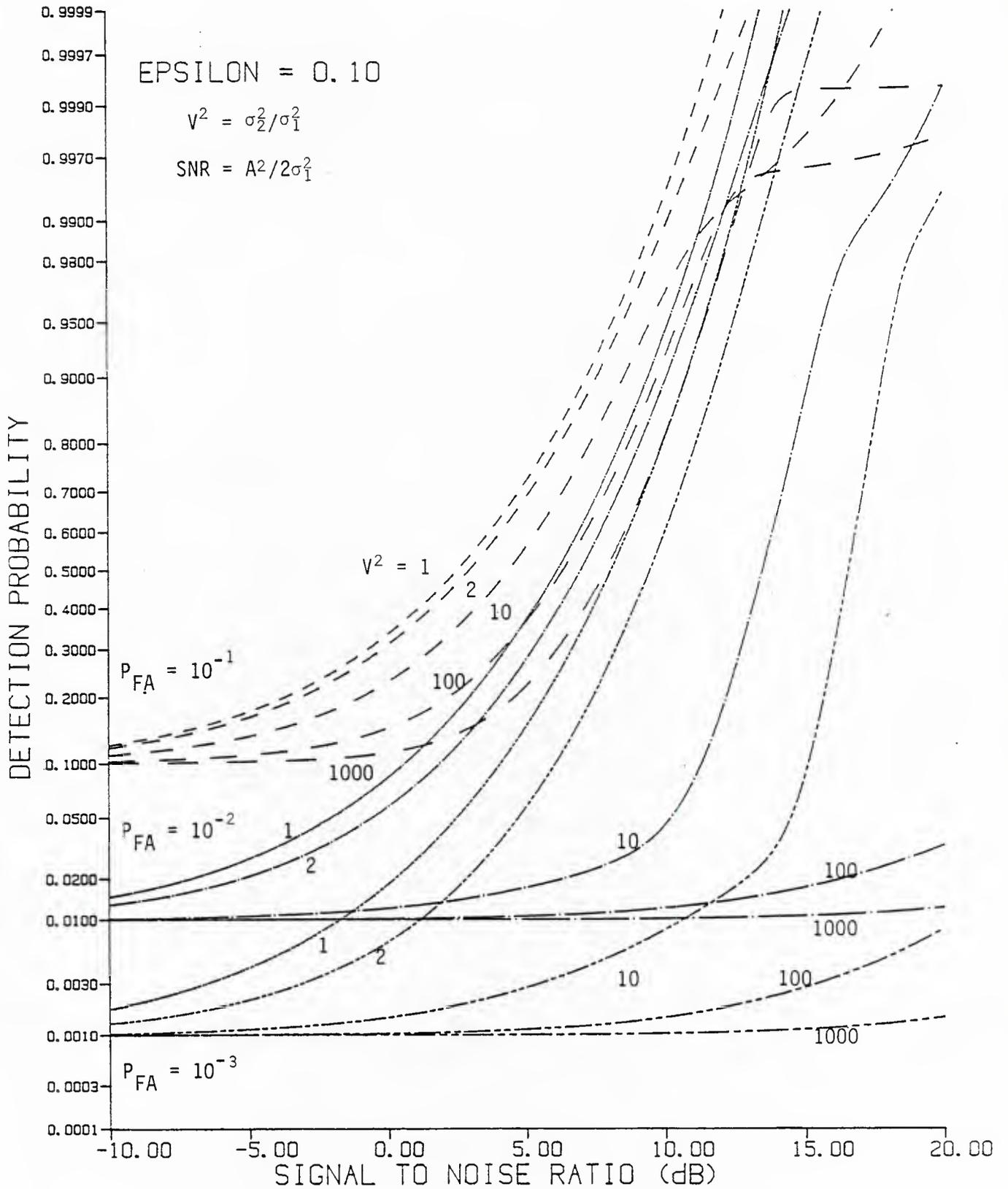


Figure 2.2-7 Receiver operating characteristics for Gaussian detector in Gaussian-Gaussian mixture noise, mixture parameter $\epsilon = 0.1$

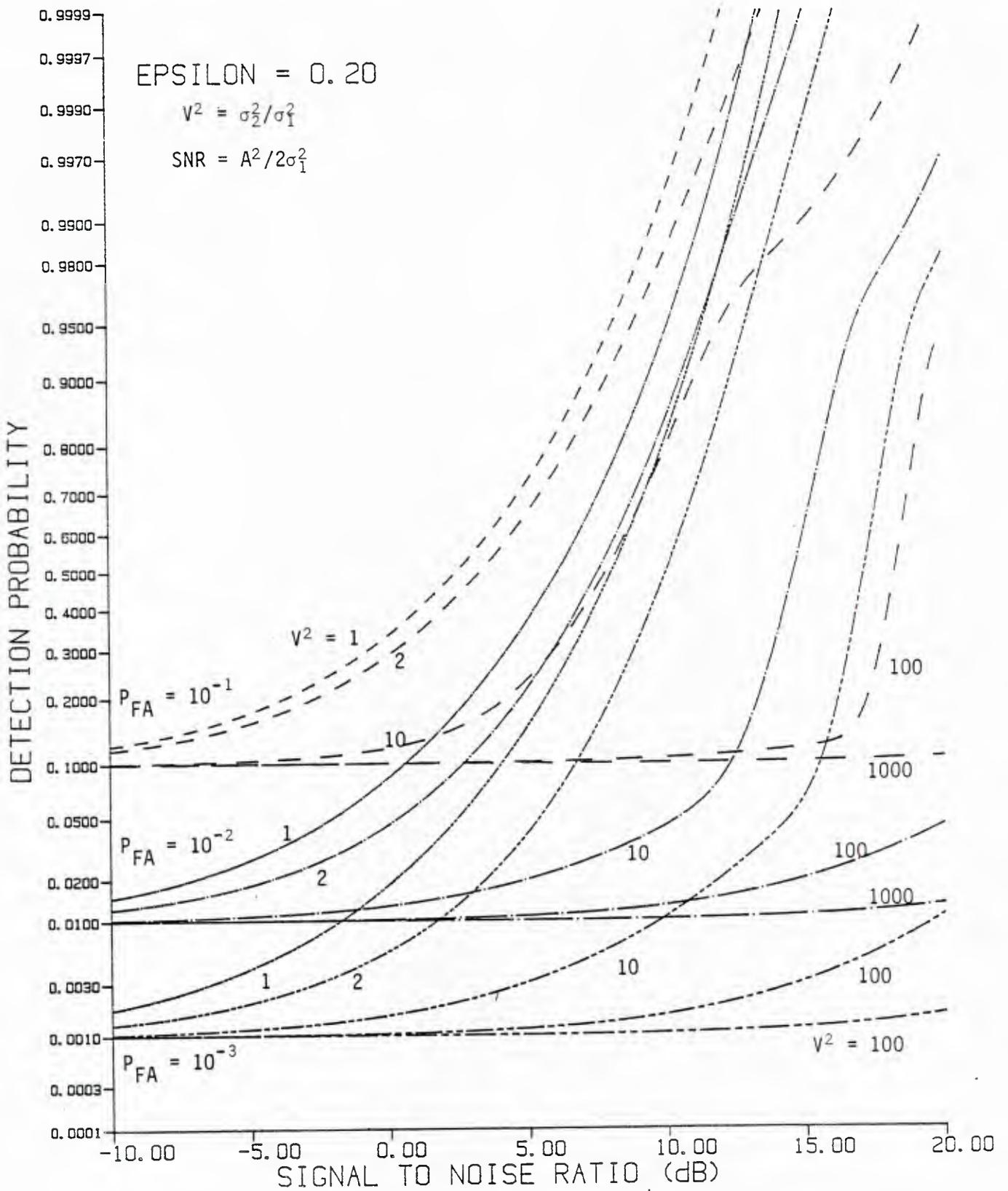


Figure 2.2-8 Receiver operating characteristics for Gaussian detector in Gaussian-Gaussian mixture noise, mixture parameter $\epsilon = 0.2$.

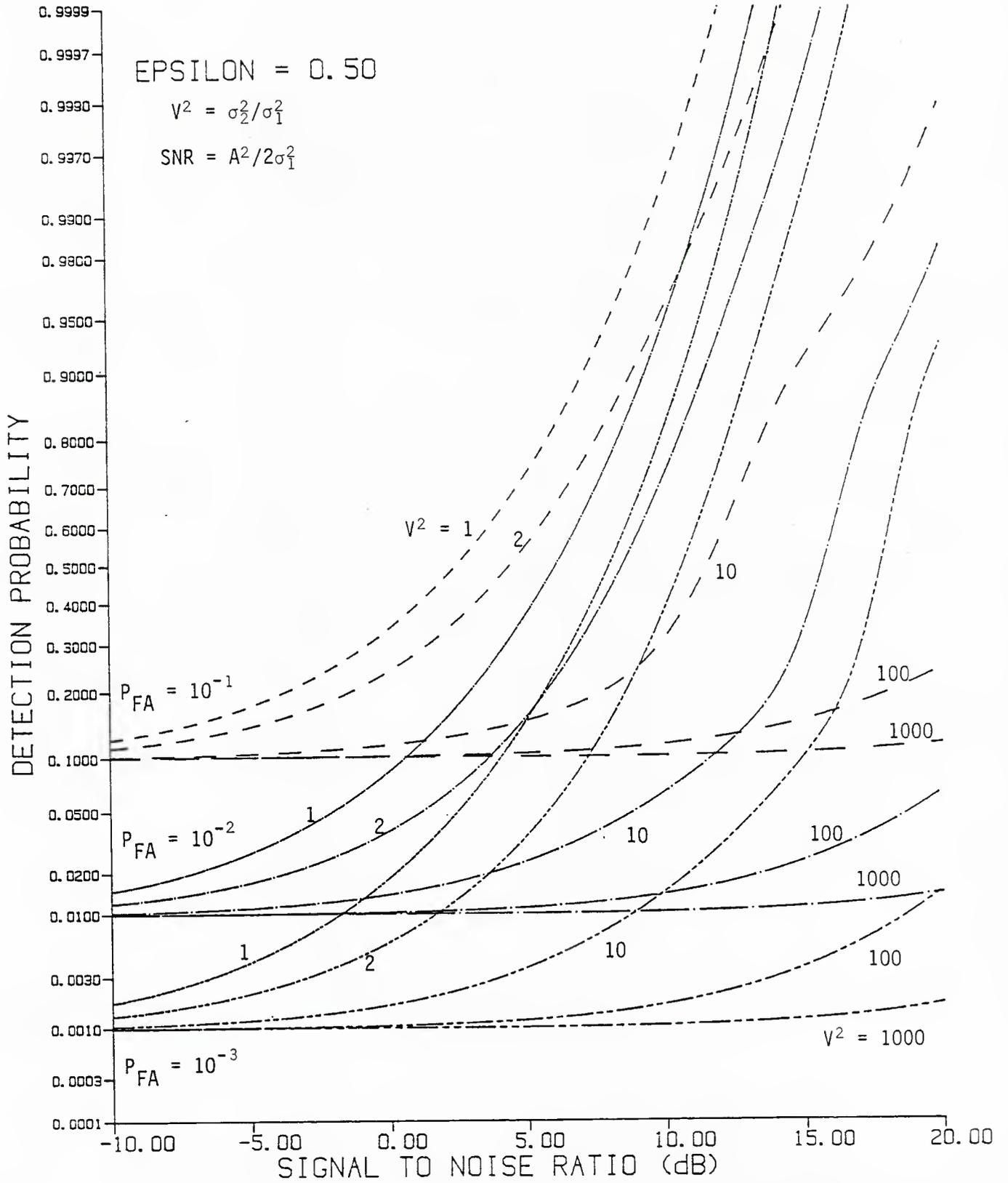


Figure 2.2-9 Receiver operating characteristics for Gaussian detector in Gaussian-Gaussian mixture noise, mixture parameter $\epsilon = 0.5$.

for $V^2=10$; this is the increase in SNR required to maintain, say, 90% detection probability as V^2 goes from the value 1 to 10.

For smaller values of P_D and $V^2 \geq 10$, we observe in Figures 2.2-6 to 2.2-9 that the Gaussian detector performance actually improves slightly as ϵ increases.

As we consider next the performance of the Gaussian detectors of Figure 2.2-1 in Gaussian-Gaussian mixture noise for multiple samples, we shall be interested to learn whether detection losses can be compensated by using multiple samples.

2.2.3 Multiple-Sample Detector Performance In Gaussian Mixture Noise

The joint pdf of K multiple, independent samples of the quadrature components of the input waveform is simply a K -fold product of the single sample pdf (2.1-3). Because this pdf has a two-term or binomial form, the K -sample joint pdf for the noise only case can be written

$$\begin{aligned}
 P_{r_c, r_s}(\alpha, \beta) &= \prod_{k=1}^K \left[\frac{1-\epsilon}{2\pi\sigma_1^2} \exp \left\{ -\frac{\alpha_k^2 + \beta_k^2}{2\sigma_1^2} \right\} + \frac{\epsilon}{2\sigma_1^2} \exp \left\{ -\frac{\alpha_k^2 + \beta_k^2}{2\sigma_2^2} \right\} \right] \\
 &= \sum_{m=0}^K \binom{K}{m} \epsilon^m (1-\epsilon)^{K-m} (2\pi)^{-K} (\sigma_1^2)^{-K+m} (\sigma_2^2)^{-m} \\
 &\quad \times \exp \left\{ -\frac{1}{2\sigma_1^2} \sum_{k_1=0}^{K-m} (\alpha_{k_1}^2 + \beta_{k_1}^2) - \frac{1}{2\sigma_2^2} \sum_{k_2=0}^m (\alpha_{k_2}^2 + \beta_{k_2}^2) \right\}.
 \end{aligned}
 \tag{2.2-14}$$

This expression conveys the information that the joint pdf consists of $K+1$ terms, each of which is a (weighted) joint pdf for K independent Gaussian random variables, m of which have variance σ_2^2 and $K-m$ of which have variance σ_1^2 , provided that the indexing or time-ordering of the samples (r_{ck}, r_{sk}) is arbitrary.

Another method for writing the multiple sample pdf is to consider the samples as conditionally Gaussian:

$$p_{r_c, r_s}(\underline{\alpha}, \underline{\beta}) = E_{V^2} \left\{ \frac{(2\pi\sigma_1^2)^{-K}}{v_1^2 \quad v_1^2 \quad \dots \quad v_k^2} \exp\left(-\sum_{k=1}^K \frac{\alpha_k^2 + \beta_k^2}{2v_k^2}\right) \right\}, \quad (2.2-15)$$

where the variance multipliers $\{v_k^2\}$ can take the values 1 or $\sigma_2^2/\sigma_1^2 \equiv V^2$, that is,

$$p_{v_k^2}(\gamma) = (1-\epsilon) \delta(\gamma-1) + \epsilon\delta(\gamma-V^2). \quad (2.2-16)$$

2.2.3.1 Sum and Square Detector

First we consider the "sum and square" quadrature detector of Figure 2.2-1(a), the GLR for a Type 1 (constant phase) signal in bandpass Gaussian noise. The test statistic for this detector may be written as

$$z = \left(\sum_{k=1}^K r_{ck} \right)^2 + \left(\sum_{k=1}^K r_{sk} \right)^2 \begin{matrix} H_1 \\ \geq \\ H_0 \end{matrix} \eta. \quad (2.2-17)$$

Since, given the variance multipliers $\{v_k^2\}$, the quadrature samples are independent Gaussian random variables, so are their sums; that is, conditionally,

$$\sum_{k=1}^K r_{ck} = \sum_{k=1}^K G(A \cos\theta, v_k^2\sigma_1^2) = G\left(KA \cos\theta, \sum_{k=1}^K v_k^2\sigma_1^2\right) \quad (2.2-18a)$$

$$\sum_{k=1}^K r_{sk} = \sum_{k=1}^K G(A \sin\theta, v_k^2\sigma_1^2) = G\left(KA \sin\theta, \sum_{k=1}^K v_k^2\sigma_1^2\right). \quad (2.2-18b)$$

Therefore conditionally z is a factor times a chi-squared random variable with two degrees of freedom:

$$z = \sigma_1^2 \left(\sum_{k=1}^K v_k^2 \right) \chi^2(2, \lambda) \quad (2.2-19a)$$

with the noncentrality parameter

$$\lambda = K^2 A^2 / \sigma_1^2 \sum_{k=1}^K v_k^2 = 2K^2 \rho / \sum_{k=1}^K v_k^2, \quad (2.2-19b)$$

using $\rho \triangleq A^2/2\sigma_1^2$. Although the detector form is based on constant phase and "slowly-varying" signal amplitude A , the performance of the detector can be evaluated for time varying amplitude and phase. The modification necessary for this evaluation is to interpret the noncentrality parameter λ in (2.2-19b) as

$$\lambda' = \left[\left(\sum_k A_k \cos\theta_k \right)^2 + \left(\sum_k A_k \sin\theta_k \right)^2 \right] / \sum_k v_k^2 \sigma_1^2, \quad (2.2-19c)$$

or the SNR ρ as

$$\rho' = \frac{1}{2\sigma_1^2} \left[\left(\frac{1}{K} \sum_k A_k \cos\theta_k \right)^2 + \left(\frac{1}{K} \sum_k A_k \sin\theta_k \right)^2 \right]. \quad (2.2-19d)$$

Conceivably the physical process giving rise to the non-Gaussian noise can introduce dependence among the variance multipliers $\{v_k^2\}$. For example, at one extreme, slow variation or low bandwidth in factors affecting the power of a conditionally Gaussian process may allow us to consider that $v_k^2 = v_1^2$, $k=2, 3, \dots, K$; that is, the value of v_k is a random

constant. In this instance it can be shown that the detection and false alarm probabilities achieved by the sum and square detector are

$$\begin{aligned}
 P_D(n; \rho, K) &= E_{V^2}[\Pr \{z > \eta | H_1\}] \\
 &= (1-\epsilon) Q\left(\sqrt{2K\rho}, \sqrt{\eta/K\sigma_1^2}\right) \\
 &\quad + \epsilon Q\left(\sqrt{2K\rho/V^2}, \sqrt{\eta/K\sigma_1^2 V^2}\right), \quad v_k^2 = v_1^2; \quad (2.2-20)
 \end{aligned}$$

where $Q(a, b)$ is Marcum's Q-function, and

$$\begin{aligned}
 P_{FA}(n; K) &= P_D(n; 0, K) \\
 &= (1-\epsilon) \exp\left\{-\eta/2K\sigma_1^2\right\} + \epsilon \exp\left\{-\eta/2K\sigma_1^2 V^2\right\}. \quad (2.2-21)
 \end{aligned}$$

Another extreme case of the statistical relationship among the $\{v_k^2\}$ is that in which high bandwidth in the variation of the power of a conditionally Gaussian process permits us to assume that the $\{v_k^2\}$ are independent. Then the detection and false alarm probabilities are

$$\begin{aligned}
 P_D(n; \rho, K) &= \sum_{m=0}^K \binom{K}{m} (1-\epsilon)^{K-m} \epsilon^m Q\left(\sqrt{\frac{2K^2\rho}{K-m+mV^2}}, \sqrt{\frac{\eta/\sigma_1^2}{K-m+mV^2}}\right), \\
 &\quad \text{independent } v_k^2; \quad (2.2-22)
 \end{aligned}$$

and

$$\begin{aligned}
 P_{FA}(n; K) &= \sum_{m=0}^K \binom{K}{m} (1-\epsilon)^{K-m} \epsilon^m \exp\{-\eta/2\sigma_1^2(K-m+mV^2)\}. \quad (2.2-23)
 \end{aligned}$$

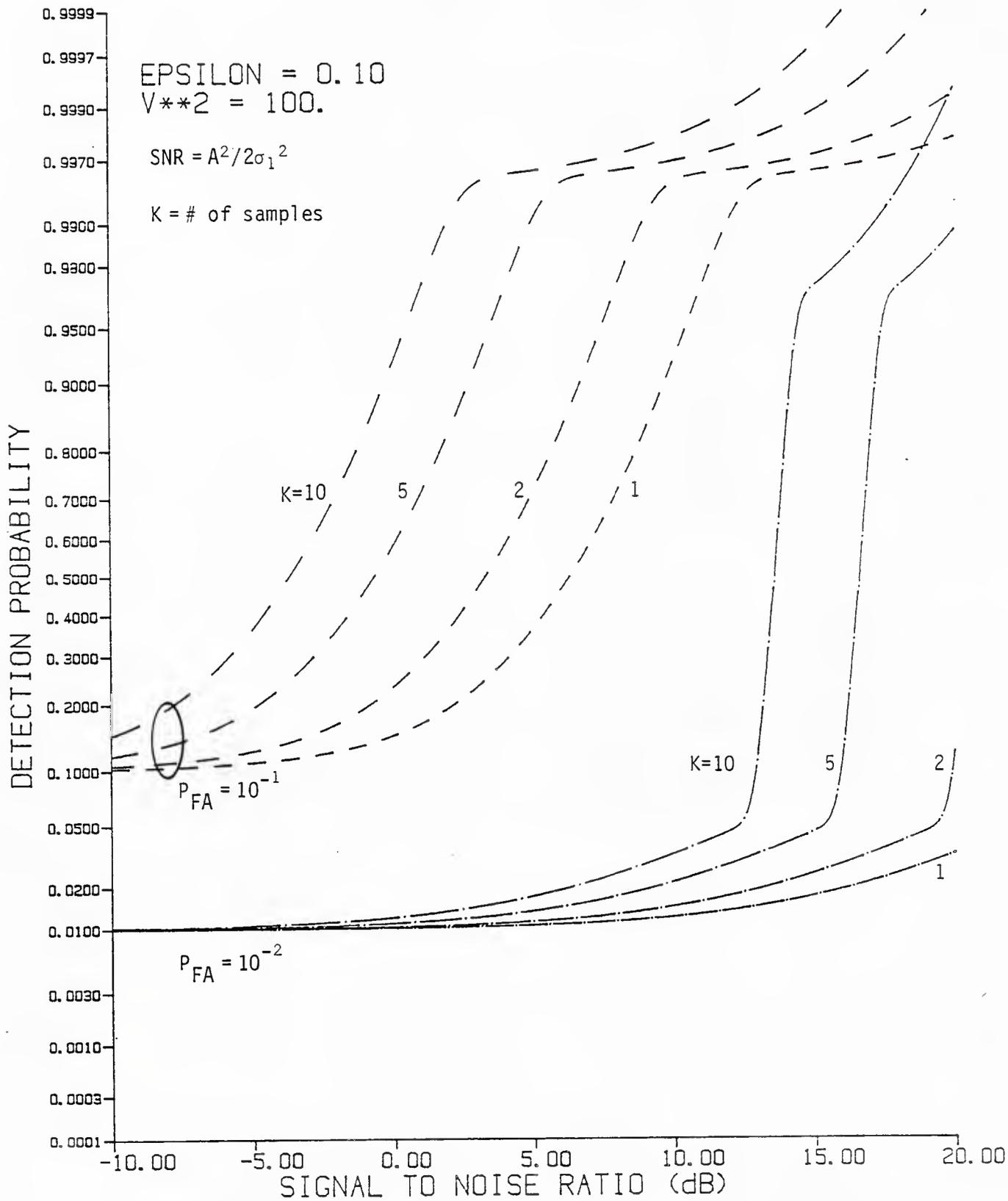


Figure 2.2-10. Receiver operating characteristics for the sum-and-square Gaussian detector in Gaussian-Gaussian mixture noise ($\epsilon = 0.1$, $V^2 = 100$) when multiple samples are used and the noise power is slowly varying.

The difference in sum-and-square detector performance due to the two different assumptions about the dependence of the variance multipliers can be observed by comparing Figures 2.2-10 and 2.2-11, in which $\epsilon=0.1$ and $V^2=100$.

In Figure 2.2-10, the equal $\{v_k^2\}$ case is evaluated, showing that an improvement in detection holds for this case. A close look at the equal $\{v_k^2\}$ P_D and P_{FA} expressions, (2.2-20) and (2.2-21), reveals that

$$P_D(n; \rho, K) = P_D(P_{FA}^{-1}; K\rho, 1), \text{ equal } v_k^2; \quad (2.2-24)$$

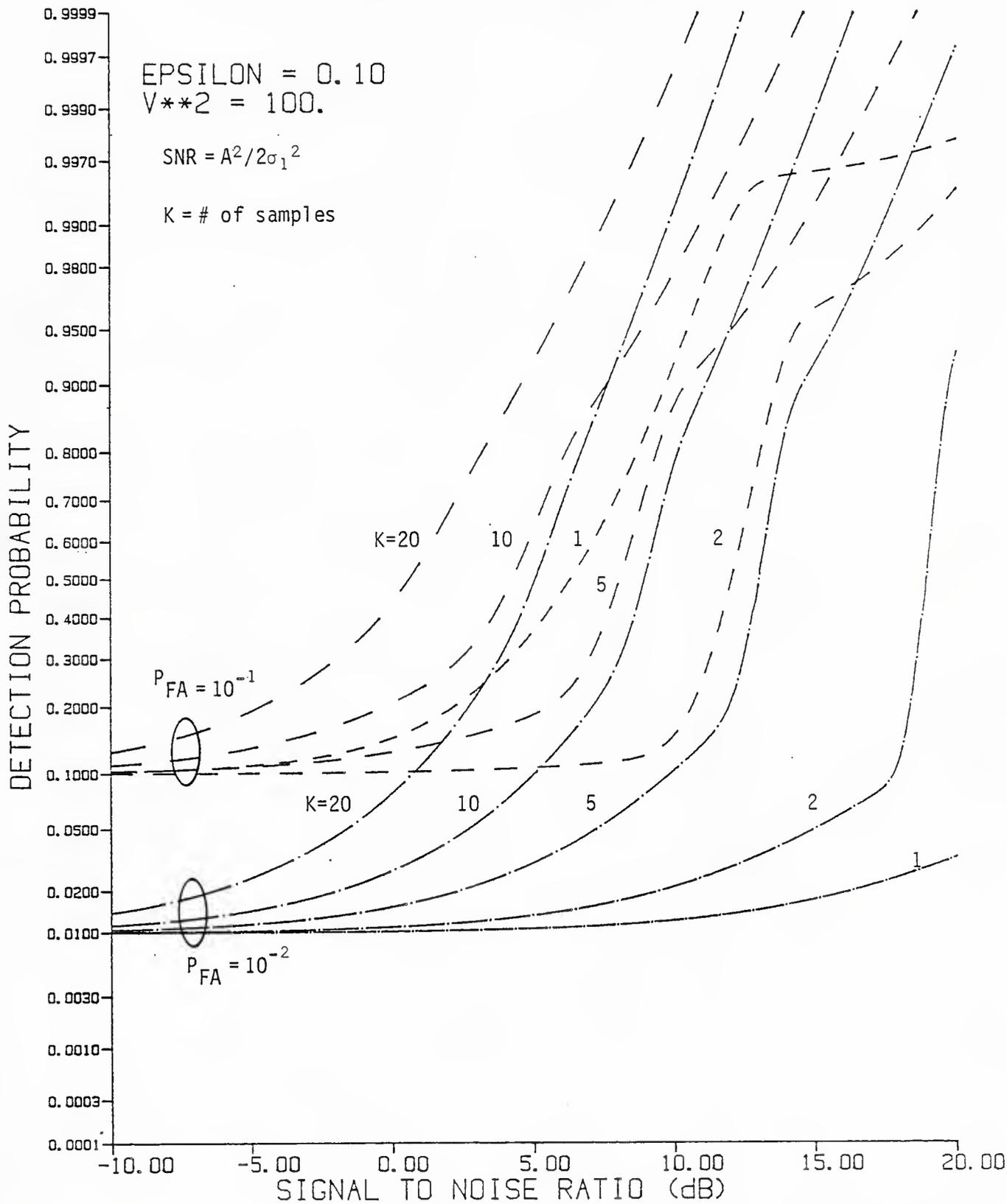
that is, the detectability of the signal is increased by the factor K . Thus the single-sample detection losses tabulated previously can be made up by using an appropriate number of samples, assuming that the variance is indeed constant for the K samples. However, relative to the performance achievable in Gaussian noise with the same number of samples, the detectability loss remains the same, regardless of the value of K .

The sharp rise in the curves for $P_{FA} = 10^{-2}$ in Figure 2.2-10 can be explained as follows: the false alarm probability (2.2-21) is dominated by the second term, yielding

$$n/\sigma_1^2 \approx -2KV^2 \ln(P_{FA}/\epsilon) = 460K. \quad (2.2-25)$$

The detection probability (2.2-20) is due to the second term for small SNR; when the SNR approaches the value at which the first term's Q -function becomes 0.5, or

$$2K\rho \approx n/K\sigma_1^2 = 460, \quad (2.2-26)$$



100,0141INDSAMPD 12-APR-85 09:44:05 1

Figure 2.2-11. Receiver operating characteristics for the sum-and-square Gaussian detector in Gaussian-Gaussian mixture noise ($\epsilon = 0.1$, $V^2 = 100$) when independent multiple samples are used.

this term rapidly increases from zero to $(1-\epsilon) = 0.9$. For example, if $K=10$ this occurs at $\rho = 23 = 13.6\text{dB}$.

The sum-and-square detector performance for independent $\{v_k^2\}$, and hence independent samples, is plotted in Figure 2.2-11. A very different behavior from that of Figure 2.2-10 is observed: for the case of $P_{FA} = 10^{-1}$, the independent sample performance actually gets worse initially as K increases; however, for the case of $P_{FA} = 10^{-2}$, the detection probability increases uniformly with the number of samples K , and is better than the results shown in Figure 2.2-10. We conclude that for low P_{FA} , the performance of this detector is better for independent noise samples, and that effects of the non-Gaussian noise can be countered by using multiple samples.

2.2.3.2 Square and Sum Detector

Next, we consider the "square and sum" quadrature detector of Figure 2.2-1(b), the optimum detector for a weak Type 2 signal (independent phase samples) in bandpass Gaussian noise. The test statistic for this detector may be written as

$$z = \sum_{k=1}^K (r_{ck}^2 + r_{sk}^2) \begin{matrix} H_1 \\ \geq \eta \\ H_0 \end{matrix} \quad (2.2-27)$$

J. S. LEE ASSOCIATES, INC.

$$P_D = Q \left[\frac{(80.99)\sqrt{K} - 2K\rho}{2\sqrt{K} \sqrt{1000.9 + 21.8\rho}} \right]. \quad (2.2-35)$$

Thus we anticipate that $P_D \approx 0.5$ when $\rho = 81/2\sqrt{K}$ and observe that the rate of increase in the detection probability as ρ increases will start slowing down at the "breakpoint" $\rho = 1001/22 = 16.6\text{dB}$. For $K=10$, both these effects are observed at or about these values of SNR, even though ten samples are too few to invoke the central limit theorem.

2.3 PERFORMANCE OF CORRELATION DETECTOR IN BANDPASS GAUSSIAN-GAUSSIAN MIXTURE NOISE

Representative of the class of multi-sensor detectors is the bandpass correlator diagrammed in Figure 2.3-1. Two bandpass waveforms $u_1(t)$ and $u_2(t)$, where

$$u_i(t) = A_i \cos(\omega_c t + \theta_i) + n_i(t), \quad i=1, 2; \quad (2.3-1a)$$

$$= u_{ci}(t) \cos \omega_c t + u_{si}(t) \sin \omega_c t, \quad (2.3-1b)$$

are multiplied, then lowpass filtered to produce the output $y(t)$. For the ideal assumption of zonal lowpass filtering, the output can be expressed as

$$y(t) = \frac{1}{2} \{u_{c1}(t) u_{c2}(t) + u_{s1}(t) u_{s2}(t)\}. \quad (2.3-2)$$

The distribution of $y(t)$ for Gaussian noises $n_1(t)$ and $n_2(t)$ was shown in [28]. Briefly, for that case the vector of quadrature components

$$\underline{u} = (u_{c1}, u_{s1}, u_{c2}, u_{s2})^T \quad (2.3-3)$$

is multivariate Gaussian with mean

$$\underline{m}_u = (A_1 \cos \theta_1, A_1 \sin \theta_1, A_2 \cos \theta_2, A_2 \sin \theta_2)^T \quad (2.3-4)$$

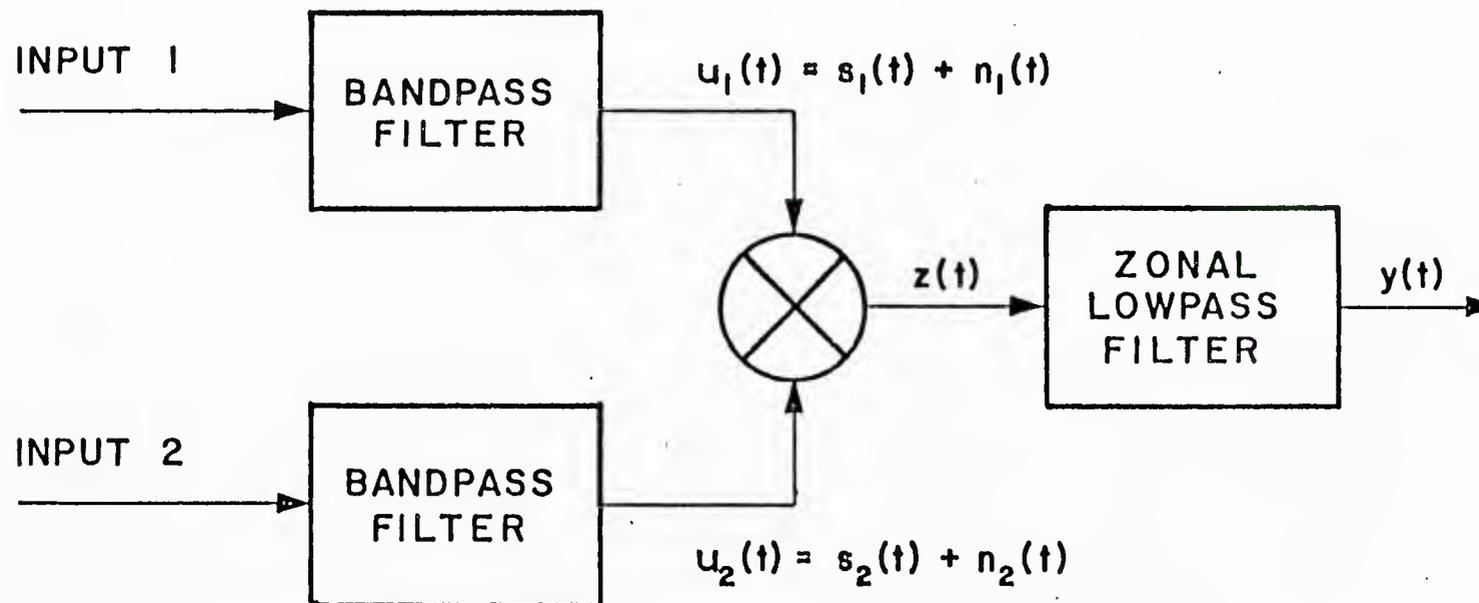


Figure 2.3-1. Bandpass Correlator

and covariance matrix

$$K_u = \begin{bmatrix} \sigma_a^2 & 0 & \xi\sigma_a\sigma_b & r\sigma_a\sigma_b \\ 0 & \sigma_a^2 & -r\sigma_a\sigma_b & \xi\sigma_a\sigma_b \\ \xi\sigma_a\sigma_b & -r\sigma_a\sigma_b & \sigma_b^2 & 0 \\ r\sigma_a\sigma_b & \xi\sigma_a\sigma_b & 0 & \sigma_b^2 \end{bmatrix} \quad (2.3-5)$$

In (2.3-5) σ_a^2 is the variance of $n_1(t)$, σ_b^2 is the variance of $n_2(t)$, ξ is the correlation coefficient between quadrature components which agree in phase and $\pm r$ is the correlation coefficient between components which are in phase quadrature.

Given these definitions, in [28] is shown that the correlator output $y(t)$ is equivalent to the difference between two independent scaled, noncentral chi-squared random variables with two degrees of freedom:

$$y \sim k_1\chi^2(2; \lambda_1) - k_2\chi^2(2; \lambda_2). \quad (2.3-6)$$

In this equivalence, we have

$$k_1 = \sigma_a\sigma_b (\sqrt{1-r^2} + \xi)/4 \quad (2.3-7a)$$

$$k_2 = \sigma_a\sigma_b (\sqrt{1-r^2} - \xi)/4 \quad (2.3-7b)$$

J. S. LEE ASSOCIATES, INC.

ρ_1 and ρ_2 (whose values follow from the covariance matrix) to be random variables. That is,

$$K_u = K_{u_m} \quad \text{with probability } \Pi_m. \quad (2.3-11)$$

For example, we may consider the case that the parameters, with probability $\Pi_1 = 1-\epsilon$, take the values

$$(\sigma_a, \sigma_b, r, \xi) = (\sigma_1, \sigma_1, 0, 0), \quad \text{prob.} = 1-\epsilon; \quad (2.3-12a)$$

and with probability $\Pi_2 = \epsilon$,

$$(\sigma_a, \sigma_b, r, \xi) = (\sigma_2, \sigma_2, 0, \xi_1(\tau)), \quad \text{prob.} = \epsilon. \quad (2.3-12b)$$

The parameter values in (2.3-12a) reflect the assumption of a "background" Gaussian noise situation with equal noise power at the two inputs and no correlation. The parameter values in (2.3-12b) are suggestive of a combined background plus "impulsive" Gaussian noise with equal power $\sigma_2^2 = V^2\sigma_1^2$ at each input, but with a finite correlation between the noise inputs. This correlation is further suggested in (2.3-12b) to be a function of the relative delay of the inputs, or the direction of arrival of the impulsive noise, due perhaps to discrete events located in a specific direction relative to the two sensors whose waveforms are being correlated.

2.3.2 Probability integral

For cases such as given in (2.3-12), where the noise powers are equal at the two inputs and it is also assumed that the signal amplitudes

are equal ($A_1=A_2$), then the probability that the correlator output exceeds a threshold is [29]

$$\begin{aligned}
 \Pr\{y > \eta\} &= (1-\epsilon) \Pr\{y > \eta; \sigma_a = \sigma_b = \sigma_1, \xi = r = 0, A_1 = A_2\} \\
 &+ \epsilon \Pr\{y > \eta; \sigma_a = \sigma_b = \sigma_1 V, r=0, \xi \neq 0, A_1 = A_2\} \\
 &= (1-\epsilon) f(\eta; \rho, \sigma_1^2, 0) \\
 &+ \epsilon f(\eta/V^2; \rho/V^2, \sigma_1^2 V^2, \xi) \qquad (2.3-13)
 \end{aligned}$$

where

$$\begin{aligned}
 f(\eta; \rho, \sigma^2, \xi) &= \Pr \left\{ \frac{\sigma^2(1+\xi)}{4} \chi^2\left(2; \frac{4\rho}{1+\xi}\right) - \frac{\sigma^2(1-\xi)}{4} \chi^2(2; 0) > \eta \right\} \\
 &= \Pr \left\{ \chi^2\left(2; \frac{4\rho}{1+\xi}\right) > \frac{1-\xi}{1+\xi} \chi^2(2) + \frac{4\eta}{\sigma^2(1+\xi)} \right\} \qquad (2.3-14a)
 \end{aligned}$$

The probability above may be solved in terms of Marcum's Q-function, yielding

$$\begin{aligned}
 f(\eta; \rho, \sigma^2, \xi) &= Q\left(\sqrt{\frac{4\rho}{1+\xi}}, \sqrt{\frac{4\eta/\sigma^2}{1+\xi}}\right) \\
 &\quad - \frac{(1-\xi)}{2} \exp\left[-\rho + \frac{2\eta/\sigma^2}{1-\xi}\right] Q\left(\sqrt{\frac{2\rho(1-\xi)}{1+\xi}}, \sqrt{\frac{8\eta/\sigma^2}{1-\xi}}\right).
 \end{aligned} \qquad (2.3-14b)$$

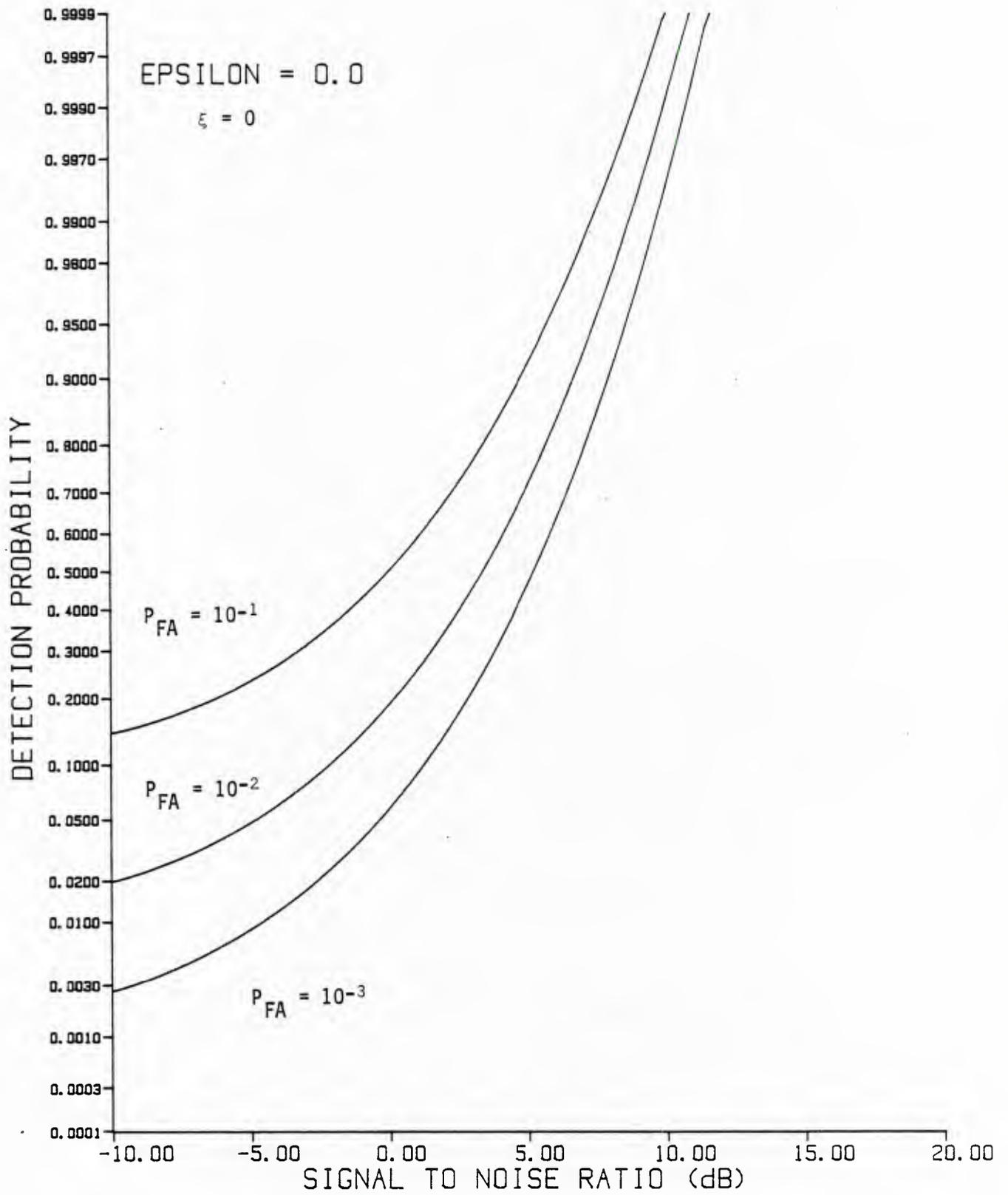


Figure 2.3-2. Performance of bandpass correlation detector in uncorrelated Gaussian noise.

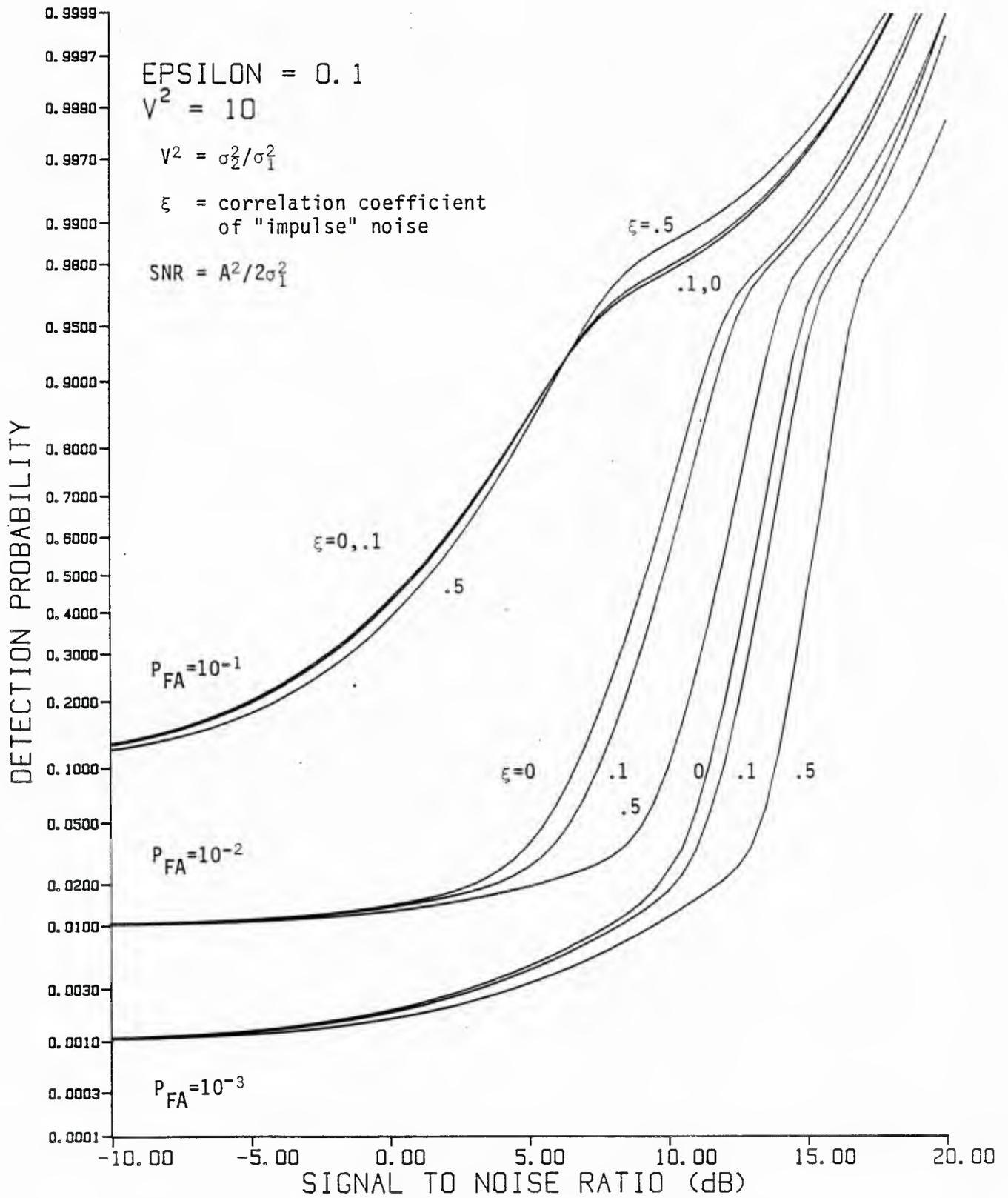


Figure 2.3-3. Performance of bandpass correlation detector in Gaussian-Gaussian mixture noise ($\epsilon=0.1$, $V^2=10$) for different degrees of correlation in "impulsive" component.

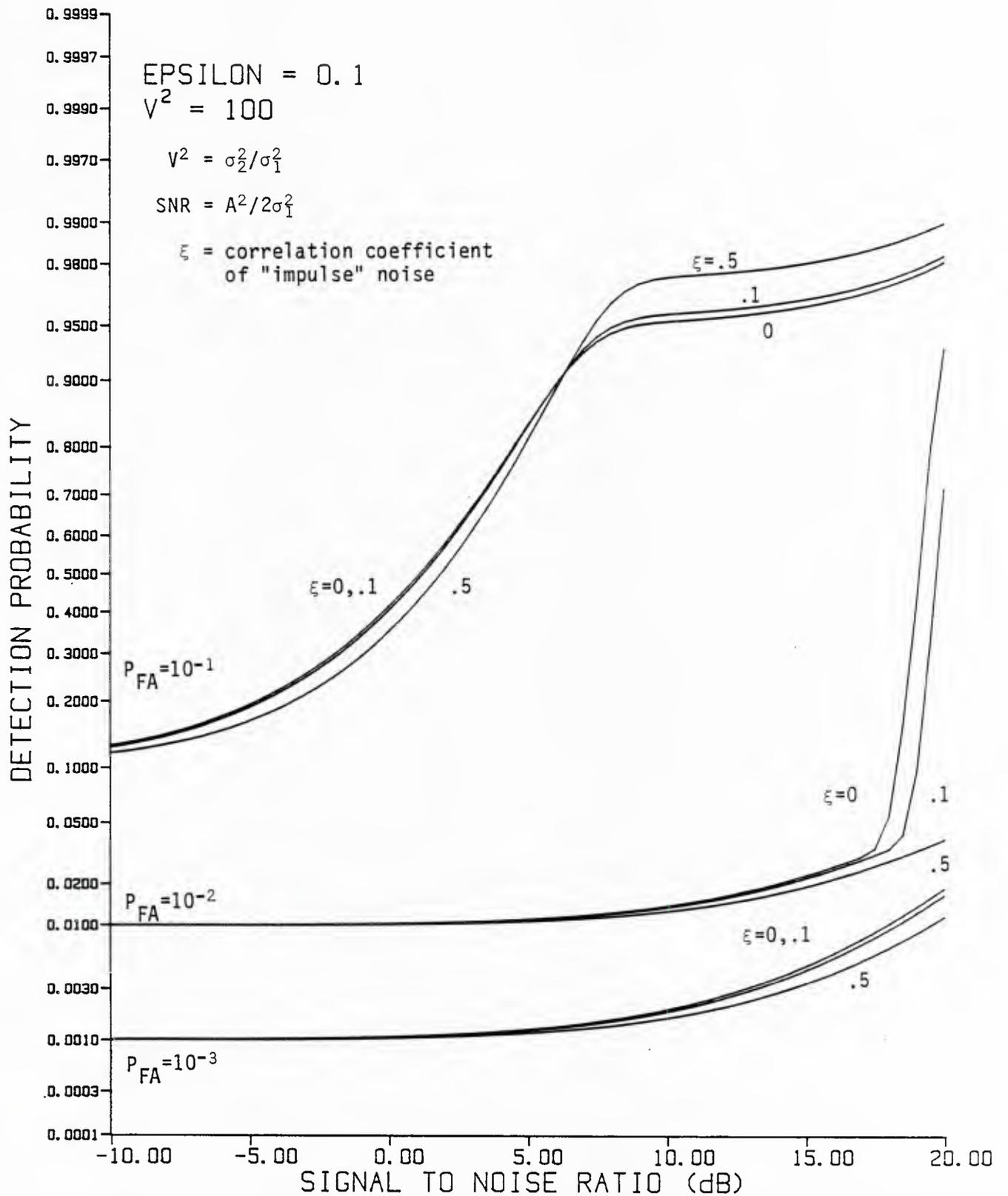


Figure 2.3-4. Performance of bandpass correlation detector in Gaussian-Gaussian mixture noise ($\epsilon=0.1$, $V^2=100$) for different degrees of correlation in "impulsive" component.

J. S. LEE ASSOCIATES, INC.

For 50% detection and $V^2 = 10$, we find that the correlation detector (after subtracting 3dB because of the two channels used) effectively requires 0.5dB less SNR for $P_{FA}=10^{-1}$ and 1.4dB less for $P_{FA}=10^{-2}$. When $V^2 = 100$, the correlation detector in effect requires 2.4dB less for $P_{FA}=10^{-1}$ and 1.6dB less for $P_{FA}=10^{-2}$. Thus in this type of noise the correlation detector seems to have a slight advantage over the conventional noncoherent Gaussian detector when the noise is uncorrelated ($\xi = 0$). However when the correlation is positive ($\xi > 0$), this advantage is decreased. The interpretation of this fact seems to be that the correlator, in using two sensors, acts as a two-element array. When this array is "steered" toward a signal source such that $\theta_1=\theta_2$ and such that the (directional) impulsive Gaussian component is either not correlated at the sensors (effectively at 90° or 270° bearing) or negatively correlated, the effect of this interference is lessened.

3.0 OPTIMUM NONCOHERENT DETECTION IN BANDPASS GAUSSIAN-GAUSSIAN MIXTURE NOISE

In the previous section we considered the performance of detectors which are designed for Gaussian noise, when the actual noise environment is a Gaussian-Gaussian mixture. Departure from Gaussian conditions was shown to result in a loss of detector performance whose severity depends on the mixture parameter ϵ and the variance ratio $\sigma_2^2/\sigma_1^2 = V^2$. It was shown also that using multiple samples to decide whether a signal is present can, but does not necessarily, improve the detector's performance, depending on the time variability of both signal and noise.

Now we consider the performance attainable by optimum detectors for signals in bandpass Gaussian-Gaussian mixture noise, that is, detectors based on the generalized likelihood ratio, and describe how that performance depends on knowledge of signal and noise parameters.

3.1 NON-GAUSSIAN DETECTOR FORMULATION

As a particular case of detection of signals in non-Gaussian noise, we turn to the problem defined as follows: on the basis of the received waveform $r(t)$, $0 < t \leq T$, we wish to accept or reject the null hypothesis

$$H_0: r(t) = n(t) \quad (\text{noise only}) \quad (3.1-1)$$

when the noise is bandpass Gaussian-Gaussian mixture noise,

$$n(t) = n_c(t)\cos\omega_0 t - n_s(t)\sin\omega_0 t \quad (3.1-2)$$

where $f_0 = \omega_0/2\pi$ is the center frequency of the band, and the joint pdf of the quadrature components $n_c(t)$, $n_s(t)$ at a given instant is the bivariate Gaussian-Gaussian mixture pdf

$$P_{nc,ns}(\alpha, \beta) = \frac{1-\epsilon}{2\pi\sigma_1^2} \exp\left\{-\frac{\alpha^2 + \beta^2}{2\sigma_1^2}\right\} + \frac{\epsilon}{2\pi\sigma_2^2} \exp\left\{-\frac{\alpha^2 + \beta^2}{2\sigma_2^2}\right\}. \quad (3.1-3)$$

Detection occurs when H_0 is rejected in favor of the alternative hypothesis

$$H_1: r(t) = n(t) + A\cos[\omega_0 t + \theta(t)], \quad (3.1-4)$$

in which the signal amplitude A is constant during the observation interval* and the signal phase $\theta(t)$ is random. Two different assumptions will be made about the phase: (a) the random phase is constant ("slowly varying") during the observation interval (type 1 signal); or (b) the random phases of samples taken during the observation interval are independent (type 2 signal).

We assume that K samples of r_c and r_s , the quadrature components of $r(t)$, are taken on the interval $(0, T)$. Under the two hypotheses, the joint pdf's of these samples are

$$H_0: P_{\underline{r}_c, \underline{r}_s}(\underline{\alpha}, \underline{\beta} | H_0) = P_{\underline{n}_c, \underline{n}_s}(\underline{\alpha}, \underline{\beta}) \quad (3.1-5a)$$

$$H_1: P_{\underline{r}_c, \underline{r}_s}(\underline{\alpha}, \underline{\beta} | H_1, \underline{s}) = P_{\underline{n}_c, \underline{n}_s}(\underline{\alpha} - \underline{s}_c, \underline{\beta} - \underline{s}_s) \quad (3.1-5b)$$

where the vector notation signifies

* As noted in Section 2, detector performances can be evaluated for non-constant signal amplitudes in a straightforward manner. However, we continue to assume constant amplitude in detector formulations, in order to simplify the analysis somewhat.

$$\underline{r}_c = [r_c(t_1), r_c(t_2), \dots, r_c(t_K)] \quad (3.1-5c)$$

$$\underline{r}_s = [r_s(t_1), r_s(t_2), \dots, r_s(t_K)]$$

$$\underline{s}_c = [s_c(t_1), s_c(t_2), \dots, s_c(t_K)]$$

$$= A \cos \theta [1, 1, \dots, 1] \quad (\text{Type 1})$$

$$= A [\cos \theta_1, \cos \theta_2, \dots, \cos \theta_K] \quad (\text{Type 2}) \quad (3.1-5d)$$

$$\underline{s}_s = [s_s(t_1), s_s(t_2), \dots, s_s(t_K)]$$

$$= A \sin \theta [1, 1, \dots, 1] \quad (\text{Type 1})$$

$$= A [\sin \theta_1, \sin \theta_2, \dots, \sin \theta_K] \quad (\text{Type 2}). \quad (3.1-5c)$$

The test for rejecting H_0 in favor of H_1 is to be based on the generalized likelihood ratio (GLR)

$$\Lambda_{\underline{r}}(\underline{\alpha}, \underline{\beta}) = \frac{E_{\theta} \left\{ p_{\underline{r}_c, \underline{r}_s}(\underline{\alpha}, \underline{\beta} | H_1, \underline{s}) \right\}}{p_{\underline{r}_c, \underline{r}_s}(\underline{\alpha}, \underline{\beta} | H_0)} \quad (3.1-6)$$

3.1.1 Conditional Gaussian Approach

The noise pdf (3.1-3) for a single sample may be viewed as the average over the variance of a conditionally Gaussian pdf. Let $v^2 = \sigma^2 / \sigma_1^2$ be a variance multiplication factor; then (3.1-3) can be understood as

$$p_{nc, ns}(\alpha, \beta) = E_v \left\{ \frac{1}{2\pi\sigma_1^2 v^2} \exp\left(-\frac{\alpha^2 + \beta^2}{2v^2\sigma_1^2}\right) \right\} \quad (3.1-7a)$$

with

$$p_{\underline{V}^2}(\gamma) = (1-\epsilon)\delta(\gamma-1) + \epsilon \delta(\gamma-V^2); \quad V \equiv \frac{\sigma_2^2}{\sigma_1^2}. \quad (3.1-7b)$$

Extension of this concept to multiple samples takes the form

$$p_{\underline{n}_c, \underline{n}_s}(\underline{\alpha}, \underline{\beta}) = E_{\underline{V}^2} \left\{ \frac{(2\pi\sigma_1^2)^{-K}}{v_1^2 v_2^2 \dots v_K^2} \exp \left(- \sum_{k=1}^K \frac{\alpha_k^2 + \beta_k^2}{2v_k^2 \sigma_1^2} \right) \right\}, \quad (3.1-8a)$$

with

$$p_{\underline{V}^2}(\gamma) = \sum_{m=1}^M C_m \delta(\gamma - v_m^2), \quad \sum_{m=1}^M C_m = 1. \quad (3.1-8b)$$

Using this form, the expectation of the H_1 joint pdf over the signal phase becomes

$$\begin{aligned} & E_{\underline{\theta}} \left\{ p_{\underline{n}_c, \underline{n}_s}(\underline{\alpha}, \underline{\beta} | H_1, \underline{s}) \right\} \\ &= E_{\underline{\theta}} \left\{ E_{\underline{V}^2} \left[\frac{(2\pi\sigma_1^2)^{-K}}{v_1^2 v_2^2 \dots v_K^2} \exp \left[- \sum_{k=1}^K \frac{(\alpha_k - A \cos \theta_k)^2 + (\beta_k - A \sin \theta_k)^2}{2v_k^2 \sigma_1^2} \right] \right] \right\} \\ &= E_{\underline{V}^2} \left\{ \frac{(2\pi\sigma_1^2)^{-K}}{v_1^2 v_2^2 \dots v_K^2} \exp \left[- \sum_{k=1}^K \frac{\alpha_k^2 + \beta_k^2 + A^2}{2v_k^2 \sigma_1^2} \right] \right\} \\ &\quad \times E_{\underline{\theta}} \left\{ \exp \left[A \sum_{k=1}^K \frac{\alpha_k \cos \theta_k + \beta_k \sin \theta_k}{v_k^2 \sigma_1^2} \right] \right\}. \quad (3.1-8c) \end{aligned}$$

3.1.2 GLR For Constant Signal Phase

For type 1 signals, the above operations yield

$$E_{\underline{V}^2} \left\{ \frac{(2\pi\sigma_1^2)^{-K}}{v_1^2 v_2^2 \dots v_K^2} \exp \left[- \sum_{k=1}^K \frac{\alpha_k^2 + \beta_k^2 + A^2}{2v_k^2 \sigma_1^2} \right] \right. \\ \left. \times I_0 \left[\frac{A}{\sigma_1^2} \sqrt{\left(\sum_{k=1}^K \frac{\alpha_k}{v_k^2} \right)^2 + \left(\sum_{k=1}^K \frac{\beta_k}{v_k^2} \right)^2} \right] \right\}. \quad (3.1-9)$$

With this result the GLR becomes

$$\Lambda_{\underline{r}}(\underline{\alpha}, \underline{\beta}) = \left(\sum_{m=1}^M C_m \frac{1}{v_{1m}^2 v_{2m}^2 \dots v_{Km}^2} \exp \left[- \sum_{k=1}^K \frac{\alpha_k^2 + \beta_k^2}{2v_{km}^2 \sigma_1^2} \right] \right)^{-1} \\ \times \left(\sum_{m=1}^M C_m \frac{1}{v_{1m}^2 v_{2m}^2 \dots v_{Km}^2} \exp \left[- \sum_{k=1}^K \frac{\alpha_k^2 + \beta_k^2 + A^2}{2v_{km}^2 \sigma_1^2} \right] \right) \\ \times I_0 \left[\frac{A}{\sigma_1^2} \sqrt{\left(\sum_{k=1}^K \frac{\alpha_k}{v_{km}^2} \right)^2 + \left(\sum_{k=1}^K \frac{\beta_k}{v_{km}^2} \right)^2} \right] \quad (3.1-10a)$$

$$= \sum_{m=1}^M W_m(\underline{\alpha}, \underline{\beta}) \Lambda_m(\underline{\alpha}, \underline{\beta}), \quad (3.1-10b)$$

where

$$W_m(\underline{\alpha}, \underline{\beta}) = \frac{C_m (v_{1m}^2 v_{2m}^2 \dots v_{km}^2)^{-1} \exp \left[- \sum_{k=1}^K \frac{\alpha_k^2 + \beta_k^2}{2v_{km}^2 \sigma_1^2} \right]}{\sum_{m=1}^M (\text{numerator})} \quad (3.1-10c)$$

and

$$\begin{aligned} \Lambda_m(\underline{\alpha}, \underline{\beta}) &= \exp \left[- \sum_{k=1}^K \frac{A^2}{2\sigma_1^2 v_{km}^2} \right] I_0 \left[\frac{A}{\sigma_1^2} \sqrt{\left(\sum_{k=1}^K \frac{\alpha_k}{v_{km}^2} \right)^2 + \left(\sum_{k=1}^K \frac{\beta_k}{v_{km}^2} \right)^2} \right], \\ &= \exp \left[-\rho \sum_{k=1}^K v_{km}^{-2} \right] I_0 \left[\frac{\sqrt{2\rho}}{\sigma_1} \sqrt{\left(\sum_{k=1}^K \frac{\alpha_k}{v_{km}^2} \right)^2 + \left(\sum_{k=1}^K \frac{\beta_k}{v_{km}^2} \right)^2} \right], \end{aligned} \quad (3.1-10d)$$

using $\rho \triangleq A^2 / 2\sigma_1^2$.

3.1.3 GLR For Independent Phase Samples

For the Type 2 signal, each $\theta_k \in (0, 2\pi)$ is assumed to be independent, yielding the H_1 joint pdf

$$p_{\underline{r}_c, \underline{r}_s}(\underline{\alpha}, \underline{\beta}; A) = E_{\underline{v}^2} \left\{ \prod_{k=1}^K \frac{(2\pi\sigma_1^2)^{-1}}{v_k^2} \exp \left[- \frac{\alpha_k^2 + \beta_k^2 + A^2}{2\sigma_1^2 v_k^2} \right] I_0 \left[\frac{A}{\sigma_1^2 v_k^2} \sqrt{\alpha_k^2 + \beta_k^2} \right] \right\} \quad (3.1-11)$$

and the GLR

$$\underline{\Lambda}_r(\underline{\alpha}, \underline{\beta}) = \frac{E_{\underline{v}^2} \left\{ p_{\underline{r}_c, \underline{r}_s}(\underline{\alpha}, \underline{\beta}; A | \underline{v}^2) \right\}}{E_{\underline{v}^2} \left\{ p_{\underline{r}_c, \underline{r}_s}(\underline{\alpha}, \underline{\beta}; 0 | \underline{v}^2) \right\}} \quad (3.1-12a)$$

$$\begin{aligned}
 &= \left(\sum_{m=1}^M C_m \frac{1}{v_{1m}^2 v_{2m}^2 \dots v_{km}^2} \exp \left[- \sum_{k=1}^K \frac{\alpha_k^2 + \beta_k^2}{2v_{km}^2 \sigma_1^2} \right] \right)^{-1} \\
 &\times \left(\sum_{m=1}^M C_m \frac{1}{v_{1m} v_{2m} \dots v_{km}} \exp \left[- \sum_{k=1}^K \frac{\alpha_k^2 + \beta_k^2 + A^2}{2v_{km}^2 \sigma_1^2} \right] \prod_{k=1}^K I_0 \left(\frac{A}{\sigma_1^2 v_{km}^2} \sqrt{\alpha_k^2 + \beta_k^2} \right) \right)
 \end{aligned} \tag{3.1-12b}$$

$$= \sum_{m=1}^M W_m(\underline{\alpha}, \underline{\beta}) \Lambda_m(\underline{\alpha}, \underline{\beta}), \tag{3.1-12c}$$

with $W_m(\underline{\alpha}, \underline{\beta})$ given in (3.1-10c), and

$$\Lambda_m(\underline{\alpha}, \underline{\beta}) = \exp \left[- \sum_{k=1}^K \frac{A}{2\sigma_1^2 v_{km}^2} \right] \prod_{k=1}^K I_0 \left[\frac{A}{\sigma_1^2 v_{km}^2} \sqrt{\alpha_k^2 + \beta_k^2} \right] \tag{3.1-12d}$$

$$= \exp \left[-\rho \sum_{k=1}^K v_{km}^{-2} \right] \prod_{k=1}^K I_0 \left(\frac{\sqrt{2\rho}}{\sigma_1 v_{km}^2} \sqrt{\alpha_k^2 + \beta_k^2} \right). \tag{3.1-12e}$$

3.1.4 Example

For example, let $K=2$. Then there are $M=2^K=4$ possible variance vectors $\underline{v}_m^2 = (v_{1m}^2, v_{2m}^2, \dots, v_{Mm}^2)$:

$$\underline{v}_1^2 = (1, 1), \underline{v}_2^2 = (V^2, 1), \underline{v}_3^2 = (1, V^2), \underline{v}_4^2 = (V^2, V^2) \tag{3.1-13a}$$

with probabilities

$$C_m = \Pr\left\{v^2 = \frac{v_m^2}{m}\right\}; m = 1, 2, \dots, M = 2^K. \quad (3.1-13b)$$

In this case, the numerator and denominator of the GLR become

$$\begin{aligned} & \frac{C_1}{\sigma_1^4} \exp\left[-\frac{\alpha_1^2 + \beta_1^2 + \alpha_2^2 + \beta_2^2 + 2A^2}{2\sigma_1^2}\right] I_0\left[A\sqrt{\left(\frac{\alpha_1 + \alpha_2}{\sigma_1^2}\right)^2 + \left(\frac{\beta_1 + \beta_2}{\sigma_1^2}\right)^2}\right] \\ & + \frac{C_2}{\sigma_2^2\sigma_1^2} \exp\left[-\frac{\alpha_1^2 + \beta_1^2 + A^2}{2\sigma_2^2} - \frac{\alpha_2^2 + \beta_2^2 + A^2}{2\sigma_1^2}\right] I_0\left[A\sqrt{\left(\frac{\alpha_1}{\sigma_2^2} + \frac{\alpha_2}{\sigma_1^2}\right)^2 + \left(\frac{\beta_1}{\sigma_2^2} + \frac{\beta_2}{\sigma_1^2}\right)^2}\right] \\ & + \frac{C_3}{\sigma_1^2\sigma_2^2} \exp\left[-\frac{\alpha_1^2 + \beta_1^2 + A^2}{2\sigma_1^2} - \frac{\alpha_2^2 + \beta_2^2 + A^2}{2\sigma_2^2}\right] I_0\left[A\sqrt{\left(\frac{\alpha_1}{\sigma_1^2} + \frac{\alpha_2}{\sigma_2^2}\right)^2 + \left(\frac{\beta_1}{\sigma_1^2} + \frac{\beta_2}{\sigma_2^2}\right)^2}\right] \\ & + \frac{C_4}{\sigma_2^4} \exp\left[-\frac{\alpha_1^2 + \beta_1^2 + \alpha_2^2 + \beta_2^2 + 2A^2}{2\sigma_2^2}\right] I_0\left[A\sqrt{\left(\frac{\alpha_1 + \alpha_2}{\sigma_2^2}\right)^2 + \left(\frac{\beta_1 + \beta_2}{\sigma_2^2}\right)^2}\right] \end{aligned} \quad (3.1-14a)$$

and

$$\begin{aligned} & \frac{C_1}{\sigma_1^4} \exp\left[-\frac{\alpha_1^2 + \beta_1^2 + \alpha_2^2 + \beta_2^2}{2\sigma_1^2}\right] + \frac{C_2}{\sigma_2^2\sigma_1^2} \exp\left[-\frac{\alpha_1^2 + \beta_1^2}{2\sigma_2^2} - \frac{\alpha_2^2 + \beta_2^2}{2\sigma_1^2}\right] \\ & + \frac{C_3}{\sigma_1^2\sigma_2^2} \exp\left[-\frac{\alpha_1^2 + \beta_1^2}{2\sigma_1^2} - \frac{\alpha_2^2 + \beta_2^2}{2\sigma_2^2}\right] + \frac{C_4}{\sigma_2^4} \exp\left[-\frac{\alpha_1^2 + \beta_1^2 + \alpha_2^2 + \beta_2^2}{2\sigma_2^2}\right]. \end{aligned} \quad (3.1-14b)$$

3.2 EFFECT OF VARIANCE DISTRIBUTION ASSUMPTIONS

So far we have not specified the joint pdf $p_{\underline{v}}(\underline{y})$, except to describe it in (3.1-8b) as taking discrete vector values $\{v_m^2\}$, possibly $2^{K=M}$ values since each noise sample has a discrete variance multiplier pdf with two possible values (1 or V^2). The joint pdf should reflect the behavior over time of the non-Gaussian noise process, which we are modelling by a bandpass Gaussian-Gaussian mixture process.

For example, at one extreme we may say that the probabilities C_m of (3.1-8b) are

$$C_1 = 1, \quad C_m = 0, \quad m > 1. \quad (3.2-1)$$

This corresponds to a single variance $\sigma_1^2 v_k^2 = \sigma_1^2$ for all the samples, or, in effect, Gaussian noise. The GLR (3.1-10) then becomes

$$\Lambda_{\underline{r}}(\underline{\alpha}, \underline{\beta}) \Big|_{C_1 = 1} = e^{-KA^2/2\sigma_1^2} I_0 \left[\frac{A}{\sigma_1^2} \sqrt{\left(\sum_{k=1}^K \alpha_k \right)^2 + \left(\sum_{k=1}^K \beta_k \right)^2} \right]. \quad (3.2-2)$$

As illustrated previously in Figure 2.2-1(a), implementation of this Gaussian GLR for the type 1 signal requires separate summing of samples (integration) in the two quadrature channels, then forming the combination of the squares of these sums and comparing this quantity to a threshold. For the type 2 signal, the combining of the squares takes place before summing, as shown in Figure 2.2-1(b).

3.2.1 Slowly-varying Noise Power.

Another limiting case is described by $C_1 = 1-\epsilon$; $C_M = \epsilon$; $C_m = 0$, $m \neq 1, M$. That is,

$$p_{\underline{V}^2}(\underline{Y}) = (1-\epsilon)\delta[\underline{Y} - (1, 1, 1, \dots, 1)] + \epsilon \delta[\underline{Y} - (V_1^2, V_2^2, \dots, V^2)]; \quad (3.2-3)$$

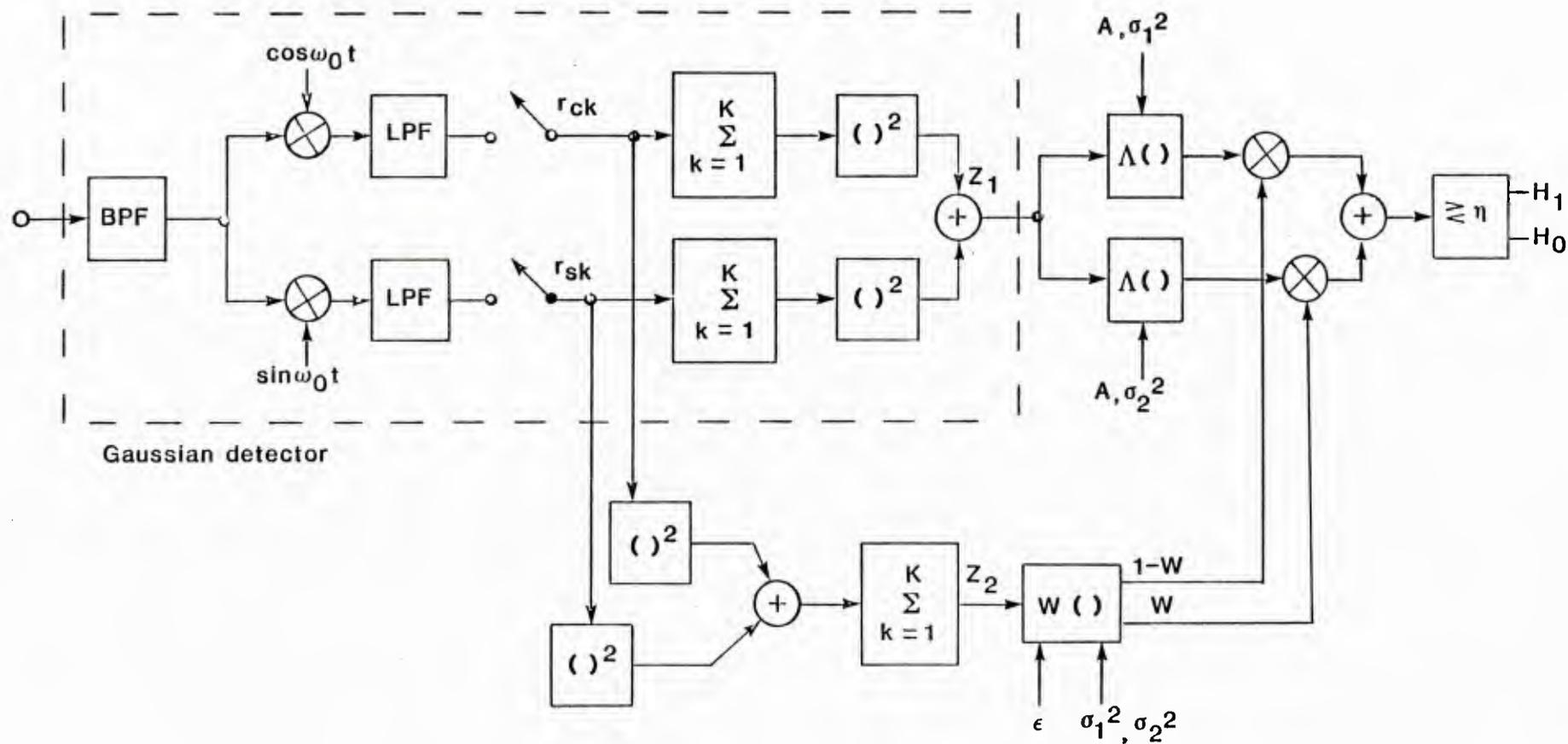
the $\sigma_1^2 V_k^2$ are all equal to σ_1^2 with probability $1-\epsilon$ and all equal to σ_2^2 with probability ϵ . This case corresponds to a "slowly-varying" non-stationary Gaussian noise model with two possible variances. For this case, the GLR is (Type 1 signal)

$$\Lambda_r(\underline{\alpha}, \underline{\beta}) \Big|_{C_1 = 1-\epsilon, C_M = \epsilon} = [1 - W(\underline{\alpha}, \underline{\beta})] e^{-KA^2/2\sigma_1^2} I_0 \left[\frac{A}{\sigma_1^2} \sqrt{\left(\sum_{k=1}^K \alpha_k\right)^2 + \left(\sum_{k=1}^K \beta_k\right)^2} \right] + W(\underline{\alpha}, \underline{\beta}) e^{-KA^2/2\sigma_2^2} I_0 \left[\frac{A}{\sigma_2^2} \sqrt{\left(\sum_{k=1}^K \alpha_k\right)^2 + \left(\sum_{k=1}^K \beta_k\right)^2} \right] \quad (3.2-4a)$$

where

$$W(\underline{\alpha}, \underline{\beta}) = \frac{\epsilon \sigma_2^{-2K} \exp\left\{-\frac{1}{2\sigma_2^2} \sum_{k=1}^K (\alpha_k^2 + \beta_k^2)\right\}}{(1-\epsilon)\sigma_1^{-2K} \exp\left\{-\frac{1}{2\sigma_1^2} \sum_{k=1}^K (\alpha_k^2 + \beta_k^2)\right\} + \epsilon \sigma_2^{-2K} \exp\left\{-\frac{1}{2\sigma_2^2} \sum_{k=1}^K (\alpha_k^2 + \beta_k^2)\right\}} \quad (3.2-4b)$$

We note that the noise samples for this slowly-varying nonstationary model are not independent, although they are uncorrelated. As shown in Figure 3.2-1, the appropriate detector is a modification of the detector for Gaussian noise.



$$\Lambda(z_1; A, \sigma^2) = e^{-KA^2/2\sigma^2} I_0\left(\frac{A}{\sigma^2} \sqrt{z_1}\right)$$

$$W(z_2; \epsilon, \sigma_1^2, \sigma_2^2) = \frac{\epsilon \sigma_2^{-2K} \exp\{-z_2/2\sigma_2^2\}}{(1-\epsilon)\sigma_1^{-2K} \exp\{-z_2/2\sigma_1^2\} + \epsilon\sigma_2^{-2K} \exp\{-z_2/2\sigma_2^2\}}$$

Figure 3.2-1 Optimum detector for sinusoidal signal in slowly-varying Gaussian-Gaussian mixture noise.

3.2.2 Independent Noise Samples

Independence of (α_k, β_k) quadrature sample pairs implies the following set of probabilities in the pdf for the variance vector:

$$\begin{aligned}
 C_1 &= \Pr\{\underline{v}^2 = (1, \dots, 1)\} = (1-\epsilon)^K \\
 C_2 &= \Pr\{\underline{v}^2 = (V_1^2, 1, \dots, 1)\} = \epsilon(1-\epsilon)^{K-1} \\
 &\vdots \\
 C_{M-1} &= \Pr\{\underline{v}^2 = (V_1^2, \dots, V_{M-1}^2, 1)\} = \epsilon^{M-1}(1-\epsilon) \\
 C_M &= \Pr\{\underline{v}^2 = (V_1^2, V_2^2, \dots, V_M^2)\} = \epsilon^K
 \end{aligned} \tag{3.2-5}$$

In general,

$$C_m = \epsilon^{w_m} (1-\epsilon)^{K-w_m} \tag{3.2-6a}$$

where w_m is the number of one's in the binary representation of $(m-1)$:

$$w_m = \text{weight}[(m-1)_2]. \tag{3.2-6b}$$

We observe that direct implementation of the GLR (3.1-10) for the case of Type 1 signal and independent, multiple samples appears to be undesirable for numbers of samples of appreciable size, since the number of separate LR's $\Lambda_m(\cdot)$ in (3.1-10b) grows exponentially with the sample size ($M = 2^K$).

For Type 2 signals and independent noise samples, the weighting concept expressed by (3.1-12) becomes cumbersome, since it is simpler to express the GLR as the product of single-sample GLR's:

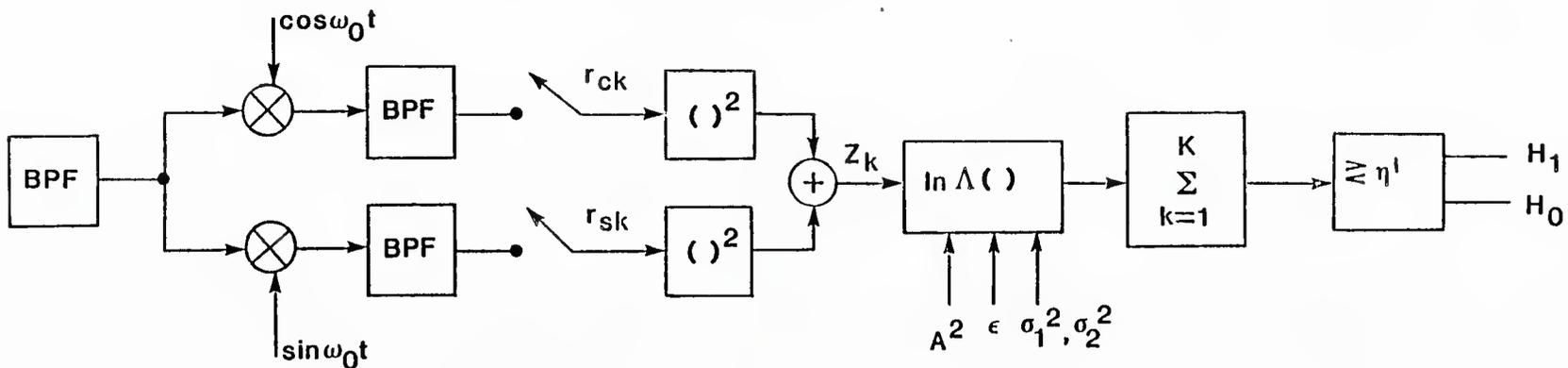
$$\Lambda_{\underline{r}}(\underline{\alpha}, \underline{\beta}) = \prod_{k=1}^K \Lambda(\alpha_k, \beta_k), \tag{3.2-7a}$$

where

$$\Lambda(\alpha_k, \beta_k) = \left\{ (1-\epsilon)\sigma_1^{-2} \exp \left\{ -\frac{\alpha_k^2 + \beta_k^2 + A^2}{2\sigma_1^2} \right\} I_0 \left[\frac{A}{\sigma_1^2} \sqrt{\alpha_k^2 + \beta_k^2} \right] \right. \\ \left. + \epsilon \sigma_2^{-2} \exp \left\{ -\frac{\alpha_k^2 + \beta_k^2 + A^2}{2\sigma_2^2} \right\} I_0 \left[\frac{A}{\sigma_2^2} \sqrt{\alpha_k^2 + \beta_k^2} \right] \right\} \\ \div \left\{ (1-\epsilon)\sigma_1^{-2} \exp \left\{ -\frac{\alpha_k^2 + \beta_k^2}{2\sigma_1^2} \right\} + \epsilon \sigma_2^{-2} \exp \left\{ -\frac{\alpha_k^2 + \beta_k^2}{2\sigma_2^2} \right\} \right\} . \quad (3.2-7b)$$

The implementation of (3.2-7) can be accomplished with accumulators, as illustrated in Figure 3.2-2, since the likelihood ratio test is equivalent to

$$\log \Lambda_{\underline{r}} = \sum_{k=1}^K \log \Lambda(\alpha_k, \beta_k) \underset{H_0}{\overset{H_1}{\geq}} n' . \quad (3.2-8)$$



$$\ln \Lambda(z; A, \epsilon, \sigma_1^2, \sigma_2^2) = \ln \left\{ (1-\epsilon)\sigma_1^{-2} \exp \left\{ -\frac{z+A^2}{2\sigma_1^2} \right\} I_0 \left[\frac{A}{\sigma_1^2} \sqrt{z} \right] + \epsilon\sigma_2^{-2} \exp \left\{ -\frac{z+A^2}{2\sigma_2^2} \right\} I_0 \left[\frac{A}{\sigma_2^2} \sqrt{z} \right] \right\} - \ln \left\{ (1-\epsilon)\sigma_1^{-2} \exp \left\{ -z/2\sigma_1^2 \right\} + \epsilon \sigma_2^{-2} \exp \left\{ -z/2\sigma_2^2 \right\} \right\}$$

Figure 3.2-2. Optimum detector for noncoherent signal and independent Gaussian-Gaussian mixture noise samples.

3.3 PERFORMANCE OF SINGLE-SAMPLE DETECTORS

Before evaluating the performance of detectors based on the GLR for multiple samples ($K > 1$), in this section we evaluate the detection performances of the GLR and other detectors for a single sample pair of quadrature components in order to develop an understanding of the non-Gaussian detection problem. For a single sample, the Type 1 and Type 2 signal phase models are the same.

3.3.1 Form of GLR Detector

For one sample ($K=1$), the GLR in (3.1-10) becomes

$$\Lambda_r(r_c, r_s) = [1 - W(r_c, r_s)] e^{-A^2/2\sigma_1^2} I_0 \left[\frac{A}{\sigma_1} \sqrt{r_c^2 + r_s^2} \right] + W(r_c, r_s) e^{-A^2/2\sigma_2^2} I_0 \left[\frac{A}{\sigma_2} \sqrt{r_c^2 + r_s^2} \right] \quad (3.3-1a)$$

where

$$W(r_c, r_s) = \frac{\epsilon \sigma_2^{-2} \exp \left\{ -\frac{r_c^2 + r_s^2}{2\sigma_2^2} \right\}}{(1-\epsilon) \sigma_1^{-2} \exp \left\{ -\frac{r_c^2 + r_s^2}{2\sigma_1^2} \right\} + \epsilon \sigma_2^{-2} \exp \left\{ -\frac{r_c^2 + r_s^2}{2\sigma_2^2} \right\}} \quad (3.3-1b)$$

We observe that the GLR is a function of the envelope only, so that its implementation involves formation of $x = R^2 = r_c^2 + r_s^2$, followed by a nonlinear function:

$$\Lambda_r = f(x; \epsilon, V^2, \sigma_1^2, \rho)$$

$$= \frac{(1-\epsilon)V^2 \exp \left\{ -\frac{x}{2\sigma_1^2} - \rho \right\} I_0(\sqrt{2\rho x}/\sigma_1) + \epsilon \exp \left\{ -\frac{1}{V^2} \left(\frac{x}{2\sigma_1^2} + \rho \right) \right\} I_0(\sqrt{2\rho x}/\sigma_1 V^2)}{(1-\epsilon)V^2 \exp \left\{ -\frac{x}{2\sigma_1^2} \right\} + \epsilon \exp \left\{ -\frac{x}{2\sigma_1^2 V^2} \right\}}$$

(3.3-2a)

using $V^2 \triangleq \frac{\sigma_2^2}{\sigma_1^2}$ and $\rho \triangleq \frac{A^2}{2\sigma_1^2}$.

(3.3-2b)

This function is parametric in signal as well as in noise parameters. To illustrate the influences of the various parameters, plots of (3.3-2) are shown in Figures 3.3-1 to 3.3-6. In each figure, ϵ and V^2 assume given values while ρ is the parameter indexing the family of curves, which are plotted as functions of x/σ_1^2 , the squared envelope sample value normalized by the smaller of the two mixture noise powers.

The curves in Figures 3.3-1 to 3.3-6 show that the form of the detector for this type of non-Gaussian noise is very dependent on the a priori value of ρ , the SNR which pertains when the signal is present. This behavior is significantly different from the Gaussian case (single sample) in only one respect: the characteristic is not monotonic. What is meant by this statement can be explained as follows:

(100,014)LRPLOTS 16-APR-85 13,57,38 3

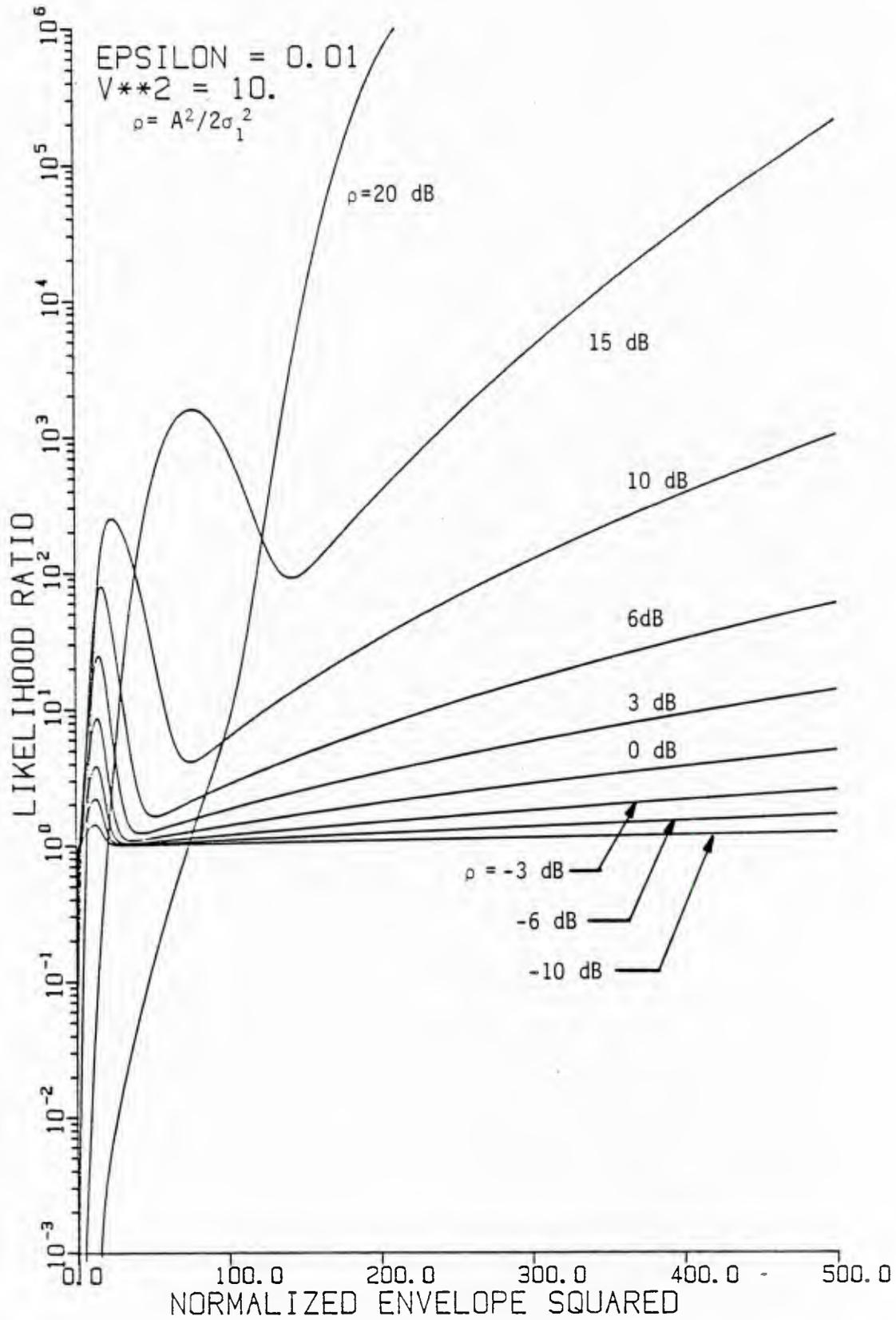


Figure 3.3-1. Likelihood ratio for Gaussian-Gaussian mixture noise ($\epsilon = 0.01, V^2 = 10$), parameterized by SNR.

[100.014]LRPLOTS 16-APR-85 13.57,38 4

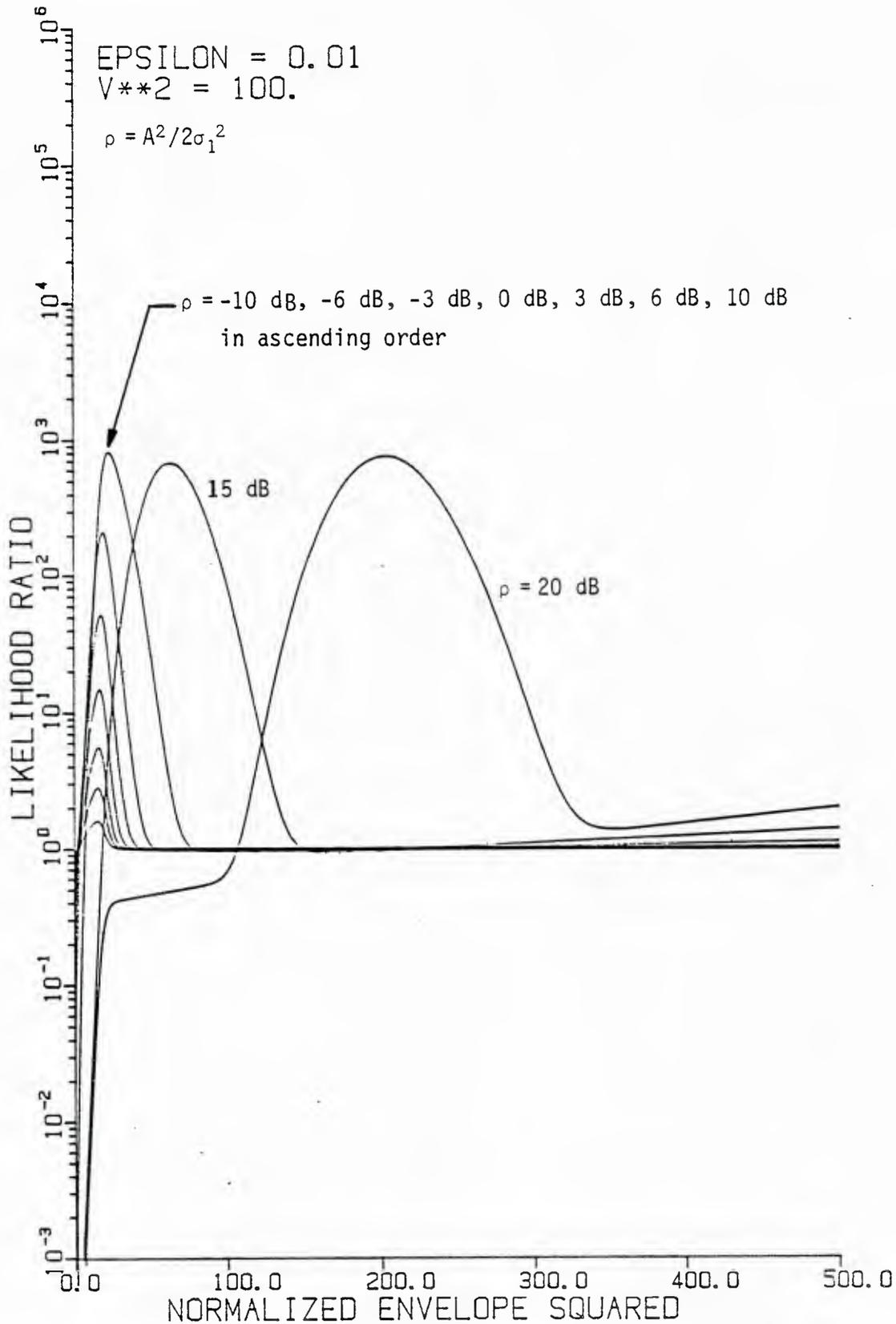


Figure 3.3-2. Likelihood ratio for Gaussian-Gaussian mixture noise ($\epsilon = 0.01$, $V^2 = 100$), parameterized by SNR.

(100.014)LRPLOTS 16-APR-85 13:57:38 5

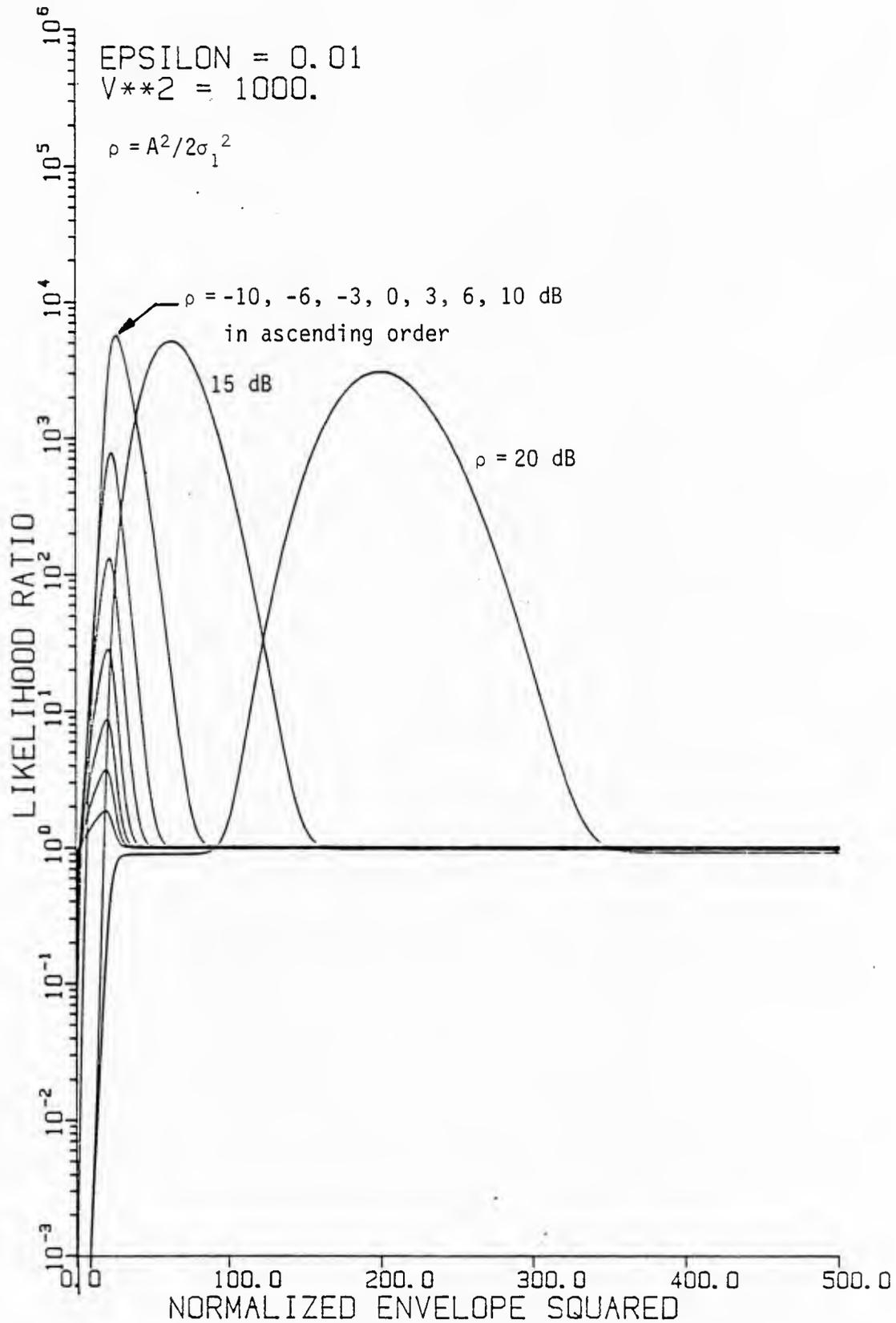


Figure 3.3-3. Likelihood ratio for Gaussian-Gaussian mixture noise ($\epsilon = 0.01$, $V^2 = 1000$), parameterized by SNR.

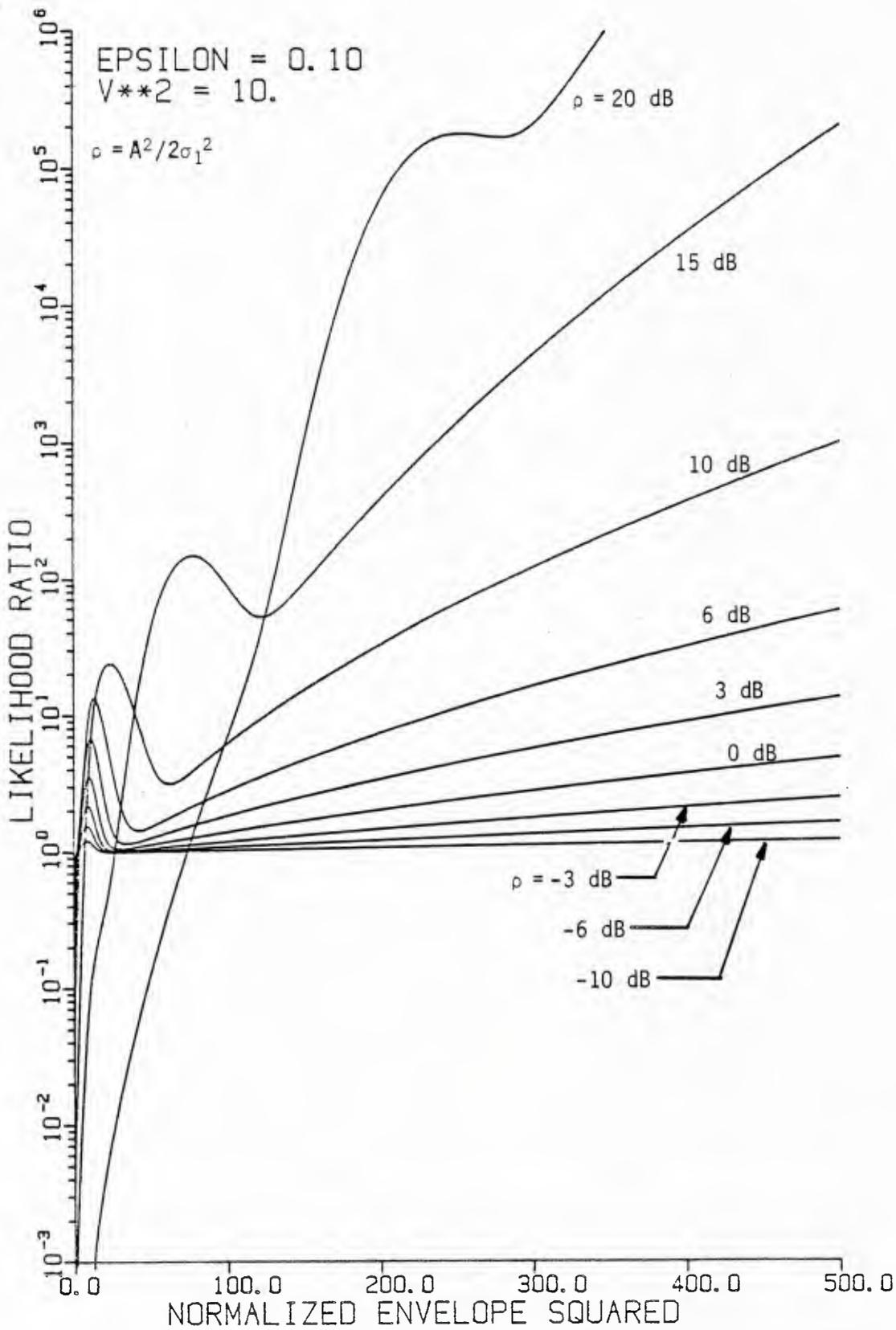


Figure 3.3-4. Likelihood ratio for Gaussian-Gaussian mixture noise ($\epsilon=0.1$, $V^2=10$), parameterized by SNR.

[100,014]LRPLOTS 16-APR-85 13.16.56 1

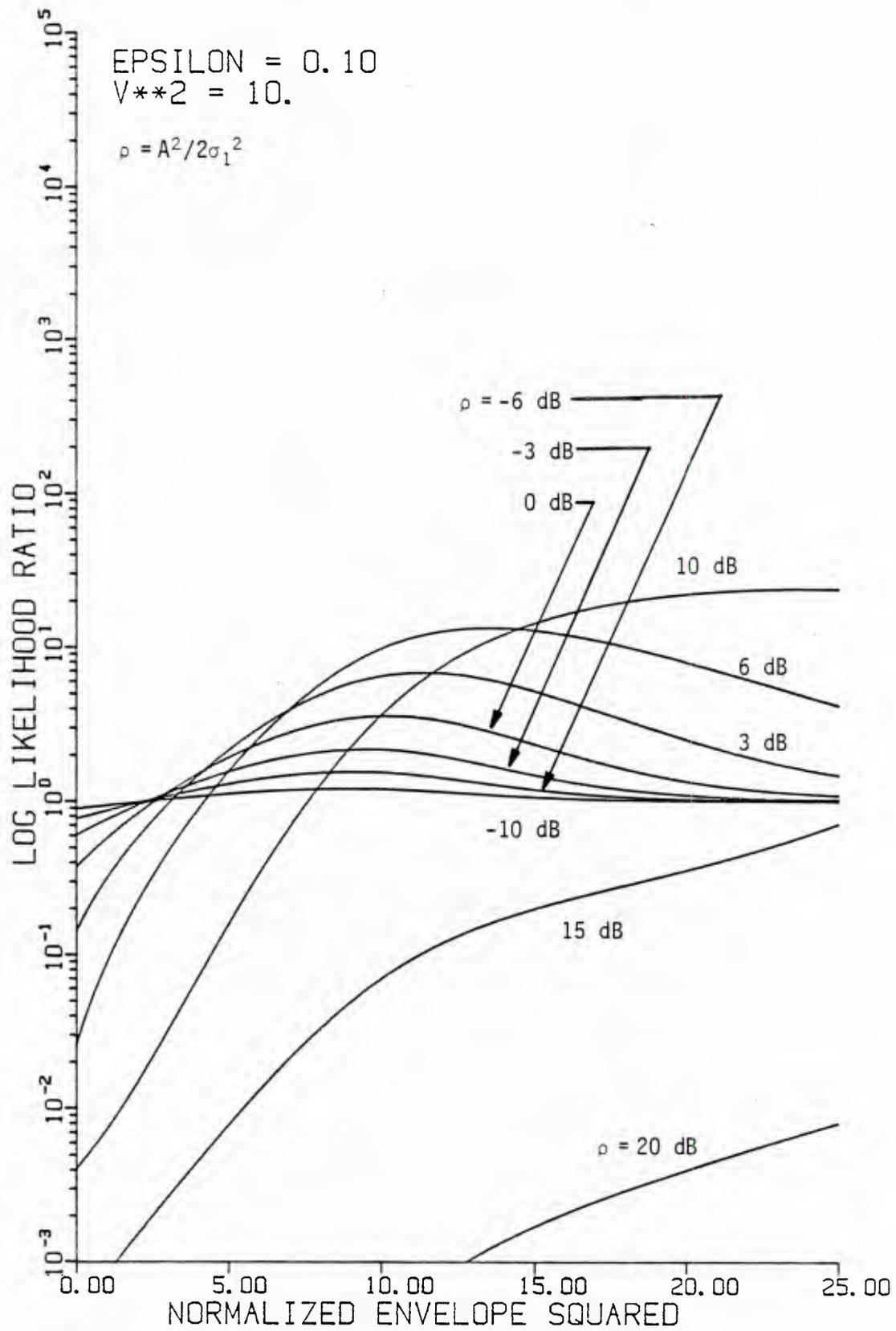


Figure 3.3-5. Likelihood ratio for Gaussian-Gaussian mixture noise ($\epsilon = 0.01$, $V^2 = 10$), parameterized by SNR (detail of Figure 3.3-4).

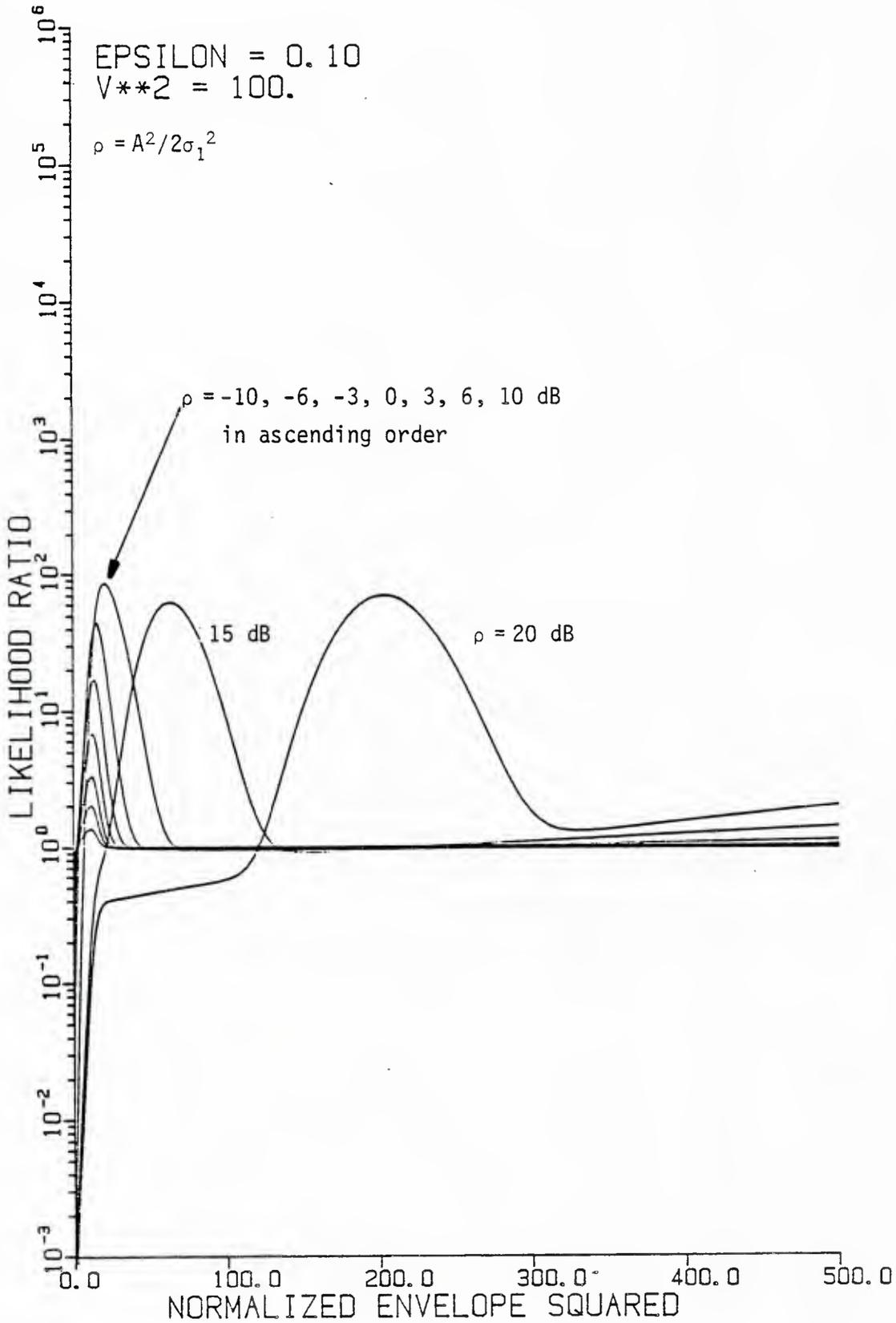


Figure 3.3-6. Likelihood ratio for Gaussian-Gaussian mixture noise ($\epsilon = 0.1$, $V^2 = 100$), parameterized by SNR.

J. S. LEE ASSOCIATES, INC.

Even in the Gaussian case, straightforward formulation of the GLR gives a function which is dependent on SNR, namely

$$\Lambda(x;\rho) = e^{-\rho} I_0 \left(\frac{1}{\sigma} \sqrt{2\rho x} \right). \quad (\text{Gaussian GLR}) \quad (3.3-3)$$

The false alarm probability for this case is

$$P_{FA} = \Pr \left\{ e^{-\rho} I_0 \left(\frac{1}{\sigma} \sqrt{2\rho x} \right) > \lambda | H_0 \right\} = \Pr \left\{ x > \eta(\sigma, \rho) | H_0 \right\}, \quad (3.3-4)$$

since $\Lambda(x;\rho)$ is monotonic. That is, the probability that the GLR is greater than some threshold λ is entirely equivalent to the probability that $R^2=x$ is greater than another threshold,

$$\eta(\sigma, \rho) = \frac{\sigma^2}{2\rho} \left[I_0^{-1} (e^{\rho \lambda(\rho)}) \right]^2, \quad \eta > 0, \quad (3.3-5)$$

using the notation $I_0^{-1}(\cdot)$ to indicate the inverse of the function $I_0(\cdot)$. In Neyman-Pearson detection, the P_{FA} is fixed at some value α . This in turn fixes $\eta(\sigma, \rho) = \eta_\alpha(\sigma)$ for all values of ρ . Therefore, in the Gaussian case no matter what the SNR is, the receiver decision is based on comparing x to the false alarm threshold η_α . The same statement is true for all GLR's which are monotonic functions of x . It follows that the single-sample detection probabilities for all decision variables which are monotonic functions of x are also equal, since

$$P_D = \Pr \left\{ f(x;\rho, \sigma) > \lambda_\alpha(\rho, \sigma) | H_1 \right\} = \Pr \left\{ x > \eta_\alpha(\sigma) | H_1 \right\} \quad (3.3-6)$$

for all of them. Now, as illustrated in Figures 3.3-1 to 3.3-6, the GLR for Gaussian-Gaussian noise is not monotonic; consequently, the inverse mapping of the GLR to x yields false alarm thresholds which depend on the SNR.

A further description of the dependence of the detector structure on the a priori SNR, ρ , is provided by the following considerations. Suppose the desired false alarm probability is $P_{FA} = \alpha$; for monotonic GLR's this requirement is equivalent to $x > \eta_\alpha$ with probability α . But for non-monotonic GLR's the requirement in general is

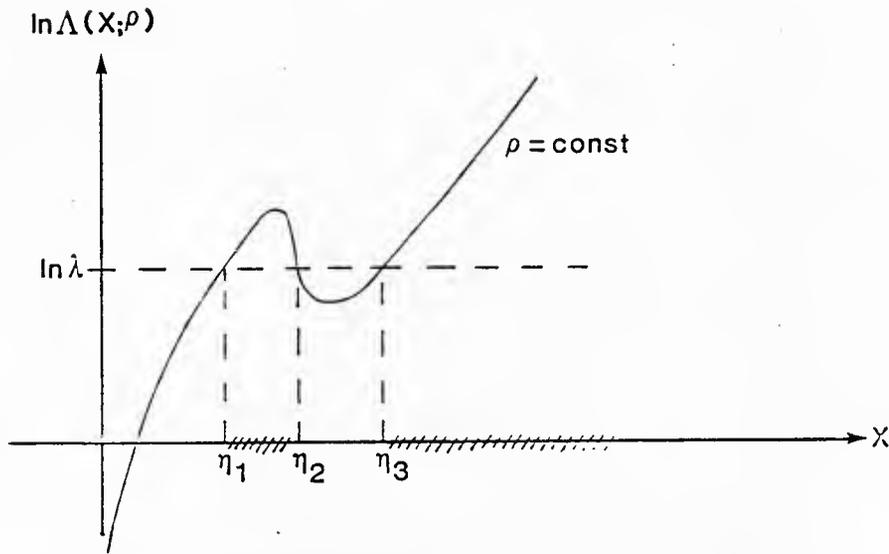
$$\begin{aligned} \alpha &= \Pr \{ \Lambda(x; \rho) > \lambda(\rho) \} \\ &= \Pr \{ \eta_1(\rho) < x < \eta_2(\rho) \} + \Pr \{ x > \eta_3(\rho) \}, \end{aligned} \quad (3.3-7)$$

as illustrated in Figure 3.3-7a; the region of x corresponding to $\Lambda > \lambda$ involves three thresholds. However, for moderate ρ values, the non-monotonic behavior of $\Lambda(x; \rho)$ is confined to a certain region of (Λ, x) as shown in Figure 3.3-7b, and if the quadrature detector false alarm threshold η_α (Table 2.2-1 and Figures 2.2-2 to 2.2-5) falls outside this region ($\eta_\alpha < \eta_{\alpha_1}$ or $\eta_\alpha > \eta_{\alpha_2}$ in Figure 3.3-6), the performance of the GLR receiver is the same as for square-law envelope detector. For large a priori ρ , then we expect the non-Gaussian GLR to yield the same performance as the square-law envelope detector.

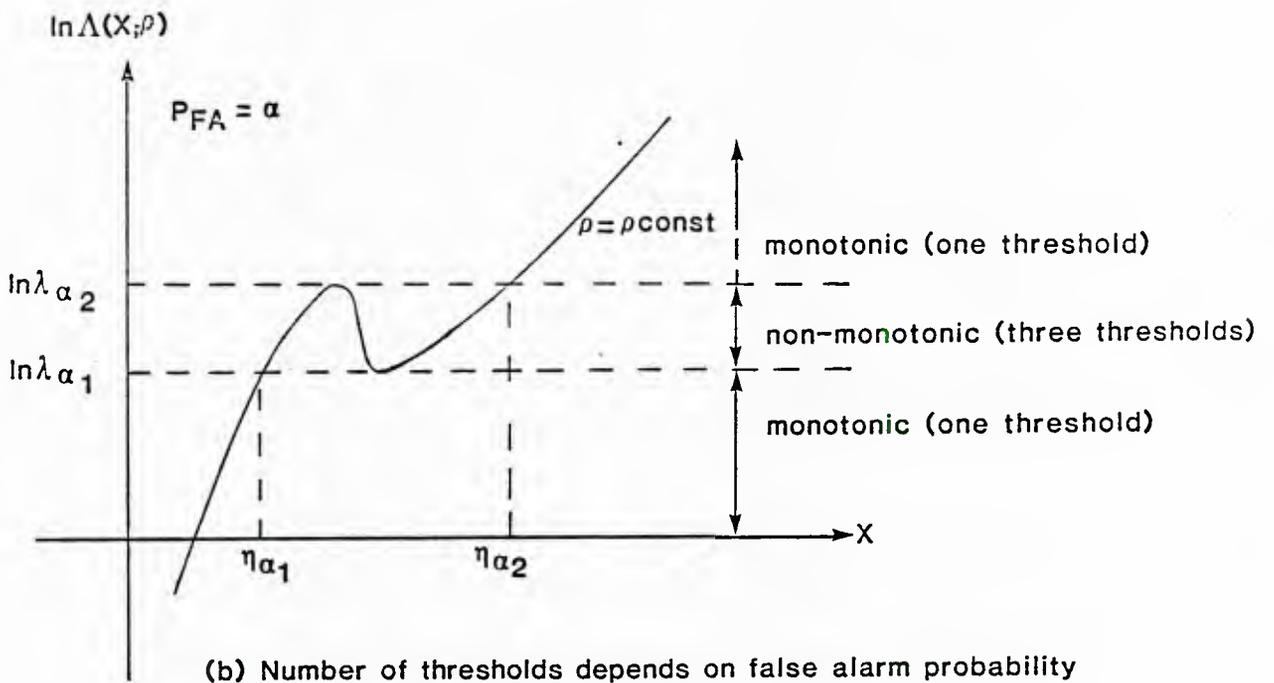
Implementation of the GLR for a single sample can be performed in concept using the configuration diagrammed in Figure 3.3-8. This implementation approach makes use of the mixture form of the GLR discussed in Section 1.2.3. We observe that two function generators are required, one for the parametric likelihood ratio and one for the weighting function. It is also clear from the diagram that the a priori information required consists of the parameters σ_1^2 , ϵ , V^2 , and ρ . In practice these parameters may be imperfectly estimated; however, for the present we shall assume that they are known or estimated precisely.

3.3.2 False Alarm Probability

The generalized likelihood ratio (3.3-2) depends on the SNR ρ in such a way that an equivalent statistic not parametric in the SNR does not exist for testing the hypotheses H_1 (signal present, with given SNR) against

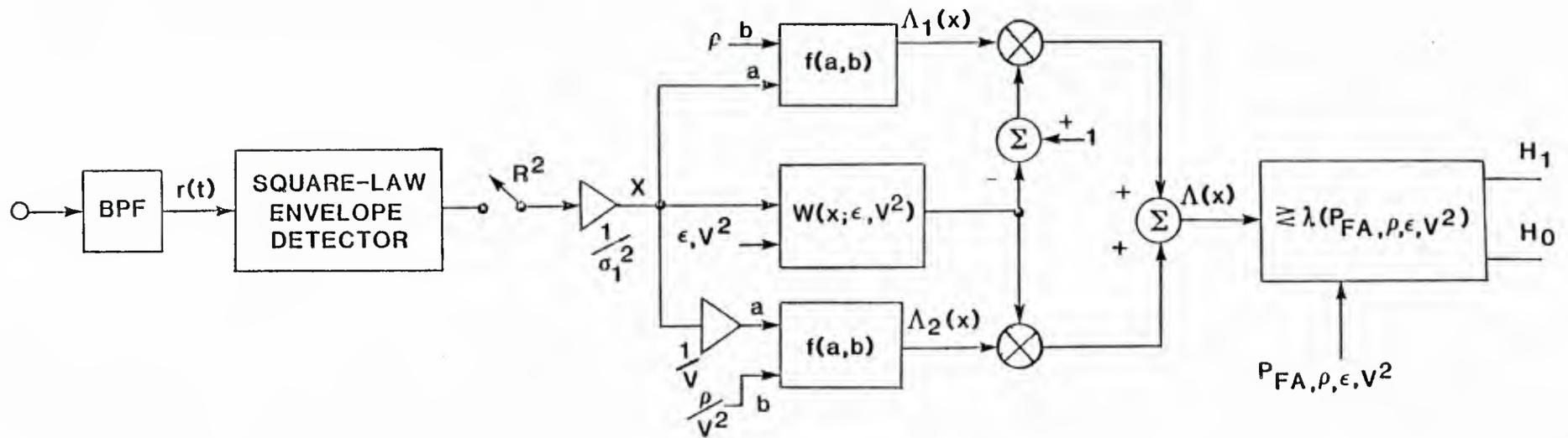


(a) General situation (three thresholds)



(b) Number of thresholds depends on false alarm probability

Fig 3.3-7 Dependence of detector false alarm thresholds on shape of likelihood ratio.



$$\Lambda(x) = [1-W(x)] \Lambda_1(x) + W(x) \Lambda_2(x)$$

$$\text{where } \Lambda_1(x) = f(x, \rho), \Lambda_2(x) = f\left(\frac{x}{V}, \frac{\rho}{V^2}\right)$$

$$f(a, b) = e^{-b} I_0(\sqrt{2ab})$$

$$\text{and } W(x) = \epsilon \exp\{-x/2V^2\} / [(1-\epsilon)V^2 \exp\{-\frac{x}{2}\} + \epsilon \exp\{-\frac{x}{2V^2}\}]$$

FIGURE 3.3-8 CONCEPTUAL IMPLEMENTATION OF GLR DETECTOR

the hypothesis H_0 (noise only). That is, a uniformly most powerful (UMP) test statistic does not exist for this problem ([19], p. 91). Therefore it is necessary to distinguish between an a priori or assumed SNR, which we shall denote by ρ_0 , and the actual SNR, which we continue to denote by ρ .

With this understanding, the false alarm probability for bandpass Gaussian-Gaussian mixture noise can be expressed by

$$\begin{aligned} P_{FA} &= \Pr \{ \Lambda_r(x; \rho_0) > \lambda | \rho=0 \} \\ &= \Pr \{ x \in R_x(\lambda, \rho_0) | \rho=0 \} , \end{aligned} \quad (3.3-8)$$

where x is the sampled envelope-squared, λ is a threshold for the likelihood function; and $R_x(\lambda, \rho_0)$ is region for x defined by λ and ρ_0 . As explained previously with the help of Figure 3.3-7, this region involves either one threshold or three thresholds:

$$R_x(\lambda, \rho_0) \equiv \begin{cases} x > \eta_1, \eta = \Lambda^{-1}(\lambda; \rho_0) \text{ single-valued;} \\ \eta_1 < x < \eta_2, x > \eta_3, \\ \eta = \Lambda^{-1}(\lambda; \rho_0) \text{ multiple-valued} \end{cases} \quad (3.3-9)$$

Thus the single-sample detector may be implemented simply by comparing the squared-envelope sample value to the threshold(s); it is not necessary to implement the GLR directly, as diagrammed in Figure 3.3-8.

Explicitly, the false alarm probability is, using (3.3-9) in (3.3-8),

$$P_{FA} = P_0(\eta_1), \quad \eta = \Lambda^{-1}(\lambda; \rho_0) \text{ single-valued}; \quad (3.3-10a)$$

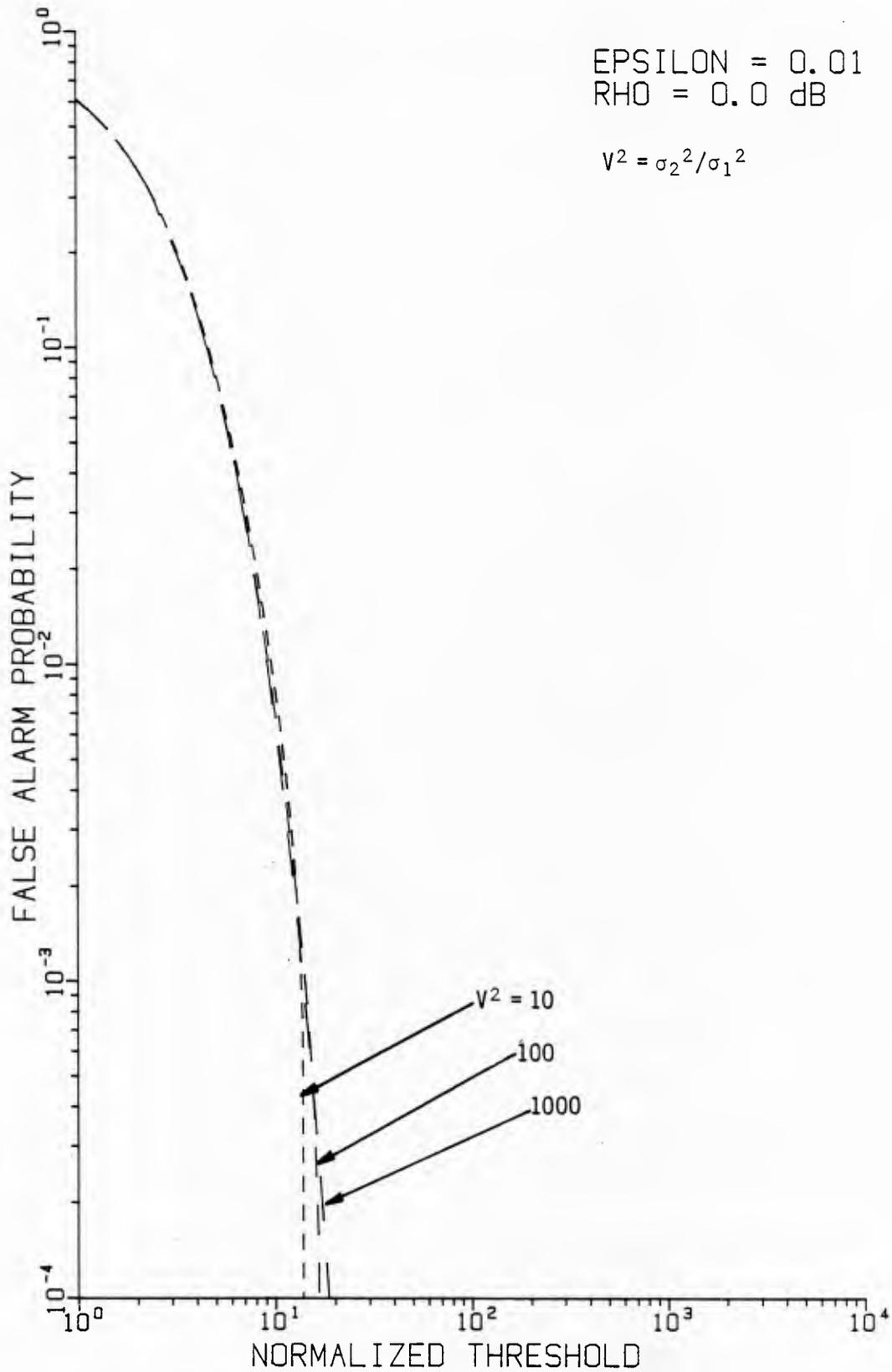
$$= P_0(\eta_1) - P_0(\eta_2) + P_0(\eta_3), \quad \eta = \Lambda^{-1}(\lambda; \rho_0) \text{ multiple-valued}; \quad (3.3-10b)$$

where

$$P_0(\eta) \triangleq (1-\epsilon) e^{-\eta/2\sigma_1^2} + \epsilon e^{-\eta/2\sigma_1^2 V^2}. \quad (3.3-11)$$

Since $P_0(\eta)$ is identical to the false alarm probability for the Gaussian detector (2.2-10), we can observe from (3.3-10) that the P_{FA} for the optimum detector is, for the same threshold η_1 , less than or equal to that obtained using the Gaussian detector. It is less when η_1 falls in the non-monotonic region of the likelihood ratio, and equal, otherwise. This interpretation of (3.3-10) is confirmed by the curves shown in Figures 3.3-9 to 3.3-12.

Figures 3.3-9 and 3.3-10 give the false alarm probability for the SNR-dependent GLR when $\epsilon = 0.01$ and $\rho_0 = 0$ dB and 15 dB, respectively. In order to compare with previous results, we have plotted P_{FA} vs η_1 , the smallest of the thresholds when there are more than one. These two figures correspond to the case shown previously in Figure 2.2-2 for the Gaussian receiver. The most obvious effect seen in the new figures, as compared with the old, is that the false alarm thresholds are reduced by orders of magnitude. The effect is especially pronounced for high SNR; the sudden decreases in P_{FA} as the threshold increases occur when the threshold $\lambda = \Lambda^{-1}(\eta_1; \rho_0)$ begins to fall in the non-monotonic portion of the GLR characteristic (compare Figures 3.3-3 and 3.3-10).



[100.014]FALSE 18-APR-85 11:43:54 3

Figure 3.3-9. False alarm probability for optimum detector in Gaussian-Gaussian mixture noise ($\epsilon = 0.01$), with assumed SNR of 0.0 dB and parametric in variance ratio.

EPSILON = 0.01
RHO = 15.0 dB

$$V^2 = \sigma_2^2 / \sigma_1^2$$

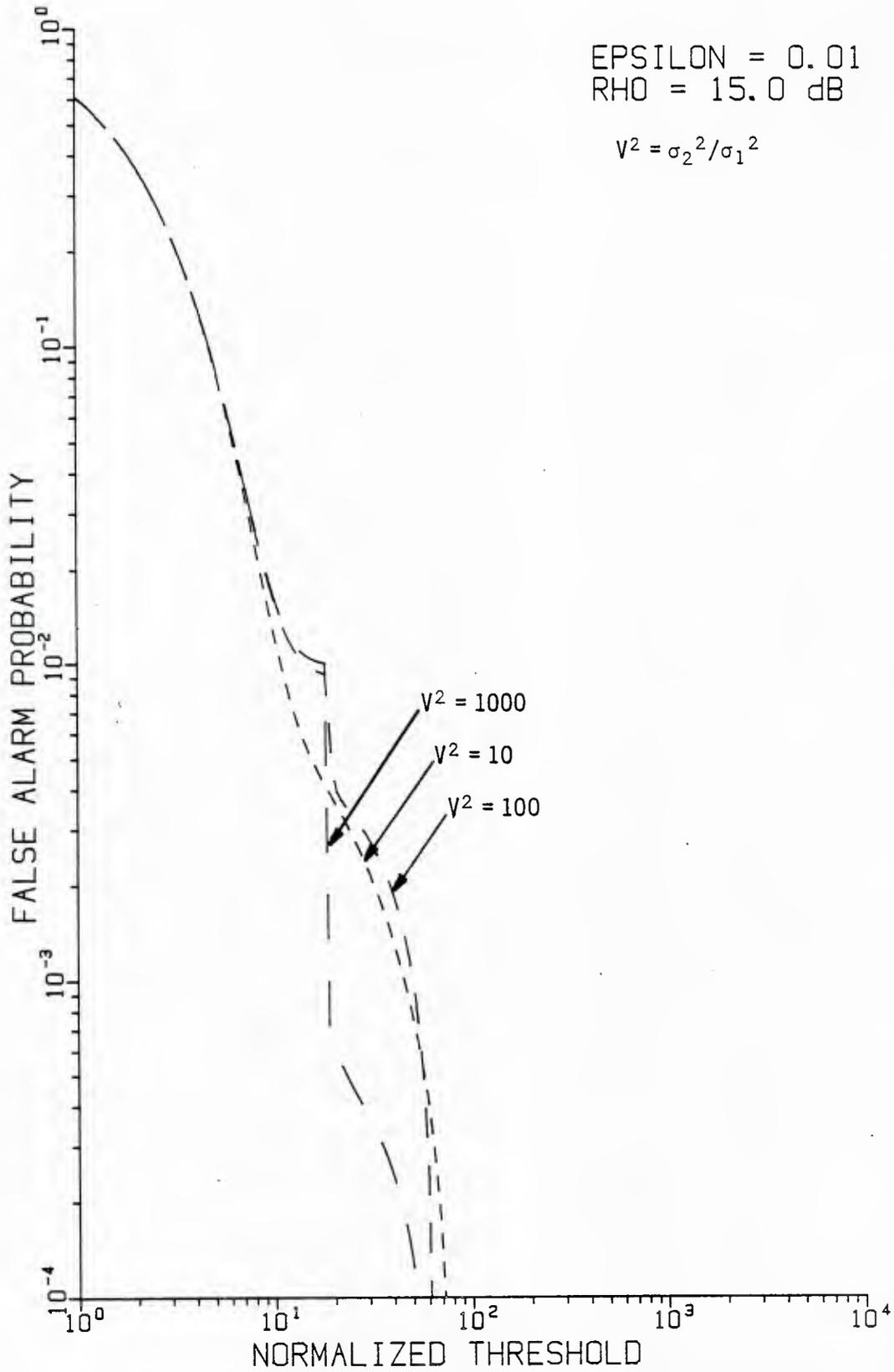


Figure 3.3-10. False alarm probability for optimum detector in Gaussian-Gaussian mixture noise ($\epsilon = 0.01$), with assumed SNR of 15 dB and parametric in variance ratio.

Similar results for $\epsilon = 0.1$ are given in Figures 3.3-11 and 3.3-12 for $\rho_0 = 0$ and 15 dB, respectively. These may be compared to the Gaussian detector's false alarm probability as shown previously in Figure 2.2-3, and the threshold values for which the sudden decreases in P_{FA} occur can be identified with the non-monotonic GLR behavior for $\epsilon = 0.1$ given in Figure 3.3-7 for $\rho_0 = 15$ dB.

3.3.3 Detection Performance.

For fixed P_{FA} and assumed or a priori SNR value ρ_0 , the probability of detection for the optimum detector in Gaussian-Gaussian mixture noise can be written

$$\begin{aligned} P_D &= P_D(\rho; P_{FA}, \rho_0) \\ &= \Pr\{\Lambda_r(x; \rho_0) > \lambda_\alpha | \rho \neq 0\} \end{aligned} \quad (3.3-12)$$

where λ_α is defined by the constraint

$$P_{FA} = \Pr\{\Lambda_r(x; \rho_0) > \lambda_\alpha | \rho = 0\} = \alpha. \quad (3.3-13)$$

As discussed in the previous section, the event of the likelihood ratio $\Lambda_r(x; \rho_0)$ exceeding some threshold λ_α is equivalent to the squared envelope x being in some region $R_x(\lambda_\alpha, \rho_0)$, which can be defined by a single threshold η or by three thresholds (η_1, η_2, η_3) , depending on whether the GLR is monotonic at $\Lambda_r = \lambda_\alpha$. Therefore the P_D can be calculated by the expression

$$P_D = P_1(\rho; \eta_1) \quad , \quad \eta = \Lambda^{-1}(\lambda_\alpha; \rho_0) \text{ single-valued;} \quad (3.3-14a)$$

$$= P_1(\rho; \eta_1) - P_1(\rho; \eta_2) + P_1(\rho; \eta_3),$$

$$\eta = \Lambda^{-1}(\lambda_\alpha; \rho_0) \text{ multiple-valued;} \quad (3.3-14b)$$

[100,014]FALSE 18-APR-85 11:43:54 1

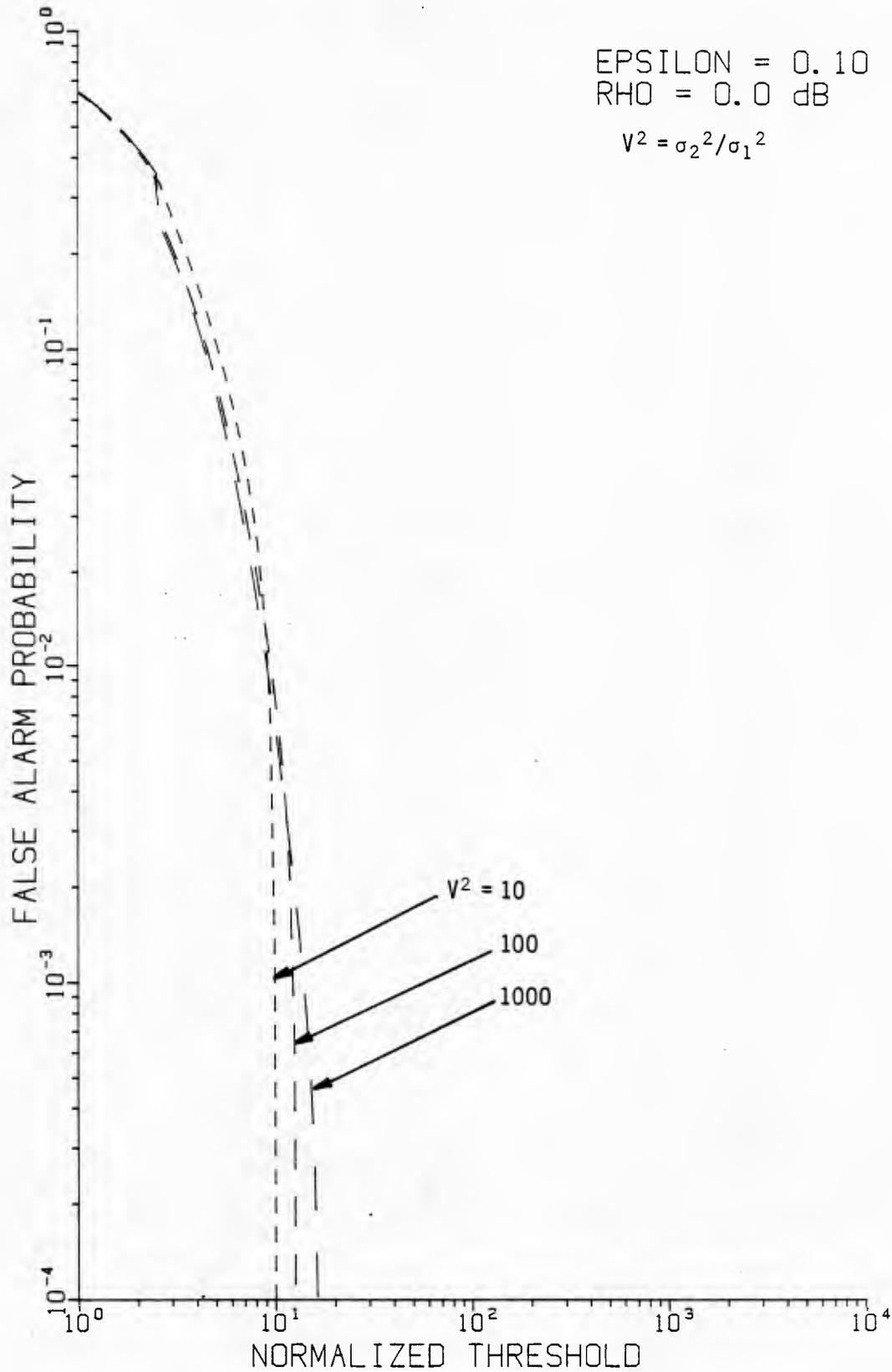
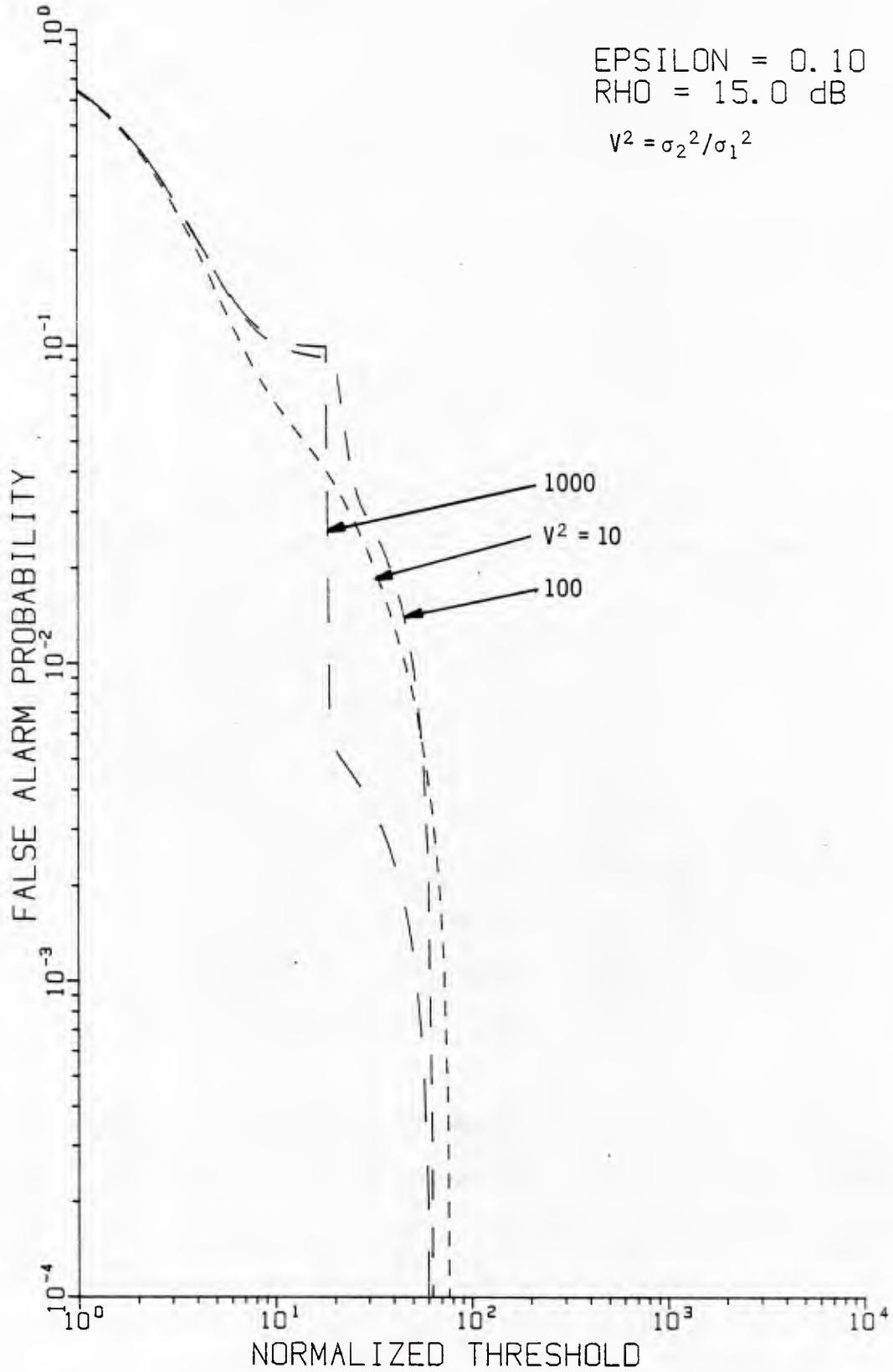


Figure 3.3-11. False alarm probability for optimum detector in Gaussian-Gaussian mixture noise ($\epsilon = 0.1$), with assumed SNR of 0.0 dB and parametric in variance ratio.



[100,014]FALSE 18-APR-85 11:43:54 2

Figure 3.3-12. False alarm probability for optimum detector in Gaussian-Gaussian mixture noise ($\epsilon = 0.1$), with assumed SNR of 15 dB and parametric in variance ratio.

where

$$P_1(\rho; n) \triangleq (1-\epsilon) Q(\sqrt{2\rho}, \sqrt{n/\sigma_1^2}) + \epsilon Q(\sqrt{2\rho/V^2}, \sqrt{n/\sigma_1^2 V^2}), \quad (3.3-15)$$

and $Q(\cdot, \cdot)$ is Marcum's Q-function.

3.3.3.1 Results for known SNR.

The best detector performance can be expected when the a priori SNR, ρ_0 , is correct, that is, equal to the exact SNR, ρ . Calculations of this best performance were made using (3.3-14); since we assume that $\rho = \rho_0$, different false alarm thresholds were obtained for each value of SNR. (The computer program used is listed in Appendix 3A.) For $\epsilon = 0.01$, the detection probability for these assumptions varies with ρ as shown in Figure 3.3-13. In this figure the P_D is shown for $P_{FA} = 10^{-1}$, 10^{-2} and 10^{-3} , and for $V^2 = 1$, 10, and 100. For $V^2 = 1$, the noise becomes Gaussian and GLR reduces to the optimum Gaussian detector, so that we can observe from the $V^2 \neq 1$ curves the effects of the non-Gaussian parameters ϵ and V^2 .

The comparable performance results for the single-sample Gaussian detector were shown previously in Figure 2.2-6. In comparison with those results, we observe the optimum detector in Gaussian-Gaussian mixture noise for $\epsilon = 0.01$ performs about as well for (a) $P_{FA} = 10^{-1}$, and (b) $V^2 = 10$ and $P_D > .5$. For $P_D < .5$ a great improvement is accomplished, particularly as V^2 increases. For example, in Figure 2.2-6, we find that an SNR in excess of 20 dB is required for $V^2 = 100$ to achieve $P_{FA} = 10^{-3}$ and $P_D > 3 \times 10^{-3}$, while in Figure 3.3-13, a P_D of 0.5 can be achieved for the same P_{FA} when $\rho = 9$ dB.

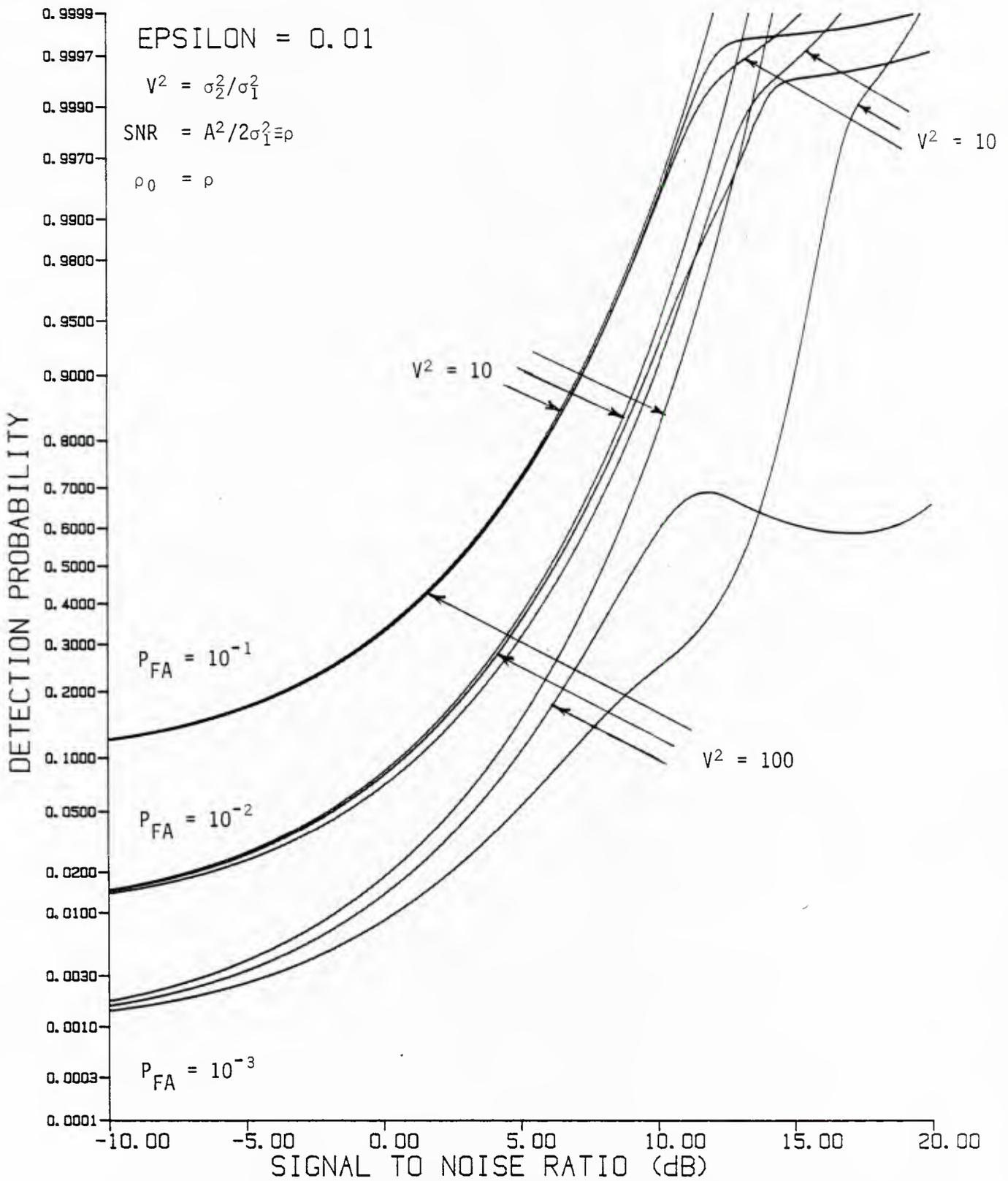


Figure 3.3-13. Receiver operating characteristics for optimum detector in bandpass Gaussian-Gaussian mixture noise ($\epsilon = 0.01$), for different false alarm probabilities and variance ratios.

J. S. LEE ASSOCIATES, INC.

Perhaps the most interesting feature in Figure 3.3-13 is the behavior of the P_D as a function the SNR for $V^2 = 100$ and $P_F = 10^{-3}$. For ρ less than about 12 dB, the P_D increases with ρ ; it increases again for $\rho > 17$ dB, but for $12 \text{ dB} < \rho < 17 \text{ dB}$, the P_D decreases with ρ . From the mathematical expression for the P_D , equation (3.3-14), we observe that such a decrease is possible since the second term is negative. Because we are assuming $\rho_0 = \rho$, that is, the a priori SNR equals the actual SNR, the thresholds (η_1, η_2, η_3) change as ρ changes in order to maintain a constant false alarm probability. Evidently, these thresholds change within such a way as ρ increases as to produce the "dip" in P_D we observe in Figure 3.3-13.

For fixed thresholds (η_1, η_2, η_3) , which corresponds to having both ρ_0 and λ fixed, we expect that P_D will "dip" because the action of the likelihood ratio characteristic is to "pass" or accentuate certain values of the detected envelope, and to "suppress" other, high values. That is, the detector discriminates against a range of high values of x , in effect considering them to be due to noise impulses.

When the mixture parameter is increased to $\epsilon = 0.1$ or to 0.5 , representing a greater departure from Gaussian noise, the optimum detector performs as shown in Figure 3.3-14 and 3.3-15, in contrast to that of the Gaussian detector, shown previously in Figure 2.2-7 and 2.2-9. We observe that for $V^2 = 10$, the detection probability is practically the same for both detectors, except for smaller values of SNR, at which the optimum detector's characteristic is not a monotonic function of the detected envelope for the false alarm thresholds considered (see Figure 3.3-4). However, the optimum detector performance is much improved for $V^2 = 100$ and $P_{FA} < 10^{-1}$. It is notable that for much of the range of SNR values shown, the performance of the detector is better for $V^2 = 100$ than for $V^2 = 10$.

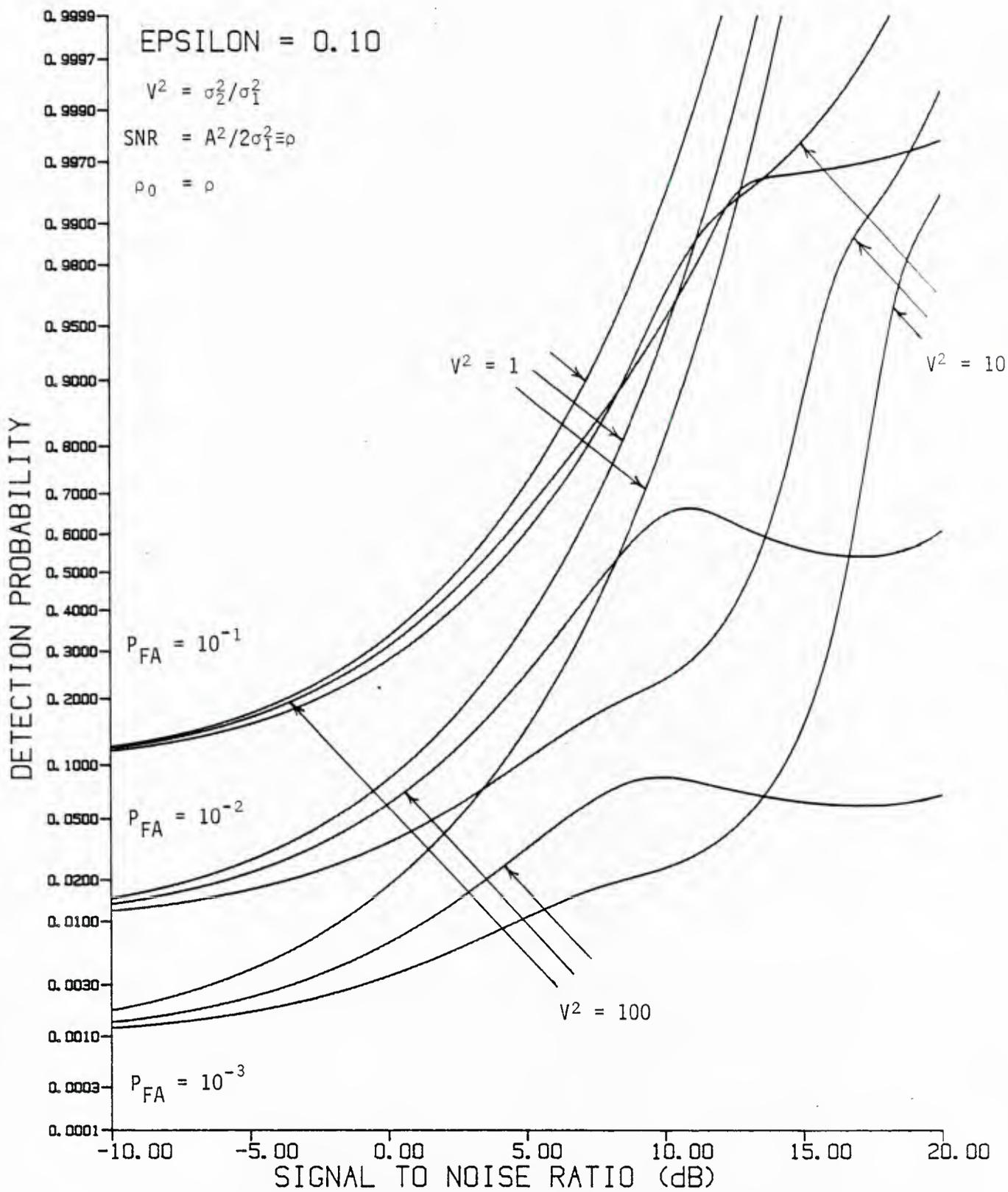


Figure 3.3-14. Receiver operating characteristics for optimum detector in bandpass Gaussian-Gaussian mixture noise ($\epsilon = 0.1$) for different false alarm probabilities and variance ratios.

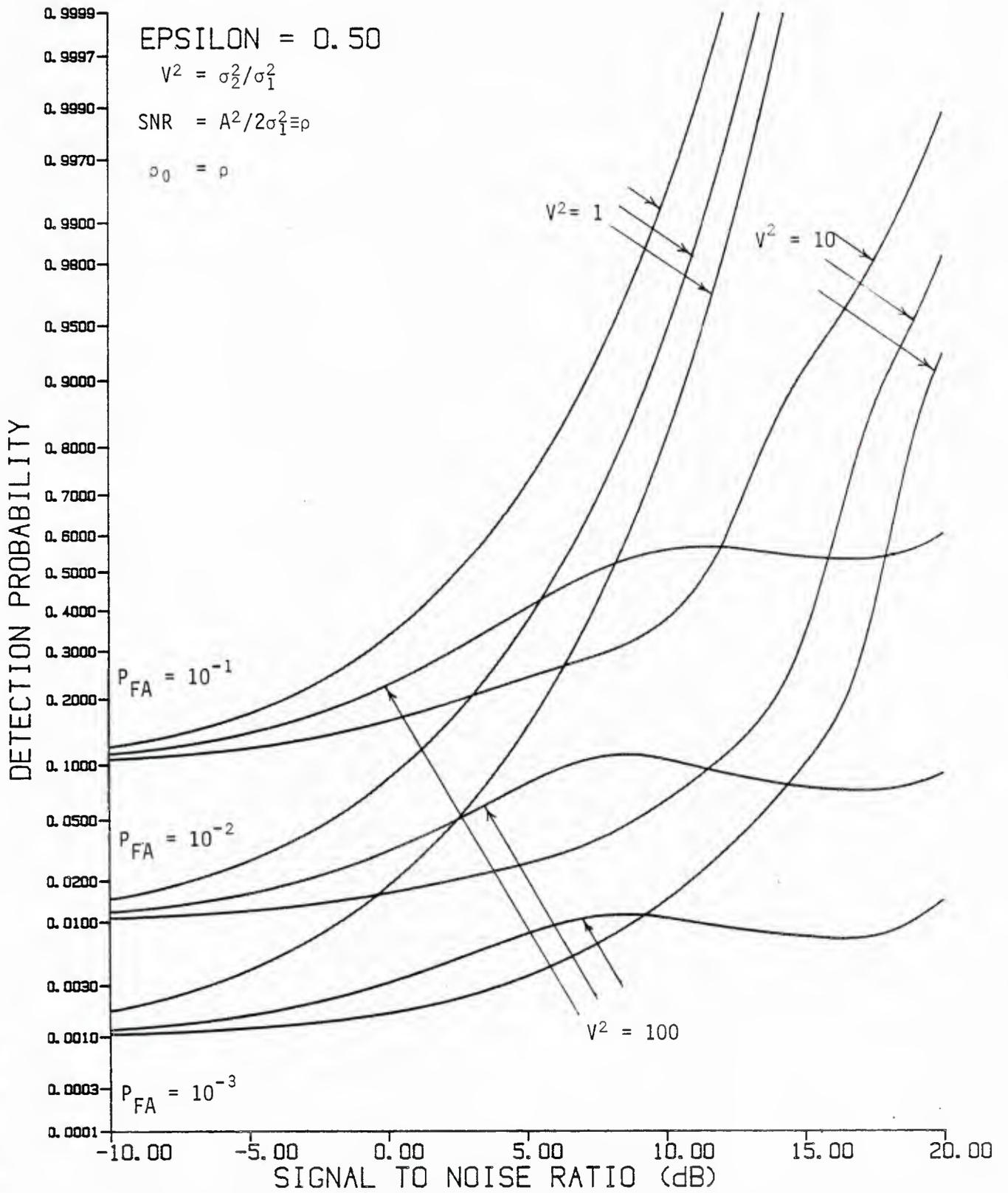


Figure 3.3-15. Receiver operating characteristics for optimum detector in bandpass Gaussian-Gaussian mixture noise ($\epsilon = 0.5$) for different false alarm probabilities and variance ratios.

1100, 0143DETECTM1 07-MAY-85 08:04:02 3

3.3.3.2 Results for fixed a priori SNR.

Since it is usually the case that the SNR of the signal to be detected is not known, the detector performances shown in Figures 3.3-13 to 3.3-15 must be considered as upper bounds to what may be realized in practice. Now we consider the effect on detection performance as a function of actual SNR when the detector GLR characteristic $\Lambda_r(x; \rho_0)$ is a fixed design, due to assuming that the SNR takes a certain fixed value, ρ_0 . For given P_{FA} and ρ_0 , this results in a comparison of the squared envelope x to a threshold η , or possibly to three thresholds (η_1, η_2, η_3), using the test (3.3-9) discussed previously.

A typical plot of detection probability vs SNR for fixed ρ_0 is shown in Figure 3.3-16, for the case of $\epsilon = 0.1$ and $V^2 = 100$. For both $P_{FA} = 10^{-1}$ and 10^{-2} , the P_D curves for $\rho_0 = -10$ dB and $\rho_0 = +10$ dB are given, and are compared to the comparable optimum ($\rho_0 = \rho$) and Gaussian detector results. As expected, the fixed- ρ_0 P_D achieves the best performance at the points for which $\rho_0 = \rho$, the actual SNR. When the actual SNR is not equal to ρ_0 , we may distinguish two different consequences, depending on ρ_0 .

For $\rho_0 = -10$ dB, the detector is predicated on the assumption of a weak signal. From Figure 3.3-16 we observe that the resulting P_D values are almost as high as the optimum values, for actual SNR as much as 5 dB, or 15 dB different than the assumed value! However, the P_D then falls to very low values, less than the false alarm probability, before rising again for extremely high SNR.

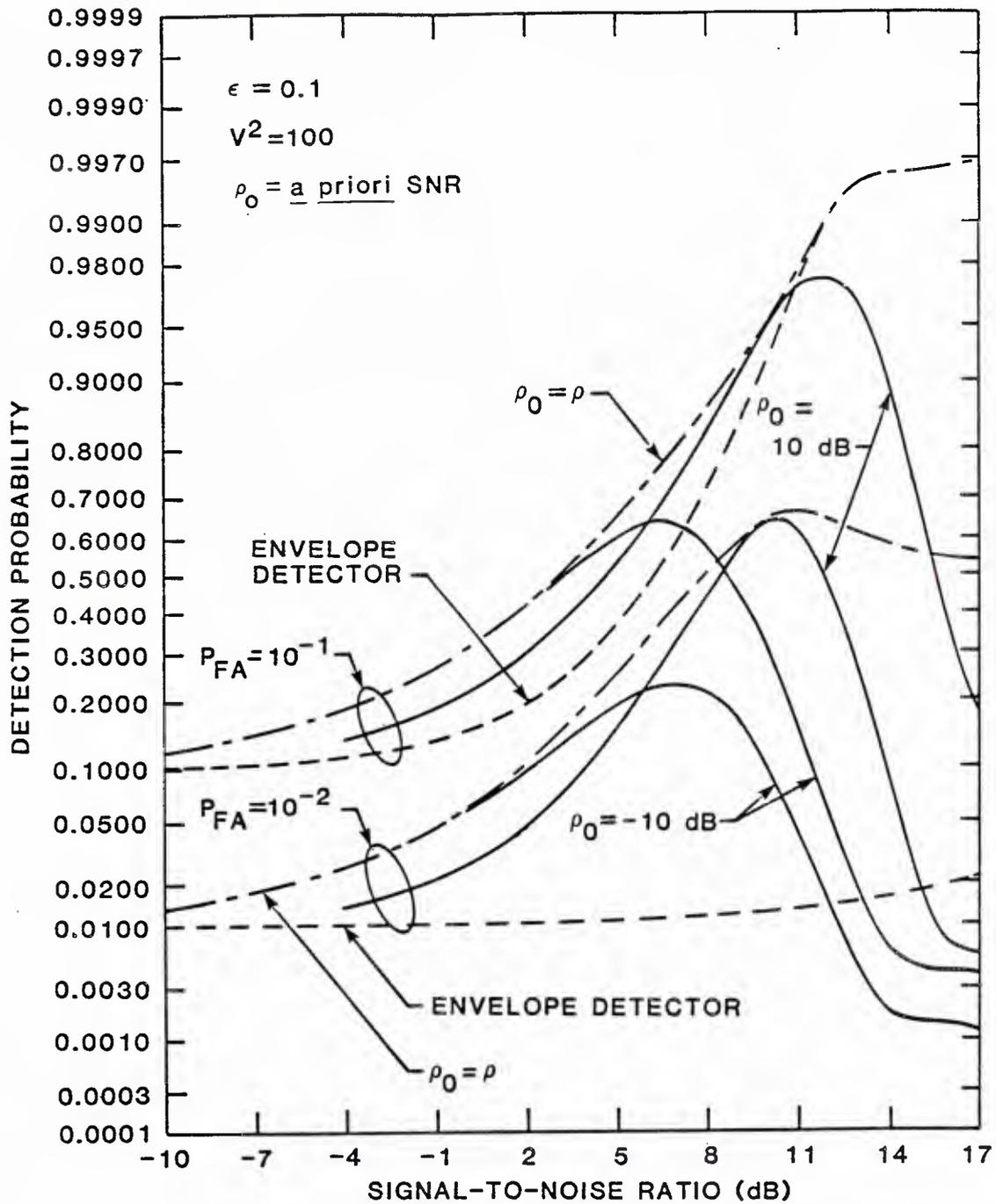


Figure 3.3-16 Receiver operating characteristics for optimum detector in bandpass Gaussian-Gaussian mixture noise: effect of using fixed value of a priori SNR.

For $\rho_0 = +10$ dB, the performance falls to low values more quickly when $\rho > \rho_0$, that is, it is more sensitive to ρ_0 when $\rho > \rho_0$. But the degradation in P_D for $\rho < \rho_0$ is relatively minor: the degraded performance is still better than that achieved by the Gaussian detector.

These results suggest that, when a fixed value of a priori SNR is used, it should be somewhat higher than the average value of SNR anticipated.

3.4 PERFORMANCE FOR MULTIPLE SAMPLES.

We have observed for a single sample that the generalized likelihood ratio (GLR) detector for signals in bandpass Gaussian-Gaussian mixture noise achieves an improvement in detection performance for low SNR over that of the conventional (quadrature or square-law envelope) detector.

Now we consider the detector performances achieved when the number of samples (K) is greater than one. Several issues become significant for $K > 1$ which do not exist for $K = 1$. First, it becomes necessary to distinguish between signal models that we have called Type 1 (slowly varying phase) and Type 2 (independent phase samples). In both cases the detection is incoherent in the sense that the instantaneous signal phase is unknown (assumed to be uniformly distributed on $(0, 2\pi)$); the difference between the two models is in the assumed rate of phase fluctuation (bandwidth) over the observation time during which the K samples are taken.

The second issue which becomes significant for $K > 1$ is the assumption concerning the joint distribution of the K noise samples. Because of the Gaussian-Gaussian mixture probability density function (pdf) assumed,

$$p_{\underline{n}_c, \underline{n}_s}(\underline{\alpha}, \underline{\beta}) = E_{\underline{v}} \left\{ \frac{(2\pi\sigma_1^2)^{-K}}{v_1^2 v_2^2 \dots v_K^2} \exp\left(-\sum_{k=1}^K \frac{\alpha_k^2 + \beta_k^2}{2\sigma_1^2 v_k^2}\right) \right\}, \quad (3.4-1)$$

the quadrature samples $\{n_{ck}, n_{sk}\}$ are uncorrelated or linearly independent regardless of the assumed pdf for the variance mixture, of the general form

$$p_{\underline{v}_2}(\underline{\alpha}) = \sum_{m=1}^M C_m \delta\left(\underline{\alpha} - \underline{v}_m^2\right), \quad \sum_{m=1}^M C_m = 1. \quad (3.4-2)$$

As discussed in Section 2.1.2, the number of terms in the pdf $p_{\underline{v}_2}(\underline{\alpha})$, and their weights $\{C_m\}$, depend on the assumptions about the independence or dependence of the non-Gaussian quadrature sample pairs.

3.4.1 Forms of the GLR for Multiple Samples

For $K > 1$ samples of the quadrature components of the received waveform, the generalized likelihood ratio (GLR) for the various assumptions about the signal phase and the variance multiplier take the various forms discussed previously in Section 3.1. We observe that, in general, the independent signal phases (Type 2) plus independent noise variance case has the most convenient form, since the detection probability admits the development

$$\begin{aligned} & \Pr\{\Lambda_k(\underline{r}) > \eta\} \\ &= \Pr\left\{\prod_k \Lambda_1(\underline{r}_k) > \eta\right\} \\ &= \Pr\left\{\sum_k \ln \Lambda_1(\underline{r}_k) > \ln \eta\right\}. \quad (\text{CASE II}) \end{aligned} \quad (3.4-3)$$

Thus an equivalent detector for this case when there are multiple samples is a simple extension of the detector $\Lambda_1(\underline{r}_k)$ for a single sample.

The second most convenient form is that for independent phase and equal v_k^2 , since it can be constructed using the statistics

$$z_1(\underline{r}) = \sum_k (\alpha_k^2 + \beta_k^2) = \sum_k R_k^2, \quad (3.4-4)$$

the sum of samples of the squared envelope, and, for $v^2 = 1$ or V^2 ,

$$\begin{aligned} z_2(\underline{r}, v^2) &= \sum_k \ln \Lambda(\underline{r}_k | v^2) \\ &= -K\rho/v^2 + \sum_k \ln I_0 \left(\frac{R_k \sqrt{2\rho}}{v^2 \sigma_1^2} \right) \end{aligned} \quad (3.4-5a)$$

$$\approx -K\rho/v^2 + \rho z_1(\underline{r}) / 2v^4 \sigma_1^2, \quad \rho \text{ small} \quad (3.4-5b)$$

$$\approx -K\rho/v^2 + \frac{\sqrt{2\rho}}{v^2 \sigma_1^2} \sum_k R_k; \quad \rho \text{ large.} \quad (3.4-5c)$$

The GLR for this case is formed from z_1 and z_2 as

$$\Lambda(\underline{r}) = \{1 - W[z_1(\underline{r})]\} e^{-z_2(\underline{r}, 1)} + W[z_1(\underline{r})] e^{-z_2(\underline{r}, v^2)} \quad (3.4-6a)$$

$$\text{where } W(z_1) = \frac{\epsilon V^{-2K} \exp\{-z_1/2\sigma_1^2 V^2\}}{(1-\epsilon) \exp\{-z_1/2\sigma_1^2\} + \epsilon V^{-2K} \exp\{-z_1/2\sigma_1^2 V^2\}} \quad (3.4-6b)$$

Similarly, the detector for constant signal phase (Type 1 signal) and slowly-varying noise variance (equal $\{v_k^2\}$) can be reasonably implemented using the statistic $z_1(\underline{r})$ and the statistic

$$z_3(\underline{r}) = \left(\sum_k \alpha_k \right)^2 + \left(\sum_k \beta_k \right)^2, \quad (3.4-7)$$

since

$$\begin{aligned} E_{\theta} \left\{ \prod_k \Lambda_1(\underline{r}_k | \theta, v) \right\} \\ = e^{-K\rho/v^2} I_0 \left(\sqrt{\frac{2\rho}{\sigma_1^2 v^4}} z_3(\underline{r}) \right). \end{aligned} \quad (3.4-8)$$

The GLR for this case is formed from z_1 and z_3 as

$$\begin{aligned} \Lambda(\underline{r}) = \{1 - W[z_1(\underline{r})]\} e^{-K\rho} I_0(\sqrt{2\rho z_3(\underline{r})/\sigma_1^2}) \\ + W[z_1(\underline{r})] e^{-K\rho/V^2} I_0(\sqrt{2\rho z_3(\underline{r})/\sigma_1^2 V^4}), \end{aligned} \quad (3.4-9)$$

where $W[z_1(\underline{r})]$ is given by (3.4-6b).

The most complicated detector is that for equal phase and independent v_k^2 , which requires generating $z_1(\underline{r})$ and $M=2^K$ statistics of the form

$$z_{4m}(\underline{r}) = \left(\sum \frac{\alpha_k}{v_{km}^2} \right)^2 + \left(\sum \frac{\beta_k}{v_{km}^2} \right)^2 ; m = 1, 2, \dots, M; \quad (3.4-10)$$

as noted previously in Section 3.1.

3.4.2 Numerical Results for Independent Samples

For independent samples of the envelope of the signal plus bandpass Gaussian-Gaussian mixture noise, the performance of the optimum detector (3.4-3) for Type 2 signal can be computed using the numerical convolution technique shown in Appendix 3B. Since the anticipated effect of using multiple samples is to increase the detection probability, it is sufficient to consider but a few cases to verify this effect.

Figure 3.4-1 gives the detection probability for the optimum detector for $P_{FA}=10^{-1}$, $\epsilon=0.1$, $V^2=10$, and the number of independent samples, K , equal to 1, 2, 5, 10, and 20. The accumulated signal energy allows 90 percent detection with about 7.3 dB less SNR for $K=10$ than for a single sample.

Figure 3.4-2 is similar to Figure 3.4-1, except that the variance multiplier is increased to $V^2=100$. For this case, about 7.5 dB in detectability is gained by observing $K=10$ samples.

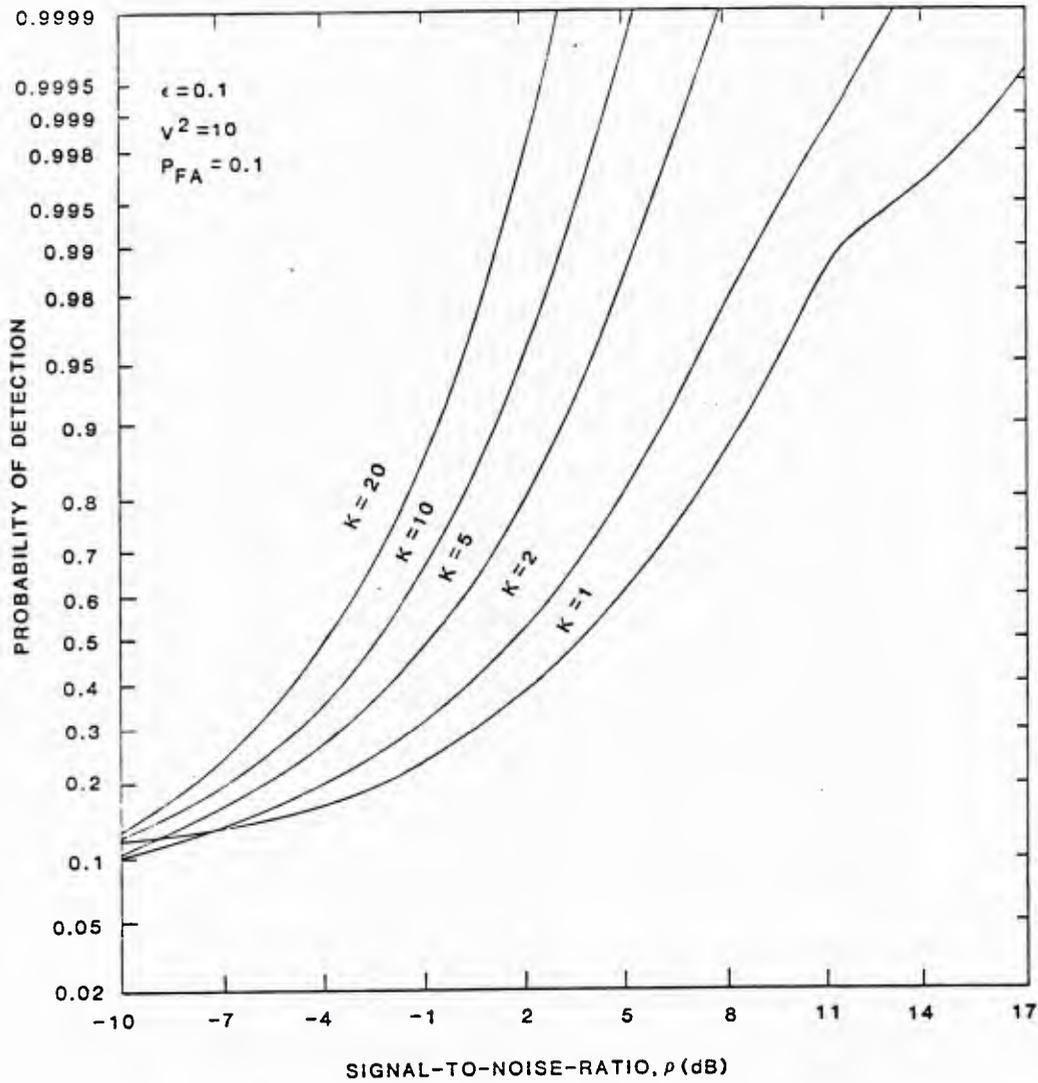


Figure 3.4-1. Performance of optimum detector for signals in bandpass Gaussian-Gaussian mixture noise ($\epsilon=0.1$, $V^2=10$) for $P_{FA}=10^{-1}$ and multiple, independent samples.

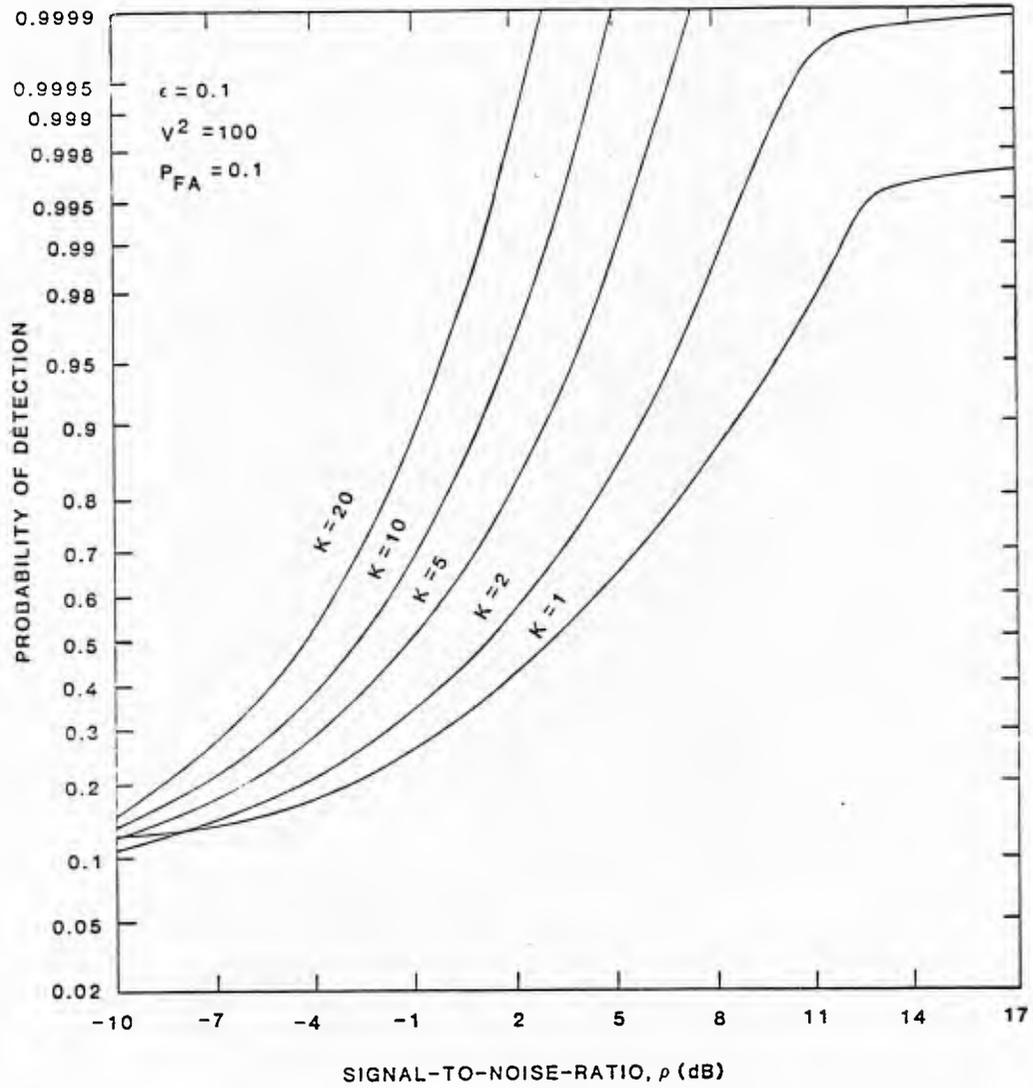


Figure 3.4-2. Performance of optimum detector for signals in bandpass Gaussian-Gaussian mixture noise ($\epsilon=0.1$, $V^2=100$) for $P_{FA}=10^{-1}$ and multiple, independent samples.

4.0 SUBOPTIMUM DETECTORS

4.1 APPROXIMATIONS TO THE OPTIMUM DETECTOR

Exact implementation of the generalized likelihood ratio (GLR) for bandpass Gaussian mixture noise, given by equation 3.3-1, requires generating the function

$$f(a, b) = e^{-b} I_0(\sqrt{2ab}), \quad (4.1-1)$$

where the argument "a" is proportional to the squared envelope of the received waveform and "b" is proportional to the a priori SNR, ρ_0 . (See Figure 3.2-1). We now consider simplifications which result from approximating $f(a, b)$ and the impact on detector performance

4.1.1 Large SNR Approximations

For large values of SNR ($b \gg 1$), we have

$$f(a, b) \approx \frac{e^{-b + \sqrt{2ab}}}{\sqrt{2\pi \sqrt{2ab}}}, \quad b \gg 1, \quad (4.1-2)$$

with the resulting GLR approximation ($x \equiv R^2/\sigma_1^2$)

$$\Lambda_r(x; \rho) \approx \frac{\text{const}}{\sqrt{x}} \cdot \frac{(1-\epsilon) \exp \left\{ -\frac{(\sqrt{x} - \sqrt{2\rho_0})^2}{2} \right\} + \frac{\epsilon}{V^2} \exp \left\{ -\frac{(\sqrt{x} - \sqrt{2\rho_0})^2}{2V^2} \right\}}{(1-\epsilon) \exp \left\{ -x/2 \right\} + \frac{\epsilon}{V^2} \exp \left\{ -x/2V^2 \right\}} \quad (4.1-3)$$

This approximation is expected to be valid [23] for $\sqrt{2ab} > 3.75$, or $\rho > 7V^4 / x$.

Examination of the numerator of (4.1-3) suggests that for large SNR the GLR will exhibit a peak near the normalized squared envelope value $x = 2\rho_0$. This phenomenon is confirmed for $\rho_0 = 20$ dB and $V^2 = 100$ or 1000 by the previous Figures 3.3-2, 3.3-3, and 3.3-6. Thus we observe that in general the GLR characteristic acts as a "window", permitting high output values only in the vicinity of input values near the anticipated SNR (if the signal is present), and suppressing the output for higher input values which are more likely to be due to noise.

Implementation of the high SNR approximation to the GLR is only slightly less complicated than that of the GLR itself. More important, this approximation is still parametric in SNR, offering no advantage in terms of a priori information requirements.

4.1.2 Small SNR Approximation and Locally Optimum Detector.

For small values of SNR ($b \ll 1$), we have

$$f(a, b) \approx 1 + b \left(\frac{a}{2} - 1 \right), \quad b \ll 1, \quad (4.1-4)$$

with the resulting GLR approximation ($x \equiv R^2/\sigma_1^2$)

$$\Lambda_p(x; \rho) \approx 1 + \frac{\rho}{2V^4} \cdot \frac{(1-\epsilon) e^{-x/2} V^4(x-2) + \frac{\epsilon}{V^2} e^{-x/2V^2} (x-2V^2)}{(1-\epsilon) e^{-x/2} + \frac{\epsilon}{V^2} e^{-x/2V^2}}. \quad (4.1-5)$$

This approximation is expected to be valid for $\sqrt{2ab} < 3.75$ or $\rho < 7/x$.

For detection purposes, we may ignore the additive constant in (4.1-5) and also the constant factor $\rho/2$, and use the weak signal "locally optimum detector" (LOD),

$$Z(x) = [1-W(x)] (x-2) + W(x) (x-2V^2)/V^4 \quad (4.1-6a)$$

where

$$W(x) = \frac{\epsilon}{V^2} e^{-x/2V^2} / \left[(1-\epsilon) e^{-x/2} + \frac{\epsilon}{V^2} e^{-x/2V^2} \right] \quad (4.1-6b)$$

The form of (4.1-6) is rather easily interpreted as a combination of LOD's for the Gaussian case, $Z_G(x) = x-2\sigma^2/\sigma_1^2$. This interpretation can also be understood from the plots of (4.1-6) given in Figures 4.1-1 to 4.1-3 for various combinations of ϵ and V^2 .

We note that the LOD is not parametric in the SNR, although it still requires a priori information in the form of ϵ and V^2 , of course. It is often argued that the weak signal case is the most interesting one. However, historically the LOD has been studied primarily because it usually involves a simpler detector structure than the GLR and therefore is more amenable to analysis.

For Gaussian and other monotonic GLR's, the LOD performs well at high SNR. As will be demonstrated below, this is not the case for the Gaussian-Gaussian mixture LOD.

4.1.3 Performance of the Locally Optimum Detector

Computations of the false alarm and detection probabilities for the bandpass Gaussian-Gaussian mixture noise locally optimum detector proceed in a way similar that described for the GLR in Section 3.3, with the important exception that the false alarm thresholds no longer depend on an a priori or assumed value of SNR.

100, 0141L00RAT10 02-MAY-85 09, 09, 01 1

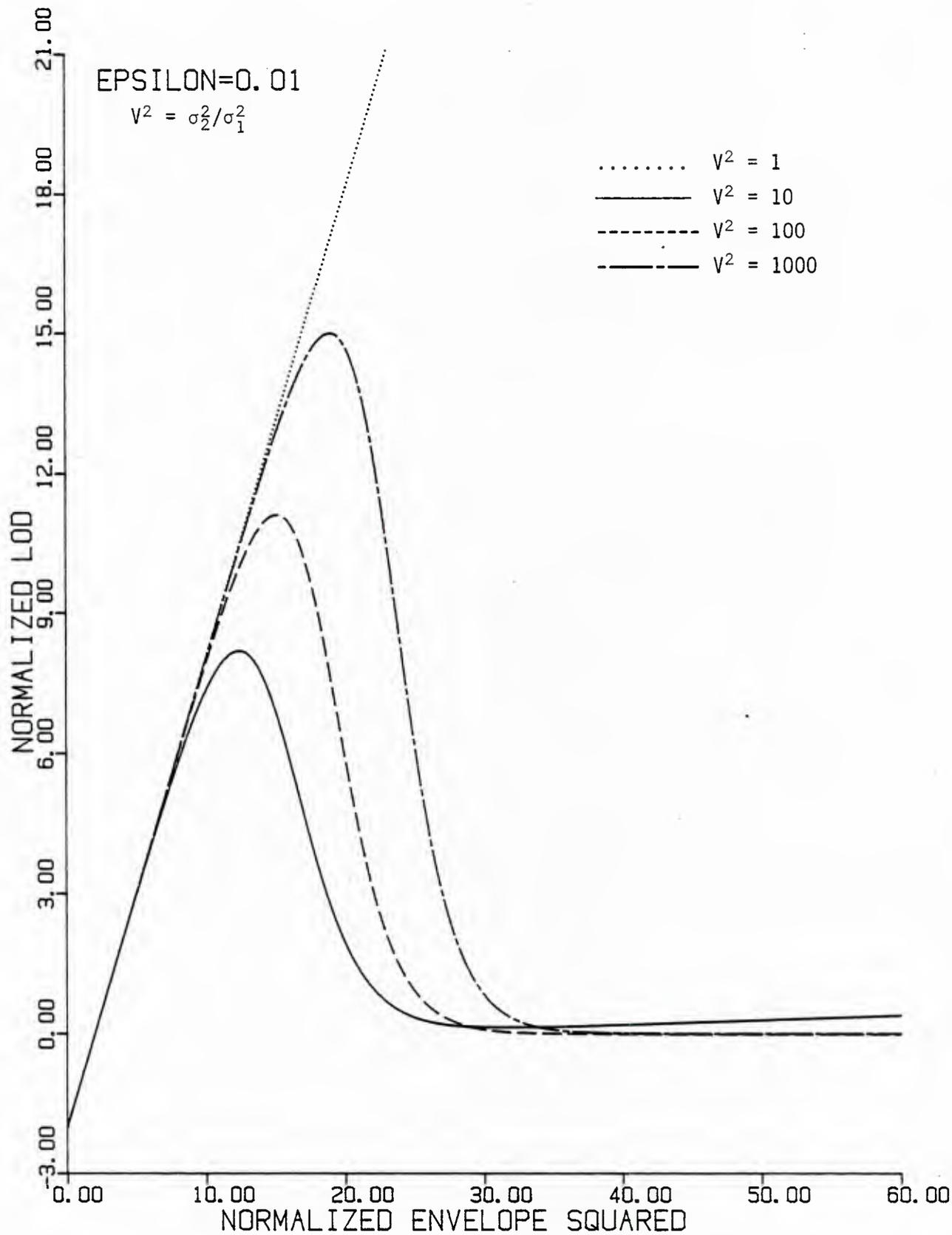


Figure 4.1-1 Locally optimum detector characteristic for bandpass Gaussian-Gaussian mixture noise ($\epsilon = 0.01$) for several values of variance ratio

1100, 0141L0DRAT10 02-MAY-85 09, 09, 01 2

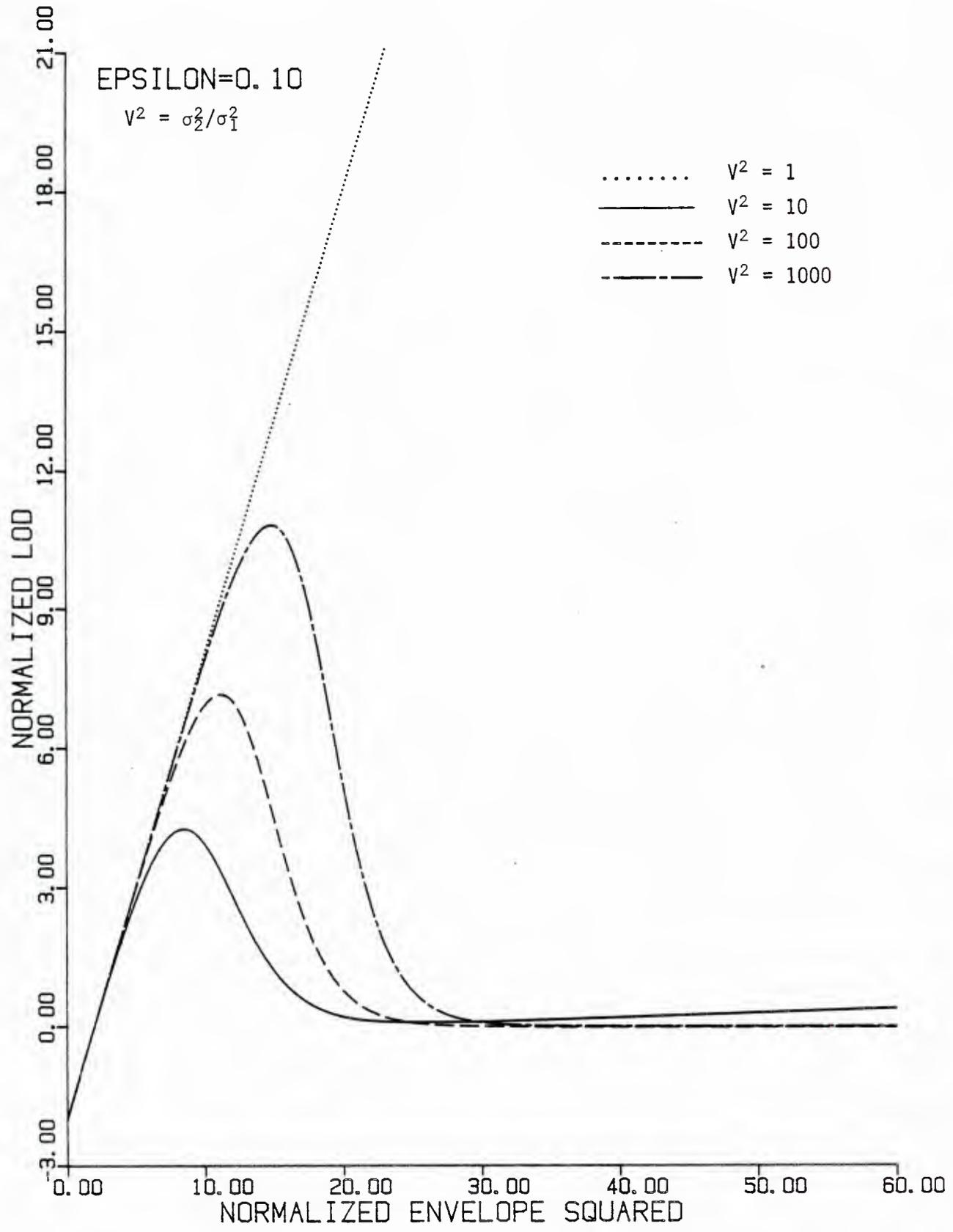


Figure 4.1-2 Locally optimum detector characteristic for bandpass Gaussian-Gaussian mixture noise ($\epsilon = 0.1$) for several values of variance ratio.

[100,014]L0DRATIO 02-MAY-85 09:09:01 3

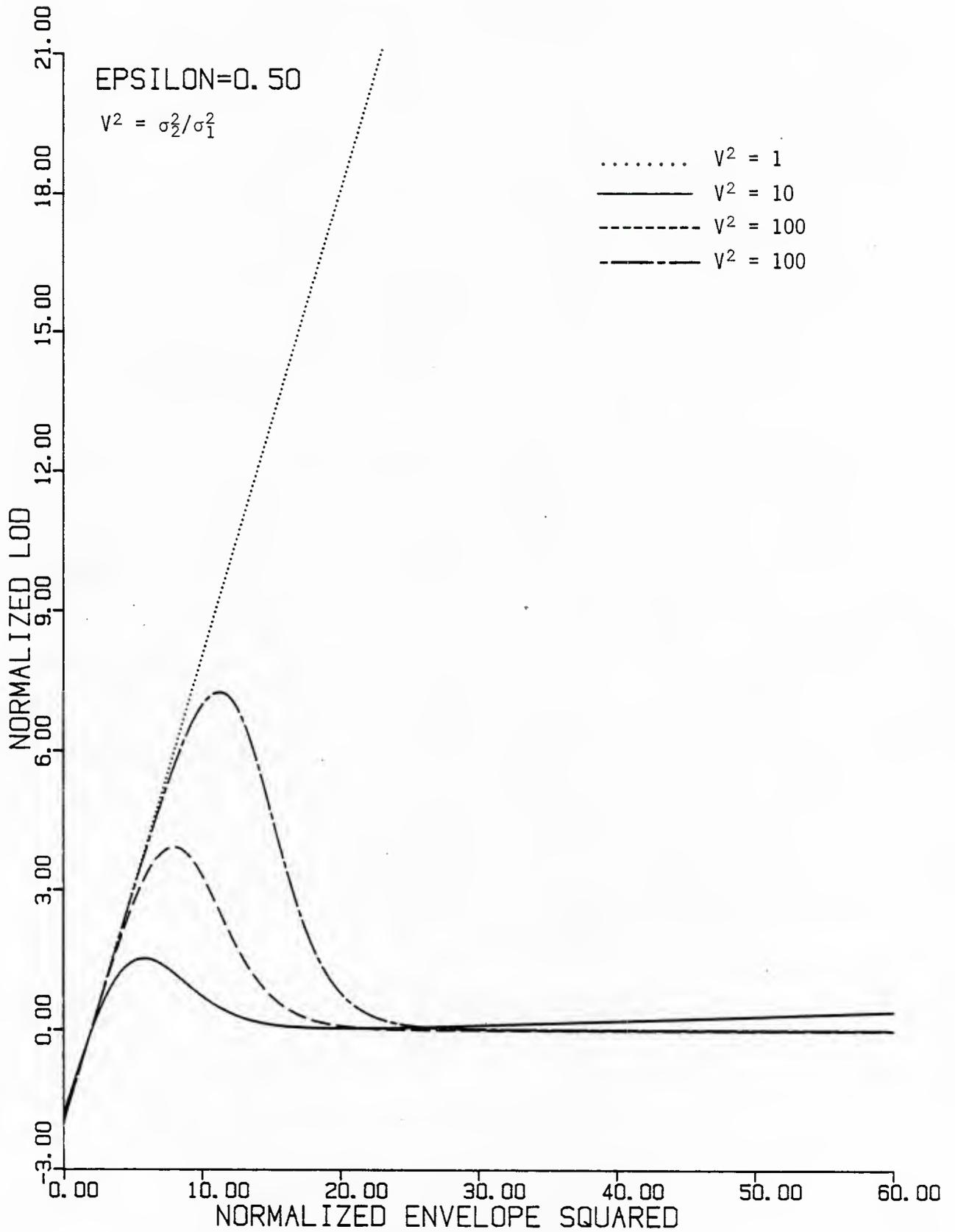


Figure 4.1-3 Locally optimum detector characteristic for bandpass Gaussian-Gaussian mixture noise ($\epsilon = 0.5$) for several values of variance ratio.

4.1.3.1 False Alarm Probability

Single-sample false alarm probabilities for the LOD given by (4.1-6) are plotted in Figures 4.1-4 to 4.1-6 as a function of the first threshold on the normalized squared envelope, η_1/σ_1^2 . It may be observed from these figures that the false alarm probability is very sensitive to variation in the threshold for $P_{FA} < \epsilon$, because at approximately this point the threshold λ on the LOD starts being above the local maximum. For example, in the plot of the LOD characteristic for $\epsilon = 0.01$ (Figure 4.1-1), the peaks for $V^2 = 10, 100, \text{ and } 1000$ occur at normalized squared envelope values of 12.5, 15.2, and 19, respectively. In Figure 4.1-4 we see that the P_{FA} curves for these cases have very steep slopes in the vicinity of these values.

A similar effect is seen for $V^2 = 100$ and 1000 in Figure 4.1-6, in which the P_{FA} is seen to decrease suddenly near the threshold value of 2; this behavior corresponds to the λ threshold on the LOD in Figure 4.1-3 starting to rise above the local minimum of the LOD.

False alarm thresholds for the LOD are given in Table 4.1-1 for various values of ϵ , V^2 , and P_{FA} .

4.1.3.2 Detection probability for a single sample.

Using the false alarm thresholds in Table 4.1-1, the detection probability for the locally optimum weak signal detector in bandpass Gaussian-Gaussian mixture noise was computed according to

$$P_D(\rho) = P_1(\rho; \eta_1) - P_1(\rho; \eta_2) + P_1(\rho; \eta_3), \quad (4.1-7)$$

[100,014]LODPFLOT 03-MAY-85 11:05:09 1

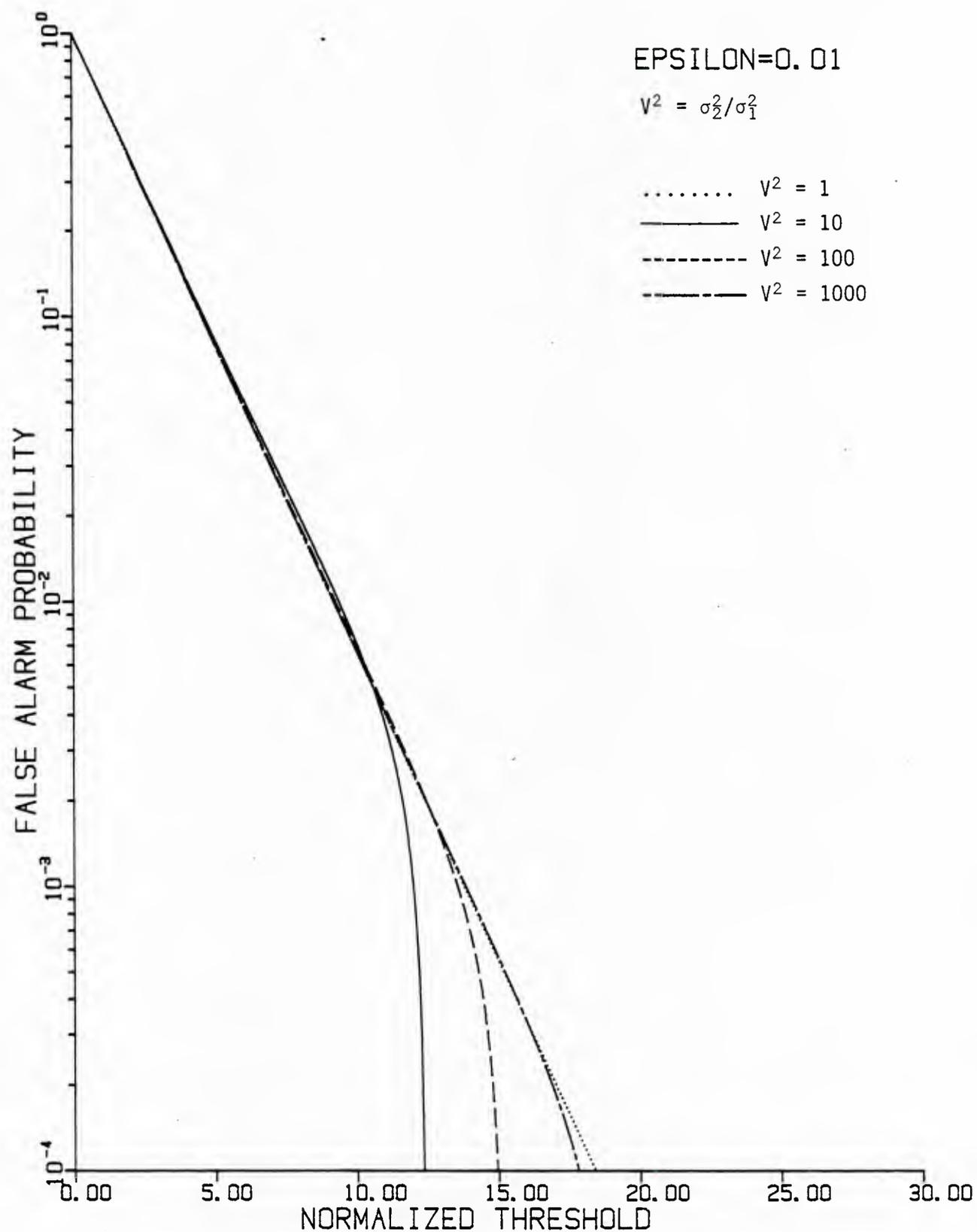
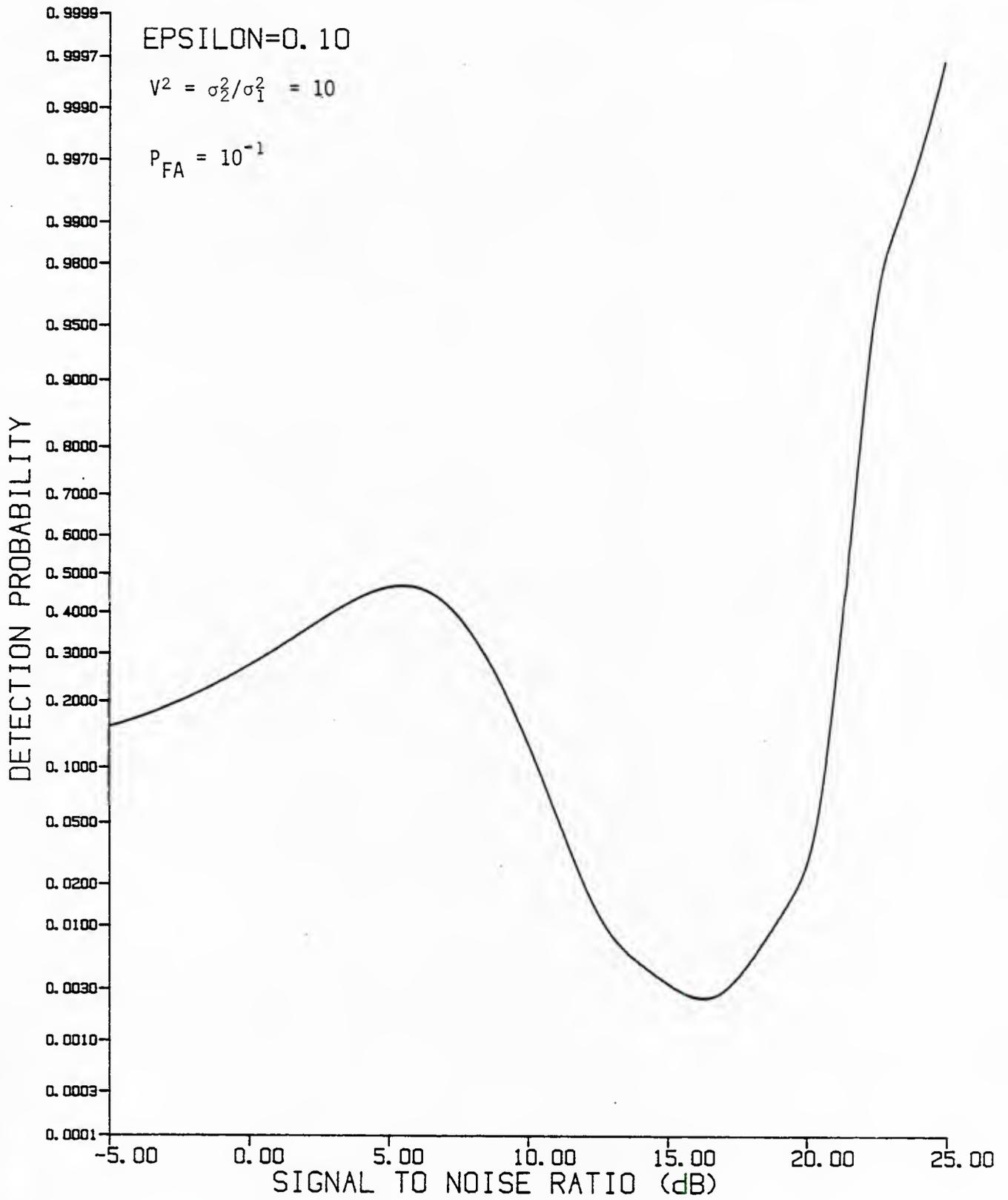


Figure 4.1-4. False alarm probability vs. first threshold for locally optimum detector in bandpass Gaussian-Gaussian mixture noise ($\epsilon = 0.01$).



I100,0141LDDPD2 06-MAY-85 09,14,44 1

Figure 4.1-10. Receiver operating characteristics for locally optimum detector in bandpass Gaussian-Gaussian mixture noise for $\epsilon = 0.1$, $V^2 = 10$, and $P_{FA} = 10^{-1}$.

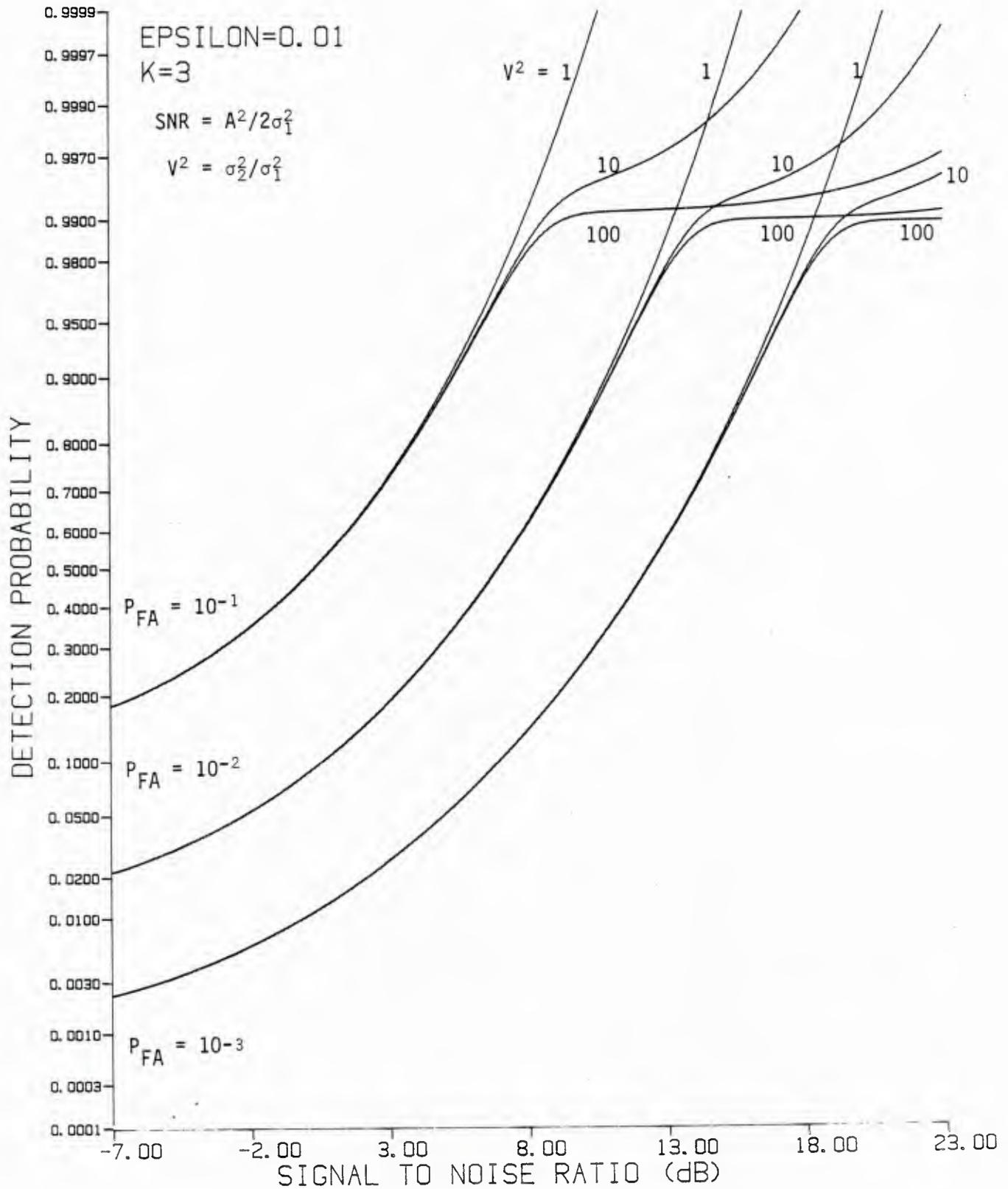


Figure 4.2-4 Performance of serial normalization detector in bandpass Gaussian-Gaussian mixture noise ($\epsilon = 0.01$) for three time samples.

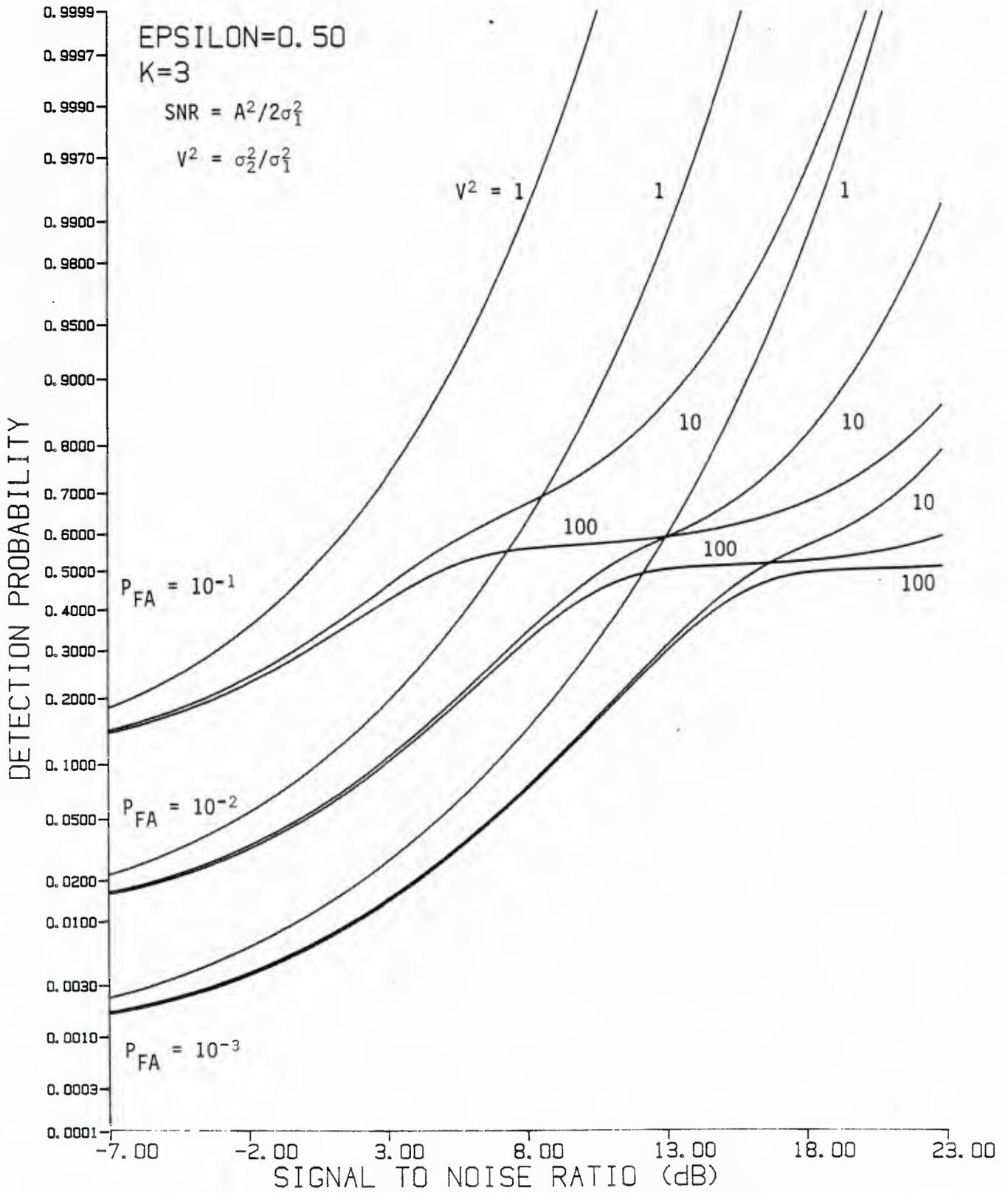
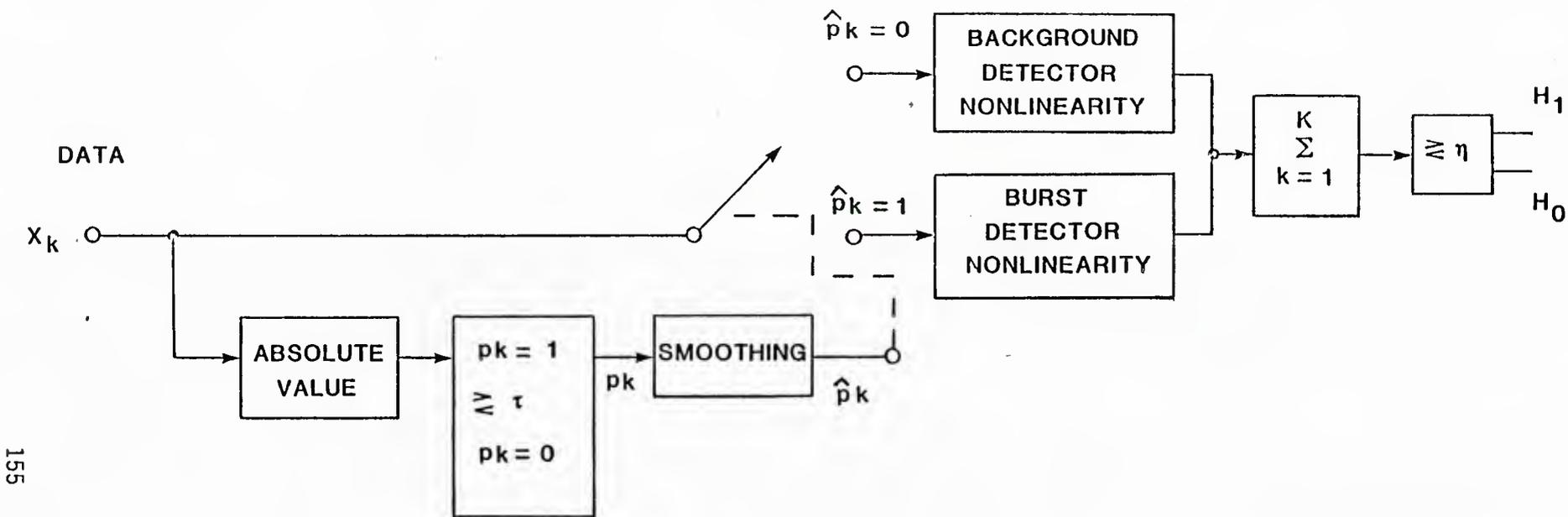


Figure 4.2-6 Performance of serial normalization detector in bandpass Gaussian-Gaussian mixture noise ($\epsilon = 0.5$) for three time samples



smoothing: $\hat{p}_k = 1$ if more than half of $p_{k \pm j}$ ($j=0, 1, \dots, m$) are equal to one

$$\tau = 1.282 \hat{\sigma}_1, \quad \hat{\sigma}_1^2 \text{ estimated from data.}$$

Figure 4.3-1 Detector for weak signal in lowpass, switched burst noise.

4.4 COMPARISON OF DETECTOR PERFORMANCES

Figures 4.4-1 and 4.4-2 provide graphical comparisons of the performances of the weak signal LOD, the serial normalization detector, and the parallel normalization detector. It is seen that the LOD is the best choice when it can be assumed that the signal is weak ($\text{SNR} < 5\text{dB}$), but it does not perform well if the signal is strong.

For strong signals both the serial normalization detector and the parallel normalization detector are superior to the LOD, with the parallel one tending to be more effective than the serial one. In addition, as discussed previously, these detectors are attractive in that they can be designed to maintain a given false alarm probability without a priori information on the noise distribution parameters.

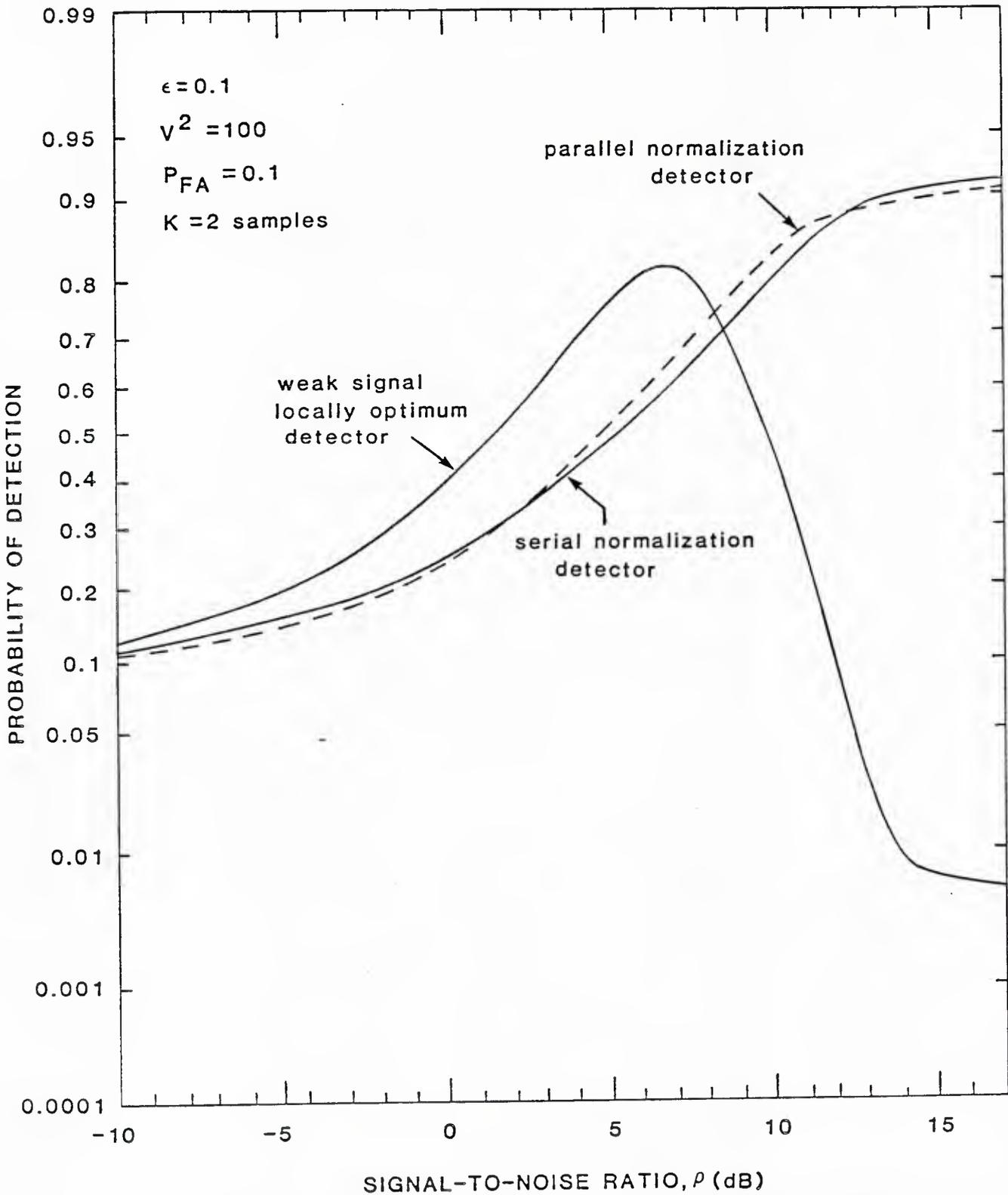


Figure 4.4-1 Comparison of suboptimum detector performances in bandpass Gaussian-Gaussian mixture noise ($\epsilon = 0.1$, $V^2 = 100$) for $P_{FA} = 0.1$ and $K = 2$ samples.

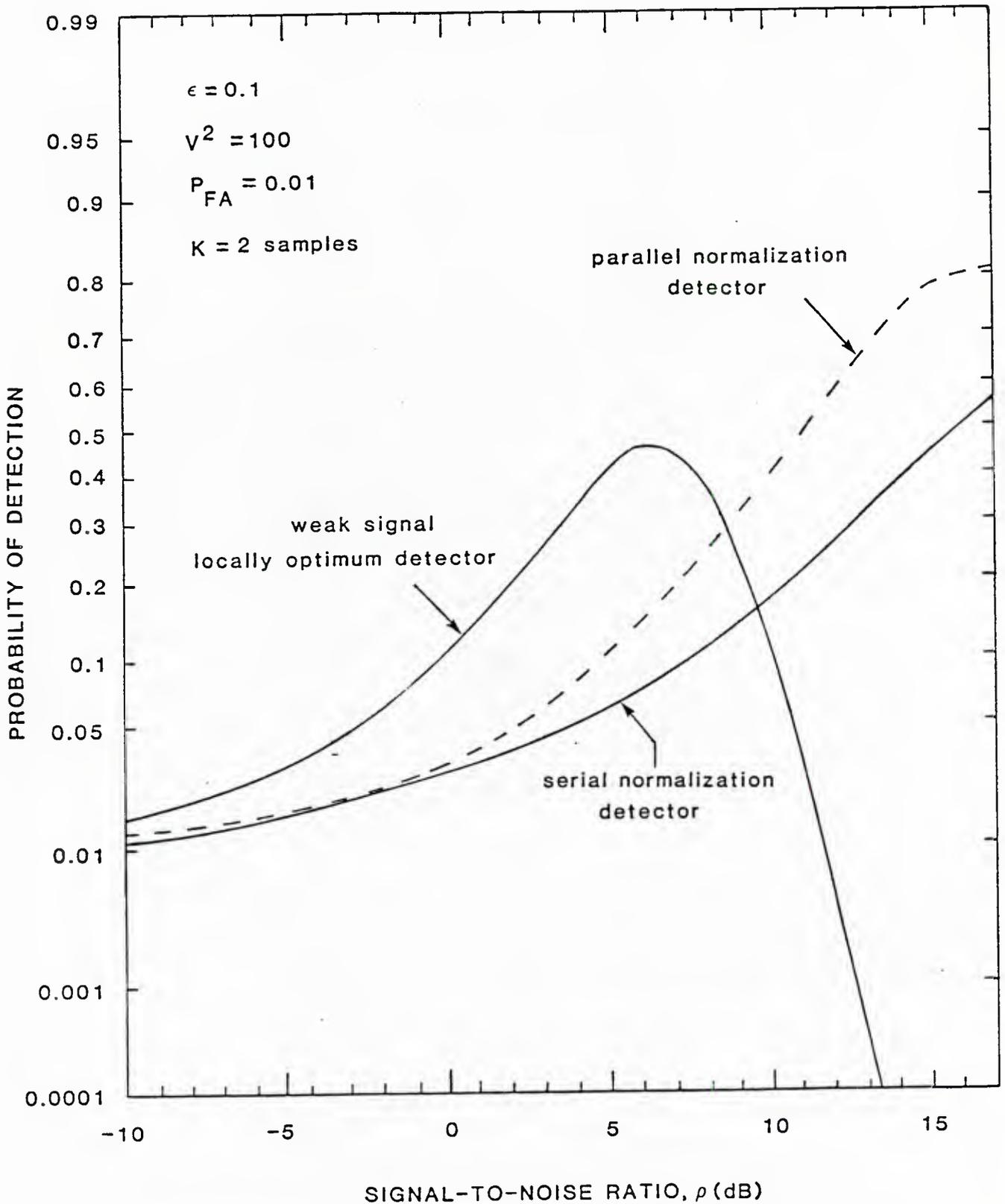


Figure 4.4-2 Comparison of suboptimum detector performances in bandpass Gaussian-Gaussian mixture noise ($\epsilon = 0.1$, $V^2 = 100$) for $P_{FA} = 0.01$ and $K = 2$ samples.

APPENDIX 3-A

FORTRAN program to calculate false alarm and detection probabilities for optimum detector in bandpass Gaussian-Gaussian mixture noise.


```
      C
      C IF NO ARCHIVE WAS AVAILABLE, CREATE ONE FOR THE NEW DATA
      C
0084      IF(.NOT.REUSE) THEN
0085          OPEN(UNIT=2,STATUS='NEW',FILE=ARCFIL,FORM='UNFORMATTED')
0086          WRITE(2) ISUB,(DBRHO(I),I=1,ISUB+2),(PD(I),I=1,ISUB+2)
0087          END IF
0088          CLOSE(UNIT=2)
      C
      C LOOPS END HERE
      C
0089      700      CONTINUE
0090      800      CONTINUE
      C
      C START NEW PAGE WHEN LOOP ON EPSILON INCREMENTS
      C
0091      IF(IEPS.EQ.3) THEN
      C LAST PAGE, JUST FLUSH PLOT BUFFER
0092          CALL PLOT(0.,0.,999)
0093      ELSE
      C INSTALLATION-STANDARD NEW PLOT ROUTINE ASKS FOR NEW
      C PAGE, WAITS FOR SIGNAL FROM TERMINAL, AND RESETS THE
      C PLOT ORIGIN TO INITIAL LOCATION
0094          CALL NEWPLT
0095          END IF
0096      900      CONTINUE
      C
      C ALL DONE
      C
0097      STOP 'DONE'
0098      END
```



```
0001      DOUBLE PRECISION FUNCTION ROOTF(X)
C
C
C   THE FUNCTION
C
C       RATIO(X) - (TARGET VALUE)
C
C   TO PASS TO THE ROOT-FINDING ROUTINES WHICH SOLVE
C   THE EQUATION F(X) = 0 FOR X
C
0002      IMPLICIT DOUBLE PRECISION(A-H,O-Z)
C
C   PASS IN THE TARGET VALUE OF THE FUNCTION
C
0003      COMMON /TARGET/ FIND
C
C   COMPUTE IT
C
0004      ROOTF=RATIO(X)-FIND
0005      RETURN
0006      END
```



```
0001          DOUBLE PRECISION FUNCTION FINDPF(ETA)
      C
      C COMPUTE THE FUNCTION
      C
      C PF(ETA) - (TARGET FALSE ALARM RATE)
      C
      C FOR USE BY ROOT FINDERS IN SEARCHING FOR FALSE
      C ALARM THRESHOLD
      C
0002          IMPLICIT DOUBLE PRECISION(A-H,O-Z)
      C
      C PASS IN THE TARGET VALUE
      C
0003          COMMON /PFATAR/ FALSEA
      C
      C COMPUTE THE VALUE
      C
0004          FINDPF=PF(ETA)-FALSEA
0005          RETURN
0006          END
```

```

0001          SUBROUTINE GETETA(PFAT,ETA)
          C
          C SUBROUTINE TO FIND THE THRESHOLD FOR WHICH
          C THE FALSE ALARM PROBABILITY IS A SPECIFIED
          C VALUE
          C
0002          IMPLICIT DOUBLE PRECISION(A-H,O-Z)
0003          EXTERNAL FINDPF
0004          LOGICAL*1 MONO,GOOD,UNIQUE
0005          COMMON /WUNRUT/ UNIQUE
0006          COMMON /VALID/ GOOD
0007          COMMON /PFATAR/ FALSEA
0008          COMMON /FLECT/ ETAMAX,ALMAX,ETAMIN,ALMIN,E3MAX,E3PLUS,
          $              MONO
0009          C SET UP TARGET VALUE FOR ROOT FINDERS
          FALSEA=PFAT
          C
          C IF THE PREVIOUS CASE WAS A SINGLE ROOT, THEN IF WE
          C STILL HAVE A SINGLE ROOT THE THRESHOLD WILL BE THE
          C SAME AND WE DON'T HAVE TO WASTE TIME RECOMPUTING IT.
          C
0010          IF(GOOD.AND.UNIQUE) THEN
0011              ALAM=RATIO(ETA)
          C IF LAMBDA(PREVIOUS ETA) IS NOT BETWEEN THE LOCAL MINIMUM
          C AND THE LOCAL MAXIMUM VALUES OF LAMBDA, THEN THERE IS ONLY
          C THE ONE SOLUTION AND THE VALUE OF ETA REMAINS GOOD
          C FOR THIS CASE.
0012              IF(ALAM.LE.ALMIN .OR. ALAM.GE.ALMAX) RETURN
0013              END IF
0014          1111 IF(MONO) THEN
          C IF MONOTONIC, ONLY ONE ROOT TO FIND.
          C SO WE SEARCH FROM 1.0 ON UP TO NEAR OVERFLOW UNTIL
          C WE FIND THE ROOT, USING SERIAL SEARCH TECHNIQUE.
0015              CALL SERETA(FINDPF,ETA,1.DO,1.DO,1.D38)
          C AND FLAG IT AS A UNIQUE ROOT
0016              UNIQUE=.TRUE.
0017          ELSE
          C WE MIGHT HAVE 3 ROOTS
          C FIRST TEST TO SEE IF BEYOND THE 3-ROOT AREA
          C
0018              PFEMAX=FINDPF(ETAMAX)
0019              IF(PFEMAX.GT.O.DO) THEN
          C
          C WE HAVE ONLY ONE ROOT BEYOND E3MAX IF FALSE ALARM
          C RATE IS TOO HIGH AT E3MAX. START SEARCHING
          C FROM E3MAX ON TOWARDS AN OVERFLOWING VALUE.
          C
0020              CALL SERETA(FINDPF,ETA,E3MAX,1.DO,1.D38)
          C AND FLAG IT AS A UNIQUE ROOT
0021              UNIQUE=.TRUE.
0022              RETURN
0023          END IF

```

```

C
C ELSE WE ARE IN THE 3-ROOT REGION
C
0024         IF(GOOD) THEN
C
C IF WE HAVE JUST STEPPED SNR WITHOUT CHANGING V**2 AND PFA,
C THE PREVIOUS THRESHOLD MAKES A GOOD STARTING POINT FOR THE
C SEARCH
C
0025         XLEFT=ETA
0026         ELSE
C
C BUT OTHERWISE WE MUST START FROM THE BEGINNING
C
0027         XLEFT=1.DO
0028         END IF
C SERIAL SEARCH TO BRACKET THE ROOT
0029 555       YLEFT=FINDPF(XLEFT)
0030 5        IF(YLEFT.GT.O.DO) THEN
C LEFT ENDPOINT FUNCTION > 0, SO INCREASE RIGHT HAND LIMIT
0031         XRIGHT=XLEFT*2.DO
0032         IF(XRIGHT.GT.ETAMAX.AND.XLEFT.LT.ETAMAX) THEN
C RIGHT END POINT MIGHT BUMP INTO ETAMAX, BE SURE WE
C DON'T EXCEED IT OR THE SEARCH WILL GO WILD
0033         XRIGHT=ETAMAX
0034         END IF
0035         ELSE
C LEFT ENDPOINT FUNCTION < 0, SO WE NEED TO TRY A
C SMALLER THRESHOLD FIRST; CUT LEFT ENDPOINT.
0036         XLEFT=XLEFT/2.DO
0037         GOTO 555
0038         END IF
0039         YRIGHT=FINDPF(XRIGHT)
C IF ROOT LIES BETWEEN THE PROSPECTIVE ENDPOINTS WE ARE READY
C TO CALL THE ROOT FINDER
0040         IF(YRIGHT*YLEFT.GE.O.DO) THEN
C BUT IF NOT THEN MUST MOVE THE INTERVAL UNTIL WE FIND ONE THAT
C BRACKETS THE ROOT. TO REDUCE SEARCH REGION, THROW OUT THIS
C WHOLE INTERVAL IN WHICH WE KNOW THE ROOT DOES NOT LIE.
0041         XLEFT=XRIGHT
0042         YLEFT=YRIGHT
0043         GOTO 5
0044         END IF
C DO THE SERIAL SEARCH FOR THE ROOT
0045         CALL SERETA(FINDPF,ETA,XLEFT,XRIGHT-XLEFT,XRIGHT)
0046         ALAM=RATIO(ETA)
C DETERMINE IF THE ROOT IS UNIQUE
0047         UNIQUE=ALAM.LE.ALMIN .OR. ALAM.GE.ALMAX
0048         END IF
0049         RETURN
0050         END

```



```

0001          SUBROUTINE SEROOT(FUNC,ETA,X1,DX)
      C
      C SERIAL SEARCH FOR ROOT OF EQUATION  FUNC(X) = 0
      C FOR USE IN FINDING ROOTS OF LIKELIHOOD RATIO.  THIS
      C SECOND ROUTINE IS NEEDED TO AVOID RECURSION.
      C
      C THE SEARCH LOGIC IS THE SAME AS ROUTINE  SERETA.
      C
0002          IMPLICIT DOUBLE PRECISION(A-H,O-Z)
0003          E1=X1
0004          P1=FUNC(E1)
0005          IF(P1.EQ.0.DO) THEN
0006              ETA=E1
0007              RETURN
0008          END IF
0009          EINC=DX
0010          1    E2=E1+EINC
0011              P2=FUNC(E2)
0012              IF(P2.EQ.0.DO) THEN
      C
      C JUST HAPPENED TO HIT IT EXACTLY
      C
0013                  ETA=E2
0014                  RETURN
0015                  ELSE IF(DSIGN(1.DO,P1).EQ.DSIGN(1.DO,P2)) THEN
      C
      C KEEP STEPPING
      C
0016                  E1=E2
0017                  P1=P2
0018                  GOTO 1
0019                  ELSE
      C
      C WE HAVE IT BRACKETED
      C
      C ... IF VERY STEEP SLOPE, JUMP TO THE INTERPOLATION STEP
0020          IF(ABS(P1-P2)/EINC.GE.2000.DO) GOTO 100
      C ... OR IF HAVE IT TO ENOUGH PLACES JUMP TO INTERPOLATION STEP
0021          IF(E1/EINC.GT.2.D8) GOTO 100
      C ... OTHERWISE CUT INCREMENT AND TRY AGAIN
0022          EINC=EINC/10.DO
0023          GOTO 1
0024          END IF
      C
      C INTERPOLATE BETWEEN FINAL TWO BRACKETING VALUES
      C
0025          100    DP=P2-P1
0026                  PP=-P1
0027                  ETA=E1+EINC*PP/DP
0028                  RETURN
0029                  END

```

```
0001          SUBROUTINE TERCON
C
C SET UP INTERPOLATION CONSTANTS FOR USE WHEN THRESHOLD IS
C NEAR ETAMAX
C
C THIS IS A TIME-SAVER. DO IT ONLY ONCE RATHER THAN
C RECOMPUTE THINGS WITHIN A SUBPROGRAM WHICH IS CALLED
C MANY TIMES IN THE COURSE OF SETTING THE THRESHOLD.
C
0002          IMPLICIT DOUBLE PRECISION(A-H,O-Z)
0003          LOGICAL*1 MONO
0004          COMMON /FLECT/ ETAMAX,ALMAX,ETAMIN,ALMIN,E3MAX,E3PLUS,
           $             MONO
0005          COMMON /TERROO/ ETA1,TERO01,TERO02,PFTER1,PFTERX
C
C BACK OFF A SMALL DISTANCE FROM THE MAXIMUM
C
0006          ETA1=ETAMAX-1.D-5
C
C SOLVE THE EQUATION FOR ROOTS LAMBDA(ETA) = LAMBDA(ETA1)
C
0007          CALL ROOTER(ETA1,TERO01,TERO02)
C
C FALSE ALARM PROBABILITY WHEN ETA=ETAMAX
C
0008          PFTERX=FAP(E3MAX)
C
C FALSE ALARM PROBABILITY WHEN ETA = ETAMAX-0.00001
C
0009          PFTER1=FAP(ETA1)-FAP(TERO01)+FAP(TERO02)
0010          RETURN
0011          END
```

APPENDIX 3B:

NUMERICAL TECHNIQUE FOR EVALUATING MULTIPLE SAMPLE DETECTOR PERFORMANCE

Given the detector form

$$U_K(\underline{r}) = \sum_k U(x_k) \equiv \sum_k u_k \equiv U, \quad (3B-1)$$

the probabilities of false alarm and detection are given by

$$P_{FA}(\eta) = \Pr \left\{ \sum_k u_k > \eta | H_0 \right\} \quad (3B-2)$$

and

$$P_D(\eta) = \Pr \left\{ \sum_k u_k > \eta | H_1 \right\}. \quad (3B-3)$$

For independent $\{x_k\}$, and therefore independent $\{u_k\}$, the characteristic function of the sum is

$$\phi_U(v) = \prod_k \phi_{u_k}(v) \quad (3B-4)$$

which implies that the probability density function (pdf) for the sum U is the K-fold convolution of the pdf's for the individual $\{u_k\}$:

$$p_U(\alpha) = p_{u_1}(\alpha) * p_{u_2}(\alpha) * \dots * p_{u_K}(\alpha). \quad (3B-5)$$

Our technique is based on using a discrete pdf to approximate the pdf of the individual detection statistics, assumed to be identically distributed, with

J. S. LEE ASSOCIATES, INC.

5.0 REFERENCES (PART I)

- [1] J. H. Fennick, "Amplitude Distributions of the Telephone Channel Noise and a Model for Impulse Noise," Bell System Technical Journal, 48, pp. 3243-3264 (December 1969).
- [2] H. M. Hall, "A New Model for 'Impulsive' Phenomena: Application to Atmospheric-Noise Communications Channels," Stanford University Electronics Labs. Tech Report Nos. 3212-8 and 7050-7, SU-SEL-66-052 (1966).
- [3] D. Middleton, "Statistical-Physical Models of Man-made Radio Noise, Part I," Dept. of Commerce Office of Telecommunications Report OT 74-36 (April 1974).
- [4] D. Middleton, "Statistical-Physical Models of Man-made and Natural Radio Noise, Part II: First Order Probability Models of the Envelope and Phase," Dept. of Commerce Office of Telecommunications Report OT 76-86 (April 1976).
- [5] A. D. Spaulding and D. Middleton, "Optimum Reception in an Impulsive Interference Environment," Dept. of Commerce Office of Telecommunications Report OT 75-67 (June 1975). Also see IEEE Transactions on Communications, COM-25, pp. 910-923 (September 1977).
- [6] L. M. Nirenberg, "Low SNR Digital Communication over Certain Additive Non-Gaussian Channels," IEEE Trans. on Communications, COM-23, pp. 332-341 (March 1975).
- [7] C. J. Wolejsza, "Non-Gaussian Characteristics of the FDM-FM Satellite Baseband Voice Channel," PhD Dissertation, The Catholic University of America, Washington, D.C. (December 1979).
- [8] D. Middleton, "Procedures for Determining the Parameters of the First-order Canonical Models of Class A and Class B Electromagnetic Interference," IEEE Trans. on Electromagnetic Compatibility, EMC-21, pp. 190-208 (August 1979).
- [9] S. C. Schwartz and J. B. Thomas, "Detection in a Non-Gaussian Environment," Information Sciences and Systems Laboratory, Report Number 5, Princeton University, September 1982.
- [10] A. B. Martinez and J. B. Thomas, "Non-Gaussian and Multivariate Noise Models for Signal Detection," Information Sciences and Systems Laboratory, Report Number 6, Princeton University, September 1982.

J. S. LEE ASSOCIATES, INC.

- [24] D. A. Shnidman, "Efficient Evaluation of Probabilities of Detection and the Generalized Q-function," IEEE Trans. on Information Theory, Vol IT-22, pp. 746-750 (November 1976).
- [25] L. E. Miller, "Multi-sensor Detection Study," Contract N60921-80-C-0107, J. S. Lee Associates, Inc. September 1980 (AD# A091954).
- [26] S. V. Czarnecki and J. B. Thomas, "Nearly Optimal Detection of Signals in non-Gaussian Noise," Information Sciences and Systems Laboratory, Report number 14, Princeton University, February 1984.
- [27] R. V. Hogg and A. T. Craig, Introduction to Mathematical Statistics (second ed.), MacMillan, New York 1965.
- [28] L.E. Miller and J.S. Lee, "Bandpass Correlator Analysis for General Input Assumptions," IEEE Trans. on Information Theory, Vol IT-28, pp. 973-977 (November 1982).
- [29] J.S. Lee et al, "Analyses of Weak Signal Extraction and Spread Spectrum Detection in the Electronic Warfare Environment," Contract N00014-80-C-0753, J.S. Lee Associates, Inc., November 1981.

PART II:

AN INVESTIGATION OF CANONICAL CORRELATION AS AN AUTOMATIC DETECTION AND BEAMFORMING TECHNIQUE

1.0 INTRODUCTION

1.1 BACKGROUND

Detection of signals in noise can be enhanced by the use of arrays of sensors. If the N sensor outputs are delayed (phased) such that the signals at each output are in phase, the signal power in the sum will be proportional to N^2 . For independent noise at each sensor, the noise power in the sum will be proportional to N . Thus an output SNR (signal-to-noise ratio) gain proportional to N . At the same time, information on the direction of the signal's arrival is embedded in the time delays (phase shifts). Figure 1-1 illustrates the array sum concept; it is understood that the operations performed are valid at a given center frequency and bandwidth of interest.

For pairs of sensors as opposed to arrays, the concept of correlation is well understood when the noise is Gaussian. Figure 1-2(a) shows how the joint operations of detection and time delay estimation can be performed using a correlator. Although the same operations can be performed by squaring the sum of the two sensor outputs, the sensitivity of the output to the delay is not as great. If the background noise contains an impulsive component, the usual assumptions (isotropic, uncorrelated noise) are, however, no longer valid.

For more than two sensors, attention has been given to the relative merits in Gaussian noise of "standard" processing (summing all sensors and squaring) and of "multiplicative" processing, in which partial array sums

SENSORS

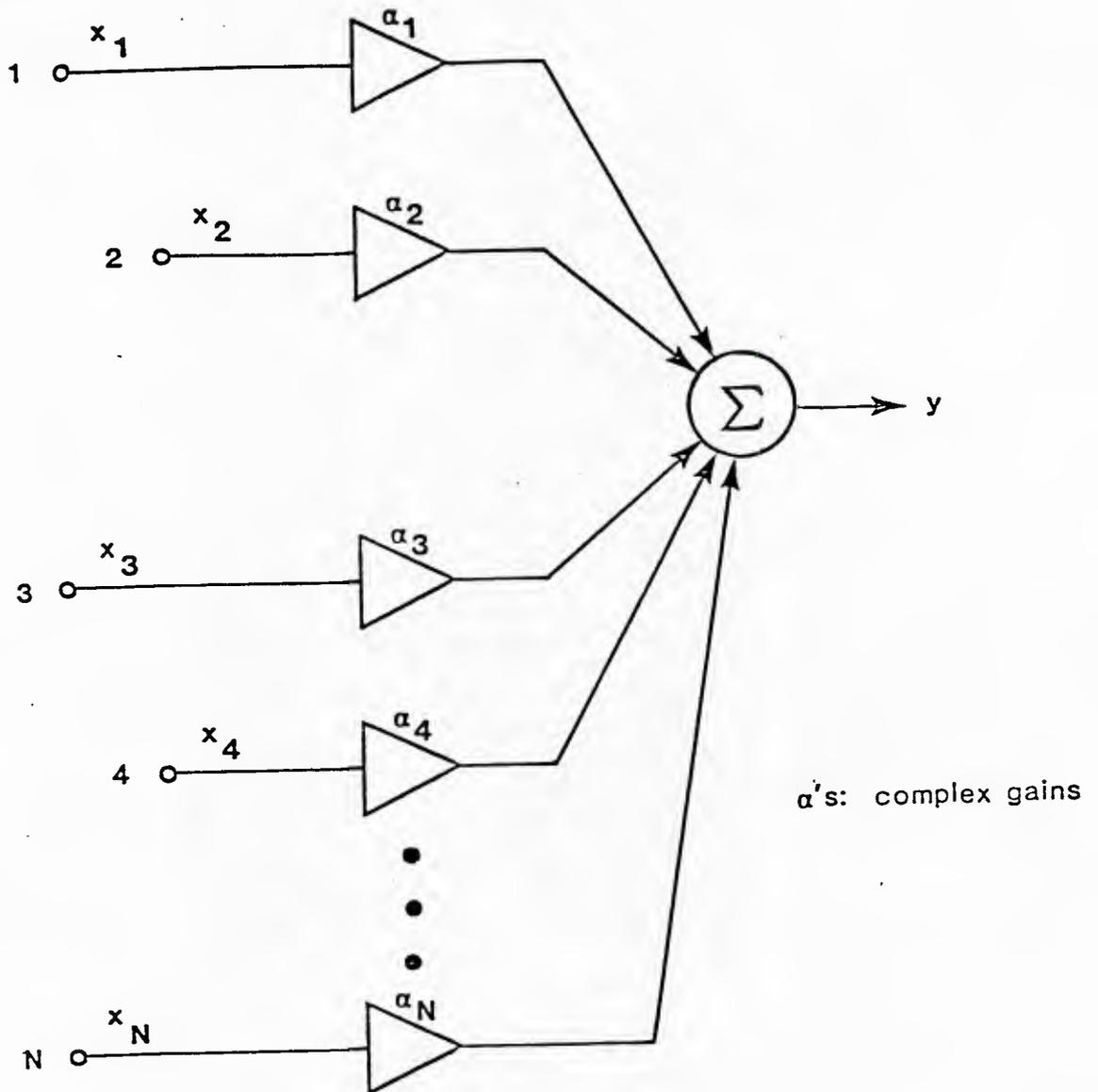
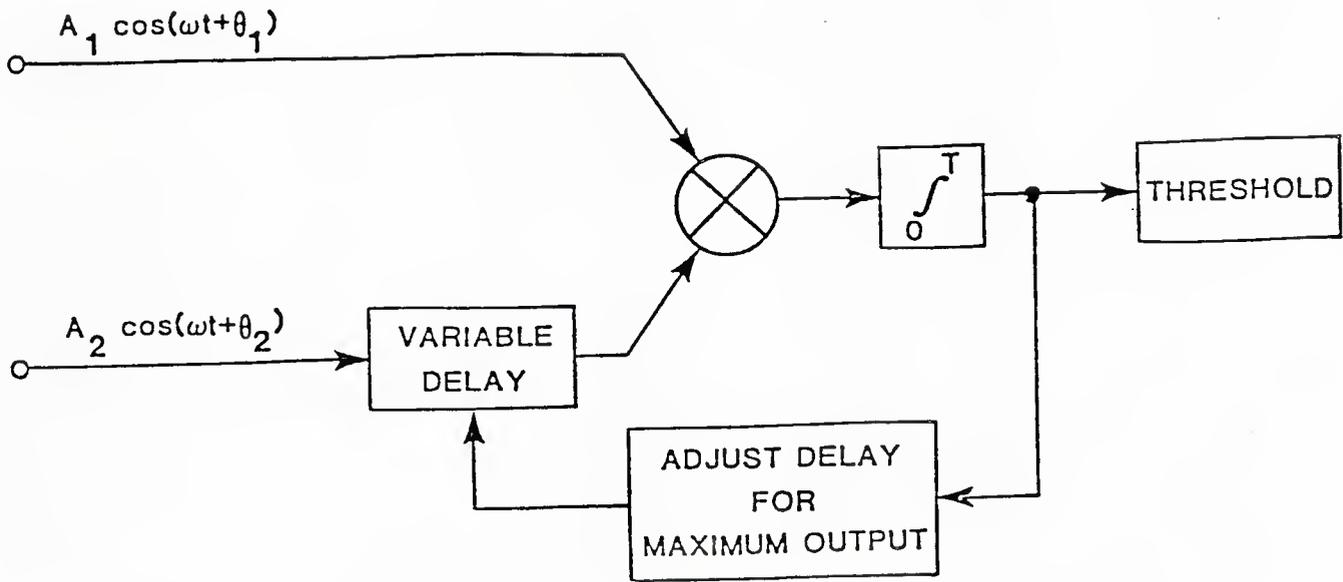
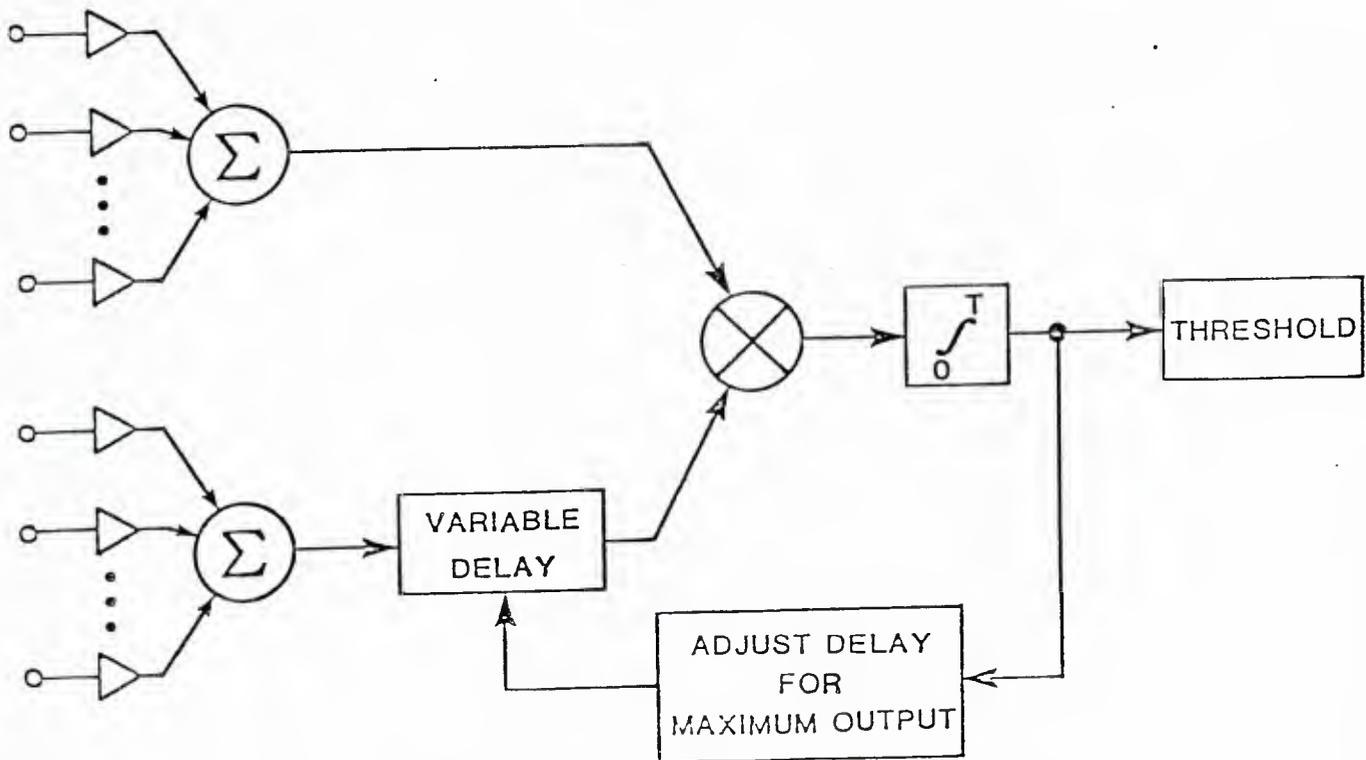


FIGURE 1-1 ARRAY SUM CONCEPT



(a) CORRELATION PROCESSING OF TWO SENSORS



(b) CORRELATION PROCESSING OF TWO ARRAYS

FIGURE 1-2 CORRELATION PROCESSING OF SENSORS AND OF ARRAYS

are formed, then multiplied [1]. In general, the multiplicative (correlator) configurations, such as shown in Figure 1-2(b), provide the same directivity for fewer sensors but are slightly less sensitive in detection. In either case, the task of "steering", or assigning delays or complex weights to the individual sensors must be made. When multiple sources are present, the success of both the standard and multiplicative approaches usually depends on the notion of sweeping the "look" angle, and resolution is proportioned to the number of sensors.

Under the usual assumptions of Gaussian, isotropic ambient noise, it is well known how to combine two sensors for detection of a signal of known or assumed form; however, in the presence of impulsive noise components, the performance of this sensor application is less well understood. How to operate two arrays jointly is an open subject with or without Gaussian noise assumptions.

1.2 MOTIVATION FOR STUDY

When two arrays are separately located, the question of combining their sensor outputs to achieve the effects of a "super array" arises. Resolution is expected to improve because of the large baseline. However, the two arrays must be time-aligned or steered in the correct initial directions before any fine tuning can be done, and it needs to be ascertained whether they are observing the same or different sources. Therefore correlation (or coherence, in the frequency domain) serves the purpose of confirming that the arrays are looking at the same source, as well as actually performing the detection and localization functions.

A new method for cross-correlating arrays is believed to be promising. The approach is to exploit the principles of "canonical correlation" [2], which may be explained as follows: -

J. S. LEE ASSOCIATES, INC.

Denoting the $N = N_x + N_y$ sensor outputs for the two arrays as \underline{x} and \underline{y} , the covariance matrix of the total sensor vector is

$$\text{Cov} \begin{pmatrix} \underline{x} \\ \underline{y} \end{pmatrix} = \begin{bmatrix} \Sigma_x & \Sigma_{xy} \\ \Sigma_{xy}^* & \Sigma_y \end{bmatrix} = \Sigma \quad (1-1)$$

where $()^*$ stands for conjugate transpose and Σ is an $N \times N = (N_x + N_y)$ matrix. Two steering vectors $\underline{\alpha}$ ($N_x \times 1$) and $\underline{\beta}$ ($N_y \times 1$) can be defined; the array sums become

$$w = \sum_{i=1}^{N_x} \bar{\alpha}_i x_i = \underline{\alpha}^* \underline{x} \quad (1-2)$$

$$z = \sum_{i=1}^{N_y} \bar{\beta}_i y_i = \underline{\beta}^* \underline{y} \quad (1-3)$$

Canonical correlation procedures find vectors $\underline{\alpha}$ and $\underline{\beta}$ so that the correlation

$$E\{wz\} = \underline{\alpha}^* E(\underline{xy}^*) \underline{\beta} = \underline{\alpha}^* \Sigma_{xy} \underline{\beta} \quad (1-4)$$

is maximized. In fact, as many as N_x or N_y (whichever is smaller) correlations of w, z combinations can be determined and ranked.

Since the canonical correlation procedure is based on the covariance matrix (in practice, its estimate), its outputs (the steering vectors and the correlations) seem to constitute an adaptive solution to simultaneously steering

in multiple directions. Thresholding of the correlations would then correspond to detection of multiple targets. A multiple target capability would of course be of considerable utility in ocean surveillance applications, especially in view of the consideration that the correlations can be performed on data in a common spectral band, rather than at different frequencies.

Another advantage of the canonical correlation method would seem to be that the solutions for the steering vectors from information embedded in the sensor covariance matrix does not require knowledge of sensor positions. Thus the method is a form of automatic beamforming.

1.3 REVIEW OF CANONICAL CORRELATION METHOD FOR REAL DATA

As set forth by Anderson [2], the canonical correlation method is the solution to the following problem: Given the m -component zero-mean random vector \underline{x} with $m \times m$ covariance matrix Σ , suppose that \underline{x} is partitioned into two vectors,

$$\underline{x} = \begin{pmatrix} \underline{x}^{(1)} \\ \underline{x}^{(2)} \end{pmatrix} \quad (1-5)$$

where $\underline{x}^{(1)}$ contains m_1 components and $\underline{x}^{(2)}$ contains m_2 components ($m_1+m_2=m$).

The covariance matrix, assumed positive definite, can be partitioned correspondingly as

$$\Sigma = \begin{pmatrix} \Sigma_{11} & \Sigma_{12} \\ \Sigma_{21} & \Sigma_{22} \end{pmatrix} \quad (1-6)$$

where Σ_{11} is $m_1 \times m_1$, Σ_{12} is $m_1 \times m_2$, Σ_{21} is $m_2 \times m_1$, and Σ_{22} is $m_2 \times m_2$.

Now consider the arbitrary linear combinations U and V , where

$$U \triangleq \underline{\alpha}^T \underline{X}^{(1)}, \quad V \triangleq \underline{\beta}^T \underline{X}^{(2)} \tag{1-7}$$

and we require that U and V have unit variance, that is,

$$E \{U^2\} = E \{ \underline{\alpha}^T \underline{X}^{(1)} \underline{X}^{(1)T} \underline{\alpha} \} = \underline{\alpha}^T \Sigma_{11} \underline{\alpha} = 1 \tag{1-8a}$$

and

$$E \{V^2\} = E \{ \underline{\beta}^T \underline{X}^{(2)} \underline{X}^{(2)T} \underline{\beta} \} = \underline{\beta}^T \Sigma_{22} \underline{\beta} = 1. \tag{1-8b}$$

In (1-7) and following equations we use the notation $()^T$ to indicate the transpose of a vector or matrix.

The correlation between U and V , which have zero means, is

$$E \{UV\} = E \{ \underline{\alpha}^T \underline{X}^{(1)} \underline{X}^{(2)T} \underline{\beta} \} = \underline{\alpha}^T \Sigma_{12} \underline{\beta}. \tag{1-9}$$

The problem is to find $\underline{\alpha}$ and $\underline{\beta}$ such that the correlation (1-9) is maximized subject to the constraints (1-8). In the usual manner, the solution is obtained by first defining the function

$$\psi = \underline{\alpha}^T \Sigma_{12} \underline{\beta} - \frac{1}{2} \lambda (\underline{\alpha}^T \Sigma_{11} \underline{\alpha} - 1) - \frac{1}{2} \mu (\underline{\beta}^T \Sigma_{22} \underline{\beta} - 1), \tag{1-10}$$

where λ and μ are Lagrange multipliers. Next, ψ is differentiated with respect to the elements of $\underline{\alpha}$ and $\underline{\beta}$, and the derivatives are set to zero:

$$\frac{\partial \psi}{\partial \underline{\alpha}} = \Sigma_{12} \underline{\beta} - \lambda \Sigma_{11} \underline{\alpha} = \underline{0} \quad (1-11a)$$

$$\frac{\partial \psi}{\partial \underline{\beta}} = \Sigma_{12} \underline{\alpha} - \mu \Sigma_{22} \underline{\beta} = \underline{0}. \quad (1-11b)$$

Multiplication of (1-11a) on the left by $\underline{\alpha}^T$ and (1-11b) on the left by $\underline{\beta}^T$ yields the equations

$$\underline{\alpha}^T \Sigma_{12} \underline{\beta} - \lambda \underline{\alpha}^T \Sigma_{11} \underline{\alpha} = 0 \quad (1-12a)$$

$$\underline{\beta}^T \Sigma_{12} \underline{\alpha} - \mu \underline{\beta}^T \Sigma_{22} \underline{\beta} = 0 \quad (1-12b)$$

Using the constraints (1-8) in (1-12), we see that

$$\lambda = \mu = \underline{\alpha}^T \Sigma_{12} \underline{\beta}, \quad (1-13)$$

and (1-11) can be combined to form the matrix equation

$$\begin{pmatrix} -\lambda \Sigma_{11} & \Sigma_{12} \\ \Sigma_{21} & -\lambda \Sigma_{22} \end{pmatrix} \begin{pmatrix} \underline{\alpha} \\ \underline{\beta} \end{pmatrix} = \underline{0}. \quad (1-14)$$

Nontrivial solutions of this equation require that the matrix be singular:

$$\det \begin{pmatrix} -\lambda \Sigma_{11} & \Sigma_{12} \\ \Sigma_{21} & -\lambda \Sigma_{22} \end{pmatrix} = 0, \quad (1-15)$$

or equivalently, using $v = \lambda^2$,

$$\det [\Sigma_{12}\Sigma_{22}^{-1}\Sigma_{21} - v\Sigma_{11}] = 0, \quad v = \lambda^2. \quad (1-16)$$

It can be shown that if $m_1 \leq m_2$, there are m_1 roots to the polynomial in v generated by (1-16). The vectors $\underline{\alpha}$ and $\underline{\beta}$ corresponding to these roots generate m_1 uncorrelated linear combinations.

If the roots $\lambda = \sqrt{v}$ are ranked, then λ_i ($i = 1, 2, \dots, m$) is the i :th canonical correlation between $\underline{x}^{(1)}$ and $\underline{x}^{(2)}$. The vectors $\underline{\alpha}_i$ and $\underline{\beta}_i$ defining the linear combinations $U_i = \underline{\alpha}_i^T \underline{x}^{(1)}$ and $V_i = \underline{\beta}_i^T \underline{x}^{(2)}$ satisfy (1-15) for $\lambda = \lambda_i$.

The conditions on the λ 's, $\underline{\alpha}$'s, and $\underline{\beta}$'s can be summarized as

$$A^T \Sigma_{11} A = I \quad (1-17a)$$

$$B_1^T \Sigma_{22} B_1 = I \quad (1-17b)$$

$$A^T \Sigma_{12} B_1 = \Lambda, \quad (1-17c)$$

where

$$A \triangleq \begin{bmatrix} \underline{\alpha}_1 & \underline{\alpha}_2 & \dots & \underline{\alpha}_{m_1} \end{bmatrix}, \quad (m_1 \times m_1) \quad (1-18a)$$

$$B_1 \triangleq \begin{bmatrix} \underline{\beta}_1 & \underline{\beta}_2 & \dots & \underline{\beta}_{m_1} \end{bmatrix}, \quad (m_2 \times m_1) \quad (1-18b)$$

$$\Lambda \triangleq \text{diag} (\lambda_1, \lambda_2, \dots, \lambda_{m_1}). \quad (1-18c)$$

In addition if $m_1 < m_2$, we have the conditions

$$B_2^T \Sigma_{22} B_2 = \underline{0} \quad (1-19a)$$

$$B_2^T \Sigma_{22} B_2 = I \quad (1-19b)$$

where B_2 is an auxiliary matrix of "extra" β 's given by

$$B_2 \triangleq \begin{bmatrix} \beta_{m_1+1} & \vdots & \cdots & \vdots & \beta_{m_2} \end{bmatrix}, \quad m_2 \times (m_2 - m_1). \quad (1-20)$$

2.0 EXTENSION OF CANONICAL CORRELATION TO COMPLEX DATA

We consider now extending the canonical correlation concept and procedure to complex data, in order to treat bandpass signals.

2.1 FORMULATION OF THE PROBLEM

Figure 2-1 illustrates a situation in which $M=2m$ sensors, arbitrarily located within some area, receive one or more signals arriving from different directions. We assume that the signal wavefronts are adequately represented as planar, and for simplicity consider only a two-dimensional case in which the sensors lie in a plane. Each sensor also samples the ambient noise background and/or generates within itself a noise background.

The direction of each signal's arrival is embedded in relative delays of the arrival at the sensor. That is, for sensor i and signal k , the received waveform is

$$x_i(t) = s_k(t - \tau_i^{(k)}) + n_i(t) \tag{2-1}$$

and the direction of arrival information is present in the set of relative delays $\{\tau_{i_1, i_2}^{(k)}\}$, where

$$\tau_{i_1, i_2}^{(k)} \triangleq \tau_{i_2}^{(k)} - \tau_{i_1}^{(k)} \tag{2-2}$$

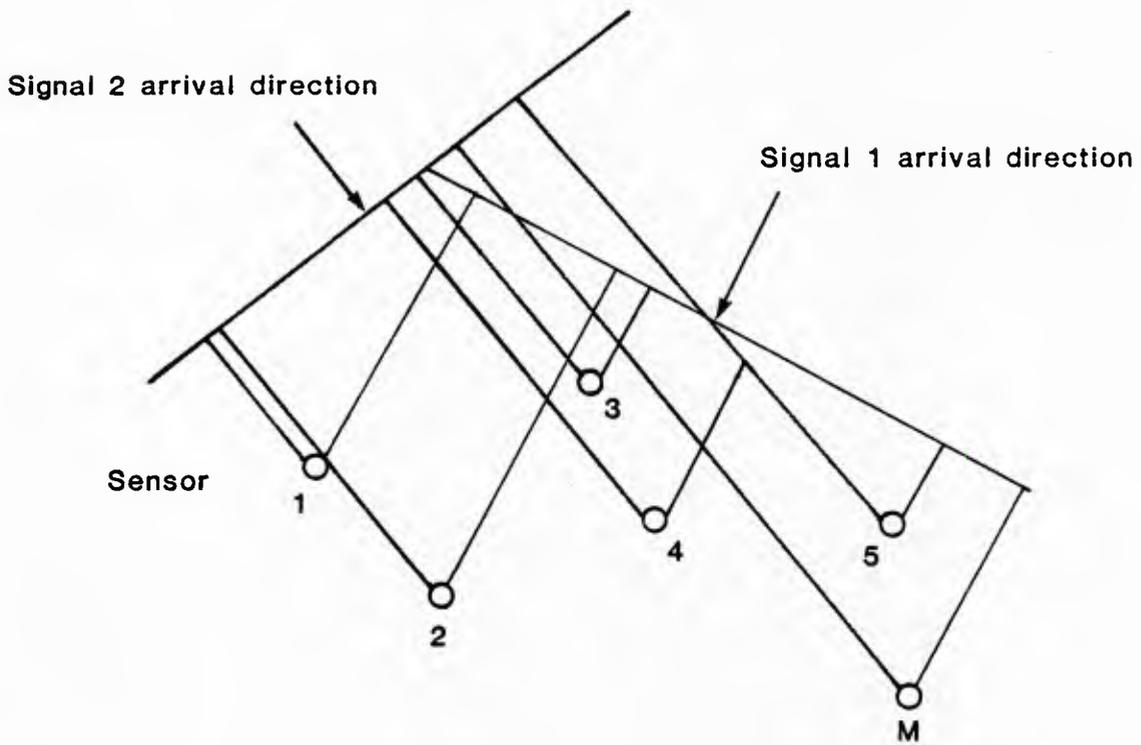


FIGURE 2-1 ILLUSTRATED SENSOR PLACEMENT AND RECEIVED SIGNAL ARRIVALS

2.1.1 Complex representation of the data. (2-3)

Bandpass filtering of the sensor outputs is assumed, so that they have the form

$$x_i(t) = R_i(t) \cos[\omega_o t + \phi_i(t)] \quad (2-3a)$$

$$= x_{ci}(t) \cos \omega_o t - x_{si}(t) \sin \omega_o t \quad (2-3b)$$

$$= \text{Re} \{ (x_{ci} + jx_{si}) e^{j\omega_o t} \} \quad (2-3c)$$

In this formulation R is an envelope and ϕ is a phase with respect to a center frequency $f_o = \omega_o / 2\pi$. The quadrature components $x_{ci} = R_i \cos \phi_i$ and $x_{si} = R_i \sin \phi_i$ are an alternate representation; samples of these components, each at the rate B Hz, where B is the bandpass bandwidth, are sufficient data to reconstruct $x_i(t)$ on a given time interval. The third form, (2-3c), indicates how $x_i(t)$ is related to its complex envelope $x_{ci}(t) + jx_{si}(t)$.

In place of $x_i(t)$, we may consider samples of the complex envelope as constituting the data. Together, the M sensors produce the data vector

$$\underline{x}(t) = \begin{bmatrix} x_{c1}(t) + jx_{s1}(t) \\ x_{c2}(t) + jx_{s2}(t) \\ \vdots \\ x_{cm}(t) + jx_{sm}(t) \end{bmatrix} = \underline{x}_c(t) + j\underline{x}_s(t). \quad (2-4)$$

We assume that the means of $\underline{x}_c(t)$ and $\underline{x}_s(t)$ are zero.

The covariance matrix for the sampled complex data vector is, after Goodman [4]

$$\begin{aligned} \frac{1}{2}E\{\underline{X}\underline{X}^*\} &= \frac{1}{2}E\{(\underline{x}_C + j\underline{x}_S)(\underline{x}_C^T - j\underline{x}_S^T)\} \\ &= \frac{1}{2}E\{\underline{x}_C\underline{x}_C^T + \underline{x}_S\underline{x}_S^T + j\underline{x}_S\underline{x}_C^T - j\underline{x}_C\underline{x}_S^T\} \triangleq \Sigma \end{aligned} \quad (2-5a)$$

with elements

$$\sigma_{ik} = \frac{1}{2}E\{x_{ci}x_{ck} + x_{si}x_{sk} + jx_{si}x_{ck} - jx_{ci}x_{sk}\} \quad (2-5b)$$

From (2-5b) we see that $\sigma_{ki} = \overline{\sigma_{ik}}$, the complex conjugate of σ_{ik} . Thus $\Sigma^* = \Sigma$, that is, Σ is Hermitian.

2.1.2 Correlation measure

Let the number of sensors be an even number $M = 2m$, and let the data vector be partitioned into two $m \times 1$ vectors.

$$\underline{x} = \begin{bmatrix} \underline{x}^{(1)} \\ \underline{x}^{(2)} \end{bmatrix}; \quad (2-6)$$

the covariance matrix then can be partitioned as

$$\Sigma = \begin{bmatrix} \Sigma_{11} & \Sigma_{12} \\ \Sigma_{21} & \Sigma_{22} \end{bmatrix}, \quad (2-7a)$$

where, since Σ is Hermitian, each submatrix is $m \times m$, and

$$\Sigma_{11}^* = \Sigma_{11}, \quad \Sigma_{22}^* = \Sigma_{22}, \quad \text{and} \quad \Sigma_{21}^* = \Sigma_{12}. \quad (2-7b)$$

A complex correlation between the linear combinations $U = \underline{\alpha}^* \underline{x}^{(1)}$ and $V = \underline{\beta}^* \underline{x}^{(2)}$ may be defined as

$$\begin{aligned} E\{U\bar{V}\} &= E\{\underline{\alpha}^* \underline{x}^{(1)} \underline{x}^{(2)} \underline{\beta}\} \\ &= \underline{\alpha}^* \underline{\Sigma}_{12} \underline{\beta}. \end{aligned} \quad (2-8)$$

In general, this quantity is complex. The variances of U and V , of course, are real when defined in the inner product sense of $E\{U\bar{U}\} = E\{|U|^2\}$ and $E\{|V|^2\}$, respectively.

2.1.3 Maximum correlation

Since the correlation (2-8) can be complex, the concept of a maximum is still ambiguous. However, as we shall demonstrate below, the solution to the maximization problem provides that the correlation, when maximized, is real.

The function to be maximized, with constraints, is

$$\psi = \underline{\alpha}^* \underline{\Sigma}_{12} \underline{\beta} - \frac{1}{2} \lambda [\underline{\alpha}^* \underline{\Sigma}_{11} \underline{\alpha} - 1] - \frac{1}{2} \mu [\underline{\beta}^* \underline{\Sigma}_{22} \underline{\beta} - 1]. \quad (2-9)$$

First, consider differentiation with respect to the elements of $\underline{\alpha} = \frac{\alpha}{R} + j \frac{\alpha}{I}$,

where $\frac{\alpha}{R}$ and $\frac{\alpha}{I}$ are the real and imaginary parts of the vector α .

This operation yields the equations

$$\frac{\partial \psi}{\partial \frac{\alpha}{R}} = \underline{\Sigma}_{12} \underline{\beta} - \lambda [\underline{\Sigma}_{11} \underline{\alpha} + \underline{\Sigma}_{11} \underline{\alpha}] = \underline{0} \quad (2-10a)$$

$$\frac{\partial \psi}{\partial \frac{\alpha}{I}} = j \underline{\Sigma}_{12} \underline{\beta} - \frac{1}{2} \lambda [-j \underline{\Sigma}_{11} \underline{\alpha} + j \underline{\Sigma}_{11} \underline{\alpha}] = \underline{0}. \quad (2-10b)$$

Premultiplying (2-10a) by $\frac{\underline{\alpha}^T}{R}$ and premultiplying (2-10b) by $\frac{\underline{\alpha}^T}{I}$, and then adding the two resulting equations yields the single equation

$$\underline{\alpha}^* \Sigma_{12} \underline{\beta} - \frac{1}{2} \lambda [\underline{\alpha}^* \Sigma_{11} \underline{\alpha} + \underline{\alpha}^T \Sigma_{11} \underline{\alpha}] = 0. \quad (2-11)$$

But since the quantity

$$\underline{\alpha}^* \Sigma_{11} \underline{\alpha} = \overline{\underline{\alpha}^T \Sigma_{11} \underline{\alpha}} = \underline{\alpha}^T \Sigma_{11} \underline{\alpha} = 1 \quad (2-12)$$

is real, (2-11) reduces to

$$\lambda = \underline{\alpha}^* \Sigma_{12} \underline{\beta}. \quad (2-13)$$

This demonstrates that the correlation is a real quantity if the Lagrange multiplier λ is taken to be real.

By a similar process, differentiation with respect to $\underline{\beta} = \frac{\underline{\beta}}{R} + j \frac{\underline{\beta}}{I}$

yields the result

$$\mu = \underline{\beta}^T \Sigma_{12} \underline{\alpha} = \underline{\alpha}^* \Sigma_{12} \underline{\beta} = \lambda. \quad (2-14)$$

Therefore the maximization problem reduces to the matrix equation

$$\begin{bmatrix} -\lambda \Sigma_{11} & \Sigma_{12} \\ \Sigma_{21} & -\lambda \Sigma_{22} \end{bmatrix} \begin{bmatrix} \underline{\alpha} \\ \underline{\beta} \end{bmatrix} = \underline{0}. \quad (2-15)$$

Nontrivial solutions to this equation require, as in the real data case,

$$\det \begin{bmatrix} -\lambda \Sigma_{11} & \Sigma_{12} \\ \Sigma_{21} & -\lambda \Sigma_{22} \end{bmatrix} = 0, \quad (2-16a)$$

or equivalently, with $v = \lambda^2$,

$$\det [\Sigma_{12}\Sigma_{22}^{-1}\Sigma_{21} - v\Sigma_{11}] = 0 . \quad (2-16b)$$

2.1.4 Sample solution: single signal.

Before considering more complicated cases, we demonstrate the canonical correlation method's solution for the simple case of uncorrelated sensor noises and a single, sinusoidal signal. For this case, the waveforms at the sensors are

$$\begin{aligned} x_i(t) &= s(t - \tau_i) + n_i(t) \\ &= \text{Re}\{Ae^{j\omega_0(t - \tau_i) + j\phi_s} + (n_{ci} + jn_{si})e^{j\omega_0 t}\} \\ &= \text{Re}\{(Ae^{-j\phi_i} + n_{ci} + jn_{si})e^{j\omega_0 t}\} \end{aligned} \quad (2-17)$$

This formulation neglects any attenuation of the signal from sensor location to sensor location. The covariance matrix for complex samples of these waveforms is

$$\begin{aligned} \Sigma &= \frac{1}{2}\Sigma\{\underline{xx}^*\} \\ &= \frac{1}{2}\Sigma\{(\underline{Av} + \underline{n}_c + j\underline{n}_s) (\underline{Av}^* + \underline{n}_c^T - j\underline{n}_s^T)\} \\ &= \frac{1}{2}[A^2 \underline{vv}^* + 2\sigma^2 \underline{I}] \\ &= \sigma^2 [\underline{I} + \rho \underline{vv}^*] . \end{aligned} \quad (2-18)$$

In this development we have used the notation

$$\underline{v} \triangleq \begin{bmatrix} e^{-j\phi_1} \\ e^{-j\phi_2} \\ \vdots \\ e^{-j\phi_M} \end{bmatrix} \quad (2-19)$$

and assume the noise components have equal variances,

$$E\{n_{ci}^2\} = E\{n_{si}^2\} = \sigma^2, \quad (2-20)$$

with $\rho = A^2/2\sigma^2$ denoting the signal-to-noise ratio (SNR).

For $M = 2m$ sensors, we partition \underline{v} into two $m \times 1$ vectors \underline{v}_1 and \underline{v}_2 so that the partitioned covariance matrix has the form

$$\Sigma = \sigma^2 \begin{bmatrix} I + \rho \underline{v}_1 \underline{v}_1^* & \rho \underline{v}_1 \underline{v}_2^* \\ \rho \underline{v}_1 \underline{v}_1^* & I + \rho \underline{v}_2 \underline{v}_2^* \end{bmatrix} \quad (2-21)$$

The determinant to be solved for the maximum correlation is of the matrix

$$\begin{aligned} & \Sigma_{12} \Sigma_{22}^{-1} \Sigma_{21} - \nu \Sigma_{11} \\ & = [\rho \underline{v}_1 \underline{v}_2^* (I + \rho \underline{v}_2 \underline{v}_2^*)^{-1} \rho \underline{v}_2 \underline{v}_1^* - \nu (I + \rho \underline{v}_1 \underline{v}_1^*)] \sigma^2. \end{aligned} \quad (2-22)$$

The needed matrix inverse is

$$(I + \rho \frac{v}{2} \frac{v}{2} *)^{-1} = I - \frac{\rho v \frac{v}{2} *}{1 + \rho |\frac{v}{2}|^2} \quad (2-23)$$

Substituting (2-23) in (2-22) yields the determinant

$$\det \left[\left(\frac{\rho |\frac{v}{2}|^2}{1 + \rho |\frac{v}{2}|^2} - v \right) \rho \sigma^2 \frac{v}{1} \frac{v}{1} * - v \sigma^2 I \right] = 0, \quad (2-24a)$$

or, using the fact that $|\frac{v}{2}|^2 = m$,

$$\det \left[\left(v - \frac{m\rho}{1 + m\rho} \right) \rho \sigma^2 \frac{v}{1} \frac{v}{1} * + v \sigma^2 I \right] = 0. \quad (2-24b)$$

It can be shown by induction that

$$\det (aI + b \underline{v} \underline{v} *) = a^{m-1} (a + mb). \quad (2-25)$$

Applying this fact to (2-24b) results in the following equation to be solved for v :

$$(\sigma^2 v)^{m-1} \left[\sigma^2 v + m \rho \sigma^2 \left(v - \frac{m\rho}{1 + m\rho} \right) \right] = 0. \quad (2-26)$$

The solution is immediately seen to be that there are m-1 zero correlations ($\nu = 0$), and one maximum correlation (normalized) given by

$$\lambda = \sqrt{\nu} = \frac{m\rho}{1 + m\rho} \quad (2-27)$$

Substitution of this value of ν in the equation

$$\Sigma_{12}\Sigma_{22}^{-1}\Sigma_{21}\underline{\alpha} = \nu\Sigma_{11}\underline{\alpha} \quad (2-28a)$$

yields the information that

$$\underline{\alpha} = \left(\frac{v_1^*}{m}\right) \underline{v}_1 = k\underline{v}_1, \quad (2-28b)$$

where k is a constant scale factor. The appropriate scale factor is found from the requirement

$$\begin{aligned} \underline{\alpha}^* \Sigma_{11} \underline{\alpha} &= 1 = k^2 \underline{v}_1^* (\sigma^2 + \rho\sigma^2 \frac{v_1^*}{v_1}) \underline{v}_1 \\ &= k^2 \sigma^2 m (1 + m\rho) \end{aligned} \quad (2-29a)$$

or finally,

$$\underline{\alpha} = \frac{\underline{v}_1}{\sqrt{m\sigma^2 (1 + m\rho)}} \quad (2-29b)$$

In a similar manner, β is found to be

$$\beta = \sqrt{\frac{v}{2} m \sigma^2 (1 + m \rho)} . \quad (2-30)$$

For this simple case, the solution is easily interpreted. Maximum correlation between a linear combination (complex weighted sum) of signals from half of the sensors and a linear combination of signals from the other half is achieved when the weights are chosen to remove the relative propagation delays (i.e., steer a beam in the direction of signal arrival). For example, a reconstruction of time samples of the linear combination U would produce the waveform

$$\begin{aligned} u(t) &= \text{Re}\{U(t)e^{j\omega_0 t}\} \\ &= \text{Re}\{\underline{\alpha}^* \underline{x}^{(1)}(t)e^{j\omega_0 t}\} \\ &= \text{Re}\left\{\sum_{i=1}^m k e^{j\theta_i} [A e^{-j\theta_i} + n_{ci}(t) + j n_{si}(t)] e^{j\omega_0 t}\right\} \\ &= km A \cos \omega_0 t + \sum_{i=1}^m n_i(t) . \end{aligned} \quad (2-31)$$

In the more general case, this ideal solution will be affected variously by complicating factors, including

- (a) the presence of more than one signal
- (b) non-zero noise correlations between sensors

- (c) attenuation of the signal as it propagates through the array of sensors
- (d) non-tonal (modulated) signals.

2.2 SOLUTION FOR TWO SIGNALS

We consider now how the presence of more than one signal affects the canonical correlation solution. The model for the data in this situation is

$$\underline{x} = \sum_{n=1}^N A_n e^{j\theta_n} \underline{v}_n + \underline{n}_c + j\underline{n}_s, \quad (2-34)$$

in which (A_n, θ_n) are the sampled amplitude and phase of the nth of N signals. The covariance matrix for this data model is

$$\begin{aligned} \Sigma &= \frac{1}{2} E(\underline{x} \underline{x}^*) \\ &= \sigma^2 \{ I + \sum_{n=1}^N \rho_{n-n} \underline{v}_n \underline{v}_n^* \}. \end{aligned} \quad (2-35)$$

This formulation assumes that

$$E\{A_n e^{j\theta_n} \underline{v}_n A_k e^{-j\theta_k} \underline{v}_k^*\} = 0, \quad (2-36)$$

that is, the signals are uncorrelated.

2.2.1 General formulation

Analytically we can pursue a solution conveniently for two signals.

For ease of notation, let $\rho_1 \equiv \rho$, $\rho_2 \equiv r$, $\underline{v}_1 \equiv \underline{v}$, and $\underline{v}_2 \equiv \underline{w}$.

Then the covariance matrix is

$$\Sigma = \sigma^2 \{ I + \rho \underline{v} \underline{v}^* + r \underline{w} \underline{w}^* \}. \quad (2-37)$$

Suitably partitioned, this matrix has the component matrices (all $m \times m$)

$$\Sigma_{11} = \sigma^2(I + \rho \underline{v}_{-1} \underline{v}_{-1}^* + r \underline{w}_{-1} \underline{w}_{-1}^*) \quad (2-38a)$$

$$\Sigma_{12} = \sigma^2(\rho \underline{v}_{-1} \underline{v}_{-2}^* + r \underline{w}_{-1} \underline{w}_{-2}^*) \quad (2-38b)$$

$$\Sigma_{21} = \sigma^2(\rho \underline{v}_{-2} \underline{v}_{-1}^* + r \underline{w}_{-2} \underline{w}_{-1}^*) = \quad (2-38c)$$

$$\Sigma_{22} = \sigma^2(I + \rho \underline{v}_{-2} \underline{v}_{-2}^* + r \underline{w}_{-2} \underline{w}_{-2}^*). \quad (2-38d)$$

The matrix whose determinant is to be found is

$$\begin{aligned} & \Sigma_{12} \Sigma_{22}^{-1} \Sigma_{21} - \nu \Sigma_{11} \\ &= \sigma^2 (\rho \underline{v}_{-1} \underline{v}_{-2}^* + r \underline{w}_{-1} \underline{w}_{-2}^*) (I + \rho \underline{v}_{-2} \underline{v}_{-2}^* + r \underline{w}_{-2} \underline{w}_{-2}^*)^{-1} (\rho \underline{v}_{-2} \underline{v}_{-1}^* + r \underline{w}_{-2} \underline{w}_{-1}^*) \\ & \quad - \omega^2 (I + \rho \underline{v}_{-1} \underline{v}_{-1}^* + r \underline{w}_{-1} \underline{w}_{-1}^*). \end{aligned} \quad (2-39)$$

The inverse matrix has the form [3]

$$\begin{aligned} & (I + \rho \underline{v}_i \underline{v}_i^* + r \underline{w}_i \underline{w}_i^*)^{-1} \\ &= I + \frac{\rho r [z_i \underline{v}_i \underline{w}_i^* + \bar{z}_i \underline{w}_i \underline{v}_i^*] - \rho(1+mr) \underline{v}_i \underline{v}_i^* - r(1+m\rho) \underline{w}_i \underline{w}_i^*}{1 + m(\rho+r) - \rho r \Delta_i} \end{aligned} \quad (2-40a)$$

using $z_i \triangleq \underline{v}_i^* \underline{w}_i$, $\Delta_i \triangleq |z_i|^{2-m^2}$. (2-40b)

After substituting (2-40), the matrix in (2-39) becomes
(neglecting the factor σ^2)

$$\begin{aligned} & [A(z_2) - \nu\rho] \underline{v}_1 \underline{v}_1^* + [B(z_2) - \nu r] \underline{w}_1 \underline{w}_1^* \\ & + C(z_2) [z_2 \underline{v}_1 \underline{w}_1^* + \bar{z}_2 \underline{w}_1 \underline{v}_1^*] - \nu I, \end{aligned} \quad (2-41)$$

where z_2 is the complex number

$$z_2 \triangleq \frac{\underline{v}_2^* \underline{w}_2}{\underline{v}_2 \underline{w}_2^*} \quad (2-42a)$$

and the coefficients A, B, and C are

$$A(z_2) = \frac{\rho^2 (m - r\Delta_2)}{1 + m(r+\rho) - \rho r\Delta_2} \quad (2-42b)$$

$$B(z_2) = \frac{r^2 (m - \rho\Delta_2)}{1 + m(r+\rho) - \rho r\Delta_2} \quad (2-42c)$$

$$C(z_2) = \frac{\rho r}{1 + m(r+\rho) - \rho r\Delta_2} \quad (2-42d)$$

As a check on our algebraic manipulations, we note that if $r=0$, (2-39) reduces to the single signal matrix, (2-24).

2.2.2 Formulation for linear array.

When the sensors are aligned to form a linear array with equal spacing d , the delay vector for the n :th signal assumes the special form

$$\begin{aligned} \underline{v}_n &= \underline{v}(\theta_n) \\ &= e^{-j\theta_n/2} [e^{jm\theta_n}, e^{j(m-1)\theta_n}, \dots, e^{-j(m-1)\theta_n}]^T \end{aligned} \quad (2-43a)$$

where

$$\theta_n = \frac{2\pi d}{\lambda} \cos b_n, \quad b_n = \text{bearing}, \quad (2-43b)$$

using the geometry of Figure 2-2. When partitioned, we find that

$$\underline{v}_{-n}^{(2)} = e^{-jm\theta_n} \underline{v}_{-n}^{(1)} \quad (2-44)$$

and

$$\underline{v}_{-n}^{(1)*} \underline{v}_{-k}^{(1)} = m D_m(\theta_k - \theta_n) \exp\left\{ \frac{jm(\theta_k - \theta_n)}{2} \right\}, \quad (2-45a)$$

using

$$D_m(\alpha) \triangleq \frac{\sin(m\alpha/2)}{m \sin(\alpha/2)} = D_m(-\alpha). \quad (2-45b)$$

In terms of the quantities introduced in Section 2.2.1, the linear array geometry produces the relations

$$\Sigma_{11} = \Sigma_{22} \quad (2-46a)$$

$$z_1 = \bar{z}_2 \quad (2-46b)$$

$$\Delta_1 = \Delta_2 \quad (2-46c)$$

The overall covariance matrix has the form, for $m = 2$,

$$\Sigma = \|\delta_{ik} + \rho \exp\{j(k-i)\theta_1\} + r \exp\{j(k-i)\theta_2\}\| \quad (2-46d)$$

These simplify the solution somewhat, but further simplification does not seem possible.

2.2.3 Special case of four sensors.

In order to pursue numerical cases, we consider a small array size of $M = 2m = 4$. In this case, we can write

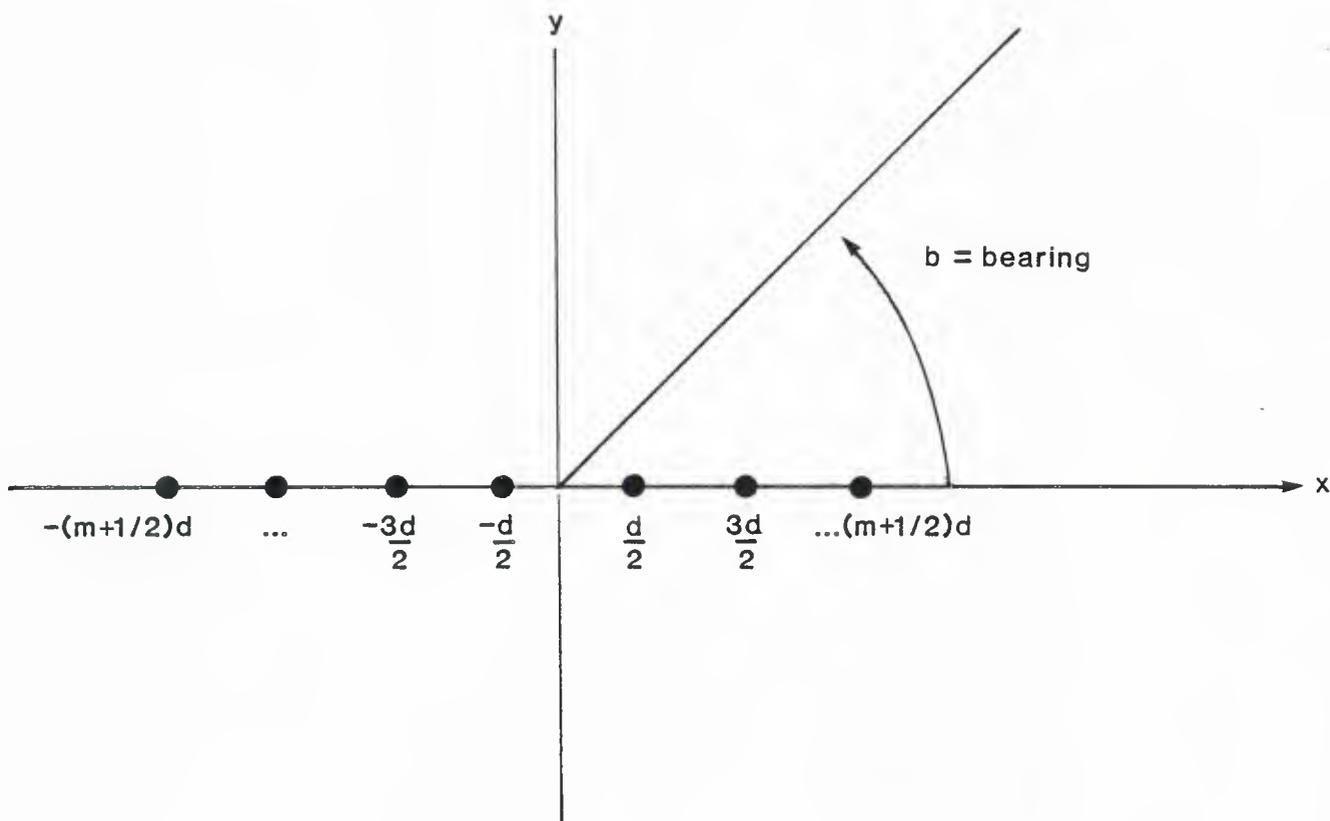


FIGURE 2-2 LINEAR ARRAY CONFIGURATION

$$\Sigma_{11} \triangleq (1 + \rho + r) \begin{bmatrix} 1 & c_1 \\ \bar{c}_1 & 1 \end{bmatrix} \quad (2-47a)$$

$$\Sigma_{22} \triangleq (1 + \rho + r) \begin{bmatrix} 1 & c_2 \\ \bar{c}_2 & 1 \end{bmatrix} \quad (2-47b)$$

and

$$\Sigma_{12} \triangleq (1 + \rho + r) \begin{bmatrix} c_3 & c_4 \\ c_5 & c_6 \end{bmatrix} \quad (2-47c)$$

The canonical correlations are then the solutions to the equation

$$\begin{aligned} 0 = & \lambda^4 (1 - |c_1|^2)(1 - |c_2|^2) \\ & + \lambda^2 \{ 2\text{Re}[c_2 c_5 \bar{c}_6 + c_1 \bar{c}_3 c_5 + c_1 \bar{c}_4 c_6 + c_2 c_3 \bar{c}_4 \\ & - c_1 \bar{c}_2 \bar{c}_3 c_6 - c_1 c_2 \bar{c}_4 c_5] \\ & - |c_3|^2 - |c_4|^2 - |c_5|^2 - |c_6|^2 \} \\ & + \lambda^0 \{ |c_3|^2 |c_6|^2 + |c_4|^2 |c_5|^2 - 2\text{Re}[\bar{c}_3 c_4 c_5 \bar{c}_6] \}. \end{aligned} \quad (2-48)$$

This equation is quadratic in $\lambda^2 = v$. Having calculated λ , the $\underline{\alpha}$ steering vector is found to have components which satisfy

$$\frac{\alpha_2}{\alpha_1} = \frac{|c_3|^2 + |c_4|^2 - 2\text{Re}[c_2 c_3 \bar{c}_4] - \lambda^2 (1 - |c_2|^2)}{c_1 \lambda^2 (1 - |c_2|^2 - c_3 \bar{c}_5 + c_2 c_3 \bar{c}_6 - c_4 \bar{c}_6 + \bar{c}_2 c_4 \bar{c}_6)} \quad (2-49a)$$

and

$$|\alpha_1|^2 + |\alpha_2|^2 + 2\text{Re}[c_1 \bar{\alpha}_1 \alpha_2] = 1. \quad (2-49b)$$

These constraints determine $\underline{\alpha}$ to within a complex factor with unit magnitude, so conveniently we may take α_1 to be real.

Having found $\underline{\alpha}$, $\underline{\beta}$ is determined by

$$\underline{\beta} = \frac{1}{\lambda} \Sigma_{22}^{-i} \Sigma_{21} \underline{\alpha}, \lambda > 0, \quad (2-50a)$$

or

$$\beta_1 = [(\bar{c}_3 - c_2 \bar{c}_4) \alpha_1 + (\bar{c}_5 - c_2 \bar{c}_6) \alpha_2] / \lambda (1 - |c_2|^2) \quad (2-50b)$$

and

$$\beta_2 = [(\bar{c}_4 - \bar{c}_2 \bar{c}_3) \alpha_1 + (\bar{c}_6 - \bar{c}_2 \bar{c}_5) \alpha_2] / \lambda (1 - |c_2|^2). \quad (2-50c)$$

For the special case of linear arrays with four elements, we have $c_1 = c_2 = c_5$ and $c_3 = c_6$, resulting in the simplified equations

$$\begin{aligned} 0 = & \lambda^4 (1 - |c_1|^2)^2 \\ & + \lambda^2 \{ 2\text{Re}[2c_1(c_1 \bar{c}_3 + c_3 \bar{c}_4) - c_1^3 \bar{c}_4] \\ & \quad - 2|c_3|^2 - 2|c_1|^2 |c_3|^2 - |c_1|^2 - |c_4|^2 \} \\ & \lambda^0 \{ |c_3|^4 + |c_1|^2 |c_4|^2 - 2\text{Re}[c_1 \bar{c}_3^2 c_4] \} \end{aligned} \quad (2-51)$$

$$\frac{\alpha_2}{\alpha_1} = \frac{|c_3|^2 + |c_4|^2 - 2\text{Re}[c_1 c_3 \bar{c}_4] - \lambda^2 (1 - |c_1|^2)}{c_1 \lambda^2 (1 - |c_1|^2) - \bar{c}_1 c_3 + c_1 |c_3|^2 - \bar{c}_3 c_4 - \bar{c}_1 \bar{c}_3 c_4}$$

$$\beta_1 = [(\bar{c}_3 - c_1 \bar{c}_4) \alpha_1 + (\bar{c}_1 - c_1 \bar{c}_3) \alpha_2] / \lambda (1 - |c_1|^2) \quad (2-53a)$$

$$\beta_2 = [(\bar{c}_4 - \bar{c}_1 \bar{c}_3) \alpha_1 + (\bar{c}_3 - \bar{c}_1^2) \alpha_2] / \lambda (1 - |c_1|^2). \quad (2-53b)$$

3.0 NUMERICAL STUDIES

Since an easily interpreted analytical solution for the canonical correlations and their corresponding steering vectors has not been found, we resort to selected numerical studies to explore the dependence of these quantities upon various parameters. In all the numerical cases presented, four sensors are assumed ($M=2$), and the array configurations illustrated in Figure 3-1 were used. As indicated in that figure, the direction of arrival of the planewave signals is given in terms of the bearing η relative to the x-axis.

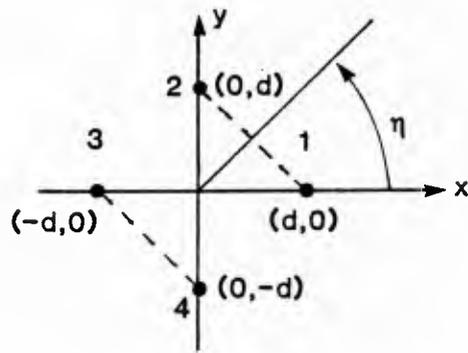
The parameters used in the numerical studies are listed in Table 3-1.

3.1 RESULTS FOR SINGLE SIGNAL

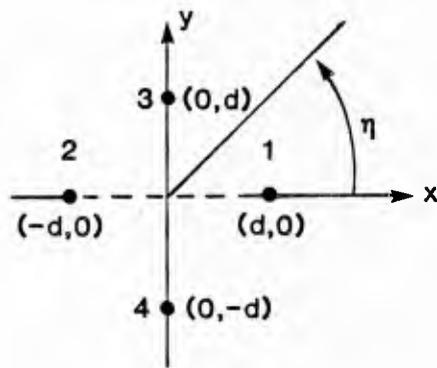
Although in Section 2.1 it was shown that the canonical correlation method yields an accurate steering vector for a single signal, irrespective of array configuration or spacing, a number of single signal cases were calculated in order to verify the analysis and also investigate effects of noise correlation.

According to the analysis presented earlier, the maximum canonical correlation value for a single signal should be

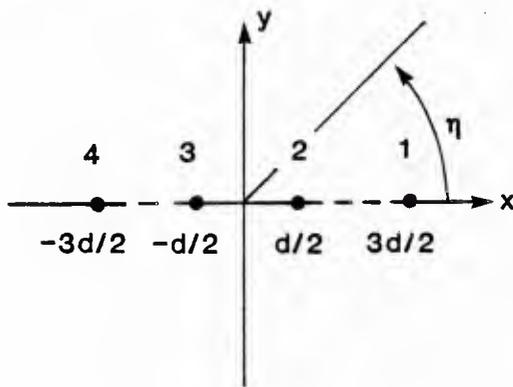
$$\lambda = \frac{m\rho}{1+m\rho} = \frac{2\rho}{1+2\rho} \quad (3-1)$$



(a) Array configuration 1: antiparallel pairs



(b) Array configuration 2: crossed pairs



(c) Array configuration 3: partitional linear array

FIGURE 3-1 ARRAY CONFIGURATIONS USED IN NUMERICAL STUDIES

Case	Array	d/λ	ρ	r	η ₁ /π	η ₂	correlation	
1	1	0.25	10	0	0(.1)1	-	none	
2		0.25		1		0.75π		
3		0.25		5		0.75π		
4	2	0.25	10	0	0(.1)1	-	none	
5		0.25		1		0.75π		
6		0.225		1		0.75π		
7		0.175		1		0.75π		
8		0.075		1		0.75π		
9		0.075		5		0.75π		
10	3	0.075	10	1	0(.1)1	0.50π	none	
11		0.075		1	0(.05)1	η ₁ - π/2	none	
12		0.25		1	0(.05)1	η ₁ - π/2	none	
13		0.125		1	0(.05)1	η ₁ - π/2	none	
14		0.075		5	0(.05)1	η ₁ - π/2	none	
15		0.075		5	0(.05)1	η ₁ - π/4	none	
16		0.075		1	0(.05)1	η ₁ - π/4	none	
17		0.25		1	0(.1)1	0.75π	none	
18		0.075		1	0(.1)1	0.75π	none	
19		0.075		1	0(.1)1	0.75π	0.01	
20		0.075		1	0(.1)1	0.75π	0.10	
21		0.075		0	0(.1)1	-	0.10	
22		0.075		0	0(.1)1	-	0.20	
23		0.075		1	0(.1)1	-	0.20	
24		0.075		.1	0(.1)1	0.75π	0.20	
25		0.075		.1	.05	0(.1)1	0.75π	0.20
26		0.075		10	0	0(.1)1	-	none
27		0.075		1	0	0(.1)1	-	0.10
28		0.075		1	0.1	0(.1)1	0.75π	0.10
29		0.075		10	1	0(.1)1	0.75π	0.20

Arrays: 1 : antiparallel pairs

2 : crossed pairs

3 : partitioned linear

$$\rho = \text{SNR}_1, \quad r = \text{SNR}_2$$

TABLE 3-1 PARAMETERS USED IN NUMERICAL STUDIES

In order to assess the agreement of the steering vector solution with the actual direction of arrival, we define the agreement metric

$$\begin{aligned} \text{Agreement} \triangleq & 1 + \cos(\theta_2 - \phi_2 + \phi_1) \\ & + \cos(\theta_3 - \phi_3 + \phi_1) \\ & + \cos(\theta_4 - \phi_4 + \phi_1), \end{aligned} \quad (3-2)$$

where the steering solution vector is

$$(\alpha_1, \alpha_2, \beta_1, \beta_2) = (|\alpha_1|e^{j\phi_1}, |\alpha_2|e^{j\phi_2}, |\beta_1|e^{j\phi_3}, |\beta_2|e^{j\phi_4}), \quad (3-3)$$

and the actual received delay vector is

$$(e^{j\theta_1}, e^{j\theta_2}, e^{j\theta_3}, e^{j\theta_4}). \quad (3-4)$$

This metric ignores any constant phase difference between the actual vector and the solution vector, as well as any differences in the magnitudes of the components.

3.1.1 Cases without noise correlation.

The elements of the normalized covariance matrix (2-47) were generated using

$$\begin{aligned} c_1 &= \rho \exp\{j(\theta_1 - \theta_2)\} / (1 + \rho) \\ c_2 &= \rho \exp\{j(\theta_3 - \theta_4)\} / (1 + \rho) \\ c_3 &= \rho \exp\{j(\theta_1 - \theta_3)\} / (1 + \rho) \\ c_4 &= \rho \exp\{j(\theta_1 - \theta_4)\} / (1 + \rho) \\ c_5 &= \rho \exp\{j(\theta_2 - \theta_3)\} / (1 + \rho) \\ c_6 &= \rho \exp\{j(\theta_2 - \theta_4)\} / (1 + \rho) \end{aligned} \quad (3-5)$$

and
$$\theta_i = \frac{2\pi}{\lambda} (x_i \cos\eta + y_i \sin\eta), \quad i = 1,2,3,4. \quad (3-6)$$

In the one-signal cases with no noise correlation (Nos. 1,4,26), without exception the canonical correlation solution yielded one non-zero root ($\lambda = 20/21 = .95238$ for $\rho=10$), and the agreement metric was always equal to 4, indicating a correct numerical solution for the delay vector.

3.1.2 Cases with noise correlation.

Several cases of noise correlation between sensors were examined for the linear array configuration. For that array type, the correlation is easily modelled by assuming that the covariance matrix is, in the absence of signals,

$$\Sigma = \|\sigma_{ik}\| = \|\sigma^2 a^{|i-j|}\| \quad , \quad (3-7)$$

where a is the correlation coefficient ($0 < a < 1$) between nearest sensors.

Table 3-2 gives the canonical correlation results as a function of signal bearing, for an SNR of $\rho = 10$ and 1 , and a noise correlation coefficient of $a = 0.1$ and $a = 0.2$. It is seen from this data that the second canonical correlation now is nonzero, but that the noise correlation has increased the first canonical correlation values from their zero-noise correlation values (.95238 for $\rho = 10$ and .66667 for $\rho = 1$). The vector agreement metric indicates that the vector solution is slightly degraded from a perfect value of 4.0000, in proportion to the noise correlation, except when the signal is broadside to the array ($\eta = \pi/2$).

ρ	η/π	a = 0.1			a = 0.2		
		λ_1	λ_2	agreement	λ_1	λ_2	agreement
10	0.0	.95216	.00722	3.9750	.95468	.01184	3.8382
	0.1	.95213	.00720	3.9772	.95462	.01177	3.8516
	0.2	.95207	.00716	3.9830	.95447	.01158	3.8886
	0.3	.95200	.00710	3.9908	.95427	.01135	3.9384
	0.4	.95193	.00705	3.9974	.95412	.01116	3.9823
	0.5	.95191	.00703	4.0000	.95406	.01109	4.0000
	0.6	.95193	.00705	3.9974	.95412	.01116	3.9823
	0.7	.95200	.00710	3.9908	.95427	.01135	3.9384
	0.8	.95207	.00716	3.9830	.95447	.01158	3.8886
	0.9	.95213	.00720	3.9772	.95462	.01177	3.8516
1.0	.95216	.00722	3.9750	.95468	.01184	3.8382	
1	0.0	.66716	.03117	3.9724	.67851	.05038	3.8663
	0.1	.66713	.03109	3.9748	.67849	.05007	3.8773
	0.2	.66704	.03090	3.9813	.67846	.04928	3.9079
	0.3	.66694	.03065	3.9898	.67844	.04829	3.9491
	0.4	.66686	.03045	3.9971	.67843	.04748	3.9854
	0.5	.66682	.03037	4.0000	.67844	.04717	4.0000
	0.6	.66686	.03045	3.9971	.67843	.04748	3.9854
	0.7	.66694	.03065	3.9898	.67844	.04829	3.9491
	0.8	.66704	.03090	3.9813	.67846	.04928	3.9079
	0.9	.66713	.03109	3.9748	.67849	.05007	3.8773
1.0	.66716	.03117	3.9724	.67851	.05038	3.8663	

TABLE 3-2 CANONICAL CORRELATION RESULTS FOR ONE SIGNAL WHEN INTER-SENSOR NOISE CORRELATION EXISTS

U221490